



Title	Residual hull girder strength of asymmetrically damaged ships
Author(s)	Muis Alie, Muhammad Zubair
Citation	大阪大学, 2013, 博士論文
Version Type	VoR
URL	<a href="https://doi.org/10.18910/26203">https://doi.org/10.18910/26203</a>
rights	
Note	

*The University of Osaka Institutional Knowledge Archive : OUKA*

<https://ir.library.osaka-u.ac.jp/>

The University of Osaka

Doctoral Dissertation

Residual hull girder strength of  
asymmetrically damaged ships

(非対称損傷を有する船体桁の残存強度に  
関する研究)

Muhammad Zubair Muis Alie

July 2013

Graduate School of Engineering  
Osaka University

## **Acknowledgements**

The present study was undertaken at the Ship Structural Integrity Subarea Laboratory (<http://www.naoe.eng.osaka-u.ac.jp/naoe/naoe4>), Osaka University, Japan. This dissertation would not have been possible to complete without help of many people, especially from the Ship Structural Integrity Subarea Laboratory member.

First of all, I would like to thank to my supervisor, Professor Masahiko FUJIKUBO for his guidance academic, frontier advice and support. Professor Masahiko FUJIKUBO is responsible during all phases from the beginning until the end of my study, and his understanding played an important role in the successful completion of my research. I also want to thank to Associate Professor Kazuhiro IJIMA for meaningful advices in my research during the past four years. I am grateful to all my committee members, Professor Hidekazu MURAKAWA and Professor Naoki OSAWA for serving and valuable guidance in my committee, their suggestions and comments were very helpful in my research.

I should thank to the Japan Bank International Cooperation (JBIC) Loan-IP 541 under Development Project of Engineering Faculty Hasanuddin University for giving the scholarship during completion of my study in Osaka University. I also extent my thanks to Professor Masahiko FUJIKUBO of additional support for living allowance. Thanks is also given to Monitoring Team of Hasanuddin University and the Consultant of Japan International Cooperation Center (JICE) during evaluation process regarding our study progress.

Finally, I would like to thanks a lot to my family in Makassar, who always pray for me, give me support, motivation and spirit during my study in Japan.

## List of figures

Figure 1.1	Ship accidents	1
Figure 2.1	Cross section with damage	14
Figure 2.2	Average stress-average strain relationship of a structural element	14
Figure 2.3	Instantaneous neutral axes for the analysis of incremental relationship of bending moment and curvature	16
Figure 2.4	Loci of Biaxial Bending Moment	22
Figure 2.5	Single Hull Bulk Carrier (Ship B1)	25
Figure 2.6	Single Hull Bulk Carrier (Ship B4)	26
Figure 2.7	Double Hull Oil Tanker (Ship T4)	26
Figure 2.8	Vertical bending moment-vertical curvature relationship (Ship B1, 70% damage)	27
Figure 2.9	Vertical bending moment-vertical curvature relationship (Ship B4, 70% damage)	27
Figure 2.10	Vertical bending moment-vertical curvature relationship (Ship T4, 70% damage)	28
Figure 2.11	Stress distribution and neutral axis (Ship B1, 70% damage, CASE 1)	29
Figure 2.12	Stress distribution and neutral axis (Ship B4, 70% damage, CASE 1)	29
Figure 2.13	Stress distribution and neutral axis (Ship T4, 70% damage, CASE 1)	30
Figure 2.14	Stress distribution and neutral axis (Ship B1, 70% damage, CASE 2)	31
Figure 2.15	Stress distribution and neutral axis (Ship B4, 70% damage, CASE 2)	31
Figure 2.16	Stress distribution and neutral axis (Ship T4, 70% damage, CASE 2)	32
Figure 2.17	Effect of damage extent on the residual hull girder strength	33
Figure 2.18	Vertical and horizontal bending moment interaction diagram curve	35
Figure 3.1	Coordinate system of a thin walled beam	39

Figure 3.2	Beam element $ij$	41
Figure 3.3	Element division on the cross section	44
Figure 3.4	Beam-HULLST Model for Analysis	45
Figure 3.5	Boundary Condition	45
Figure 3.6	Moment-Curvature relationship for intact of Ship B1, B4 and T4	46
Figure 3.7	Bending moment-average curvature relationship of a panama-size bulk carrier obtained by Beam-HULLST using the one frame-space model and the five frame-space model	47
Figure 3.8	Three-hold model of Panamax-size bulk carrier	48
Figure 4.1	Neutral axes of the elastic hull girder cross section with a symmetric damage	52
Figure 4.2	Locations of the critical deck element	54
Figure 4.3	Comparison of residual hull girder strength $M_V$ between the simplified Method and progressive collapse analysis	56
Figure 4.6	Comparison of reduction ratio of residual hull girder strength due to The rotation of the neutral axis between simplified method and Progressive collapse analysis (CASE 1/CASE 2)	56
Figure 5.1	Three-cargo-hold of single hull bulk carrier of Panamax model	60
Figure 5.2	Cross section of three-cargo-hold model	60
Figure 5.3	Rigid body object and boundary condition (Case 1)	61
Figure 5.4	Boundary condition (Case 2)	62
Figure 5.5	Illustration of the collision on the three-hold model	62
Figure 5.6	Time history of applied rotational velocity (3 hold model)	63
Figure 5.6	Moment-time and moment-curvature relationship (intact-hogging)	64
Figure 5.7	Deformation and stress distribution at point B (intact-hogging)	65
Figure 5.8	Deformation and stress distribution at point C (intact-hogging)	66
Figure 5.9	Moment-time and moment-curvature relationship (intact-sagging)	67

Figure 5.10	Deformation and stress distribution at point E (intact-sagging)	68
Figure 5.11	Deformation and stress distribution at point F (intact-sagging)	69
Figure 5.12	Moment-time and moment-curvature relationship (20% damage-hogging)	70
Figure 5.13	Moment-time and moment-curvature relationship (20% damage-sagging)	70
Figure 5.14	Stress distribution at ultimate strength (20% damage-hogging)	72
Figure 5.15	Stress distribution at ultimate strength (20% damage-sagging)	73
Figure 5.16	Moment-time and moment-curvature relationship (70% damage-hogging)	74
Figure 5.17	Moment-time and moment-curvature relationship (70% damage-sagging)	74
Figure 5.18	Stress distribution at ultimate strength (70% damage-hogging)	75
Figure 5.19	Stress distribution at ultimate strength (70% damage-sagging)	76
Figure 5.20	Moment-curvature relationship of three-hold model for intact	78
Figure 5.21	Moment-curvature relationship of one-frame space for intact	78
Figure 5.22	Moment-curvature relationship of three-hold model for 20% damage	80
Figure 5.23	Moment-curvature relationship of one-frame space for 20% damage	80
Figure 5.24	Moment-curvature relationship of three-hold model for 70% damage	81
Figure 5.25	Moment-curvature relationship of one-frame space for 70% damage	81
Figure 5.26	Moment-curvature relationship of three-hold model (70% damage)	82

## Table of contents

Acknowledgements	i
List of figures	ii
Table of contents	v
Chapter 1. Introduction	1
1.1. Background	1
1.2. Objective of the Present Study	6
1.3. Organization of the Dissertation	7
Chapter 2. Method of Progressive Collapse Analysis	11
2.1. Introduction	11
2.2. Cross-Sectional Force and Deformation Relationship	12
2.3. Incremental Relationship of Biaxial Bending Moment and Curvature	13
2.4. Solution Procedures	20
2.5. Example Calculation and Discussion	24
2.6. Conclusion	35
Chapter 3. Progressive Collapse Analysis Using Beam Finite Element	37
3.1. Introduction	37
3.2. Fundamental of Thin-Walled Beam	38
3.3. Method of Analysis	43
3.4. Case Studies	46
3.5. Conclusion	49
Chapter 4. Simple Formula of Residual Hull Girder Strength under Sagging Condition	50
4.1. Introduction	50

4.2.	Basic Assumption	51
4.3.	Estimation of the Residual Hull Girder Strength and Neutral Axis Effect	51
4.4.	Result and Discussion	54
4.5.	Conclusion	57
Chapter 5.	Finite Element Analysis	58
5.1.	Introduction	58
5.2.	Structural Modeling	59
5.3.	Analysis Cases	60
5.4.	Intact Condition	63
5.5.	Damage Condition	70
	5.4.1. 20% Damage	70
	5.4.2. 70% Damage	74
5.6.	Comparison of FE Analysis and Smith's Method	77
5.7.	Conclusion	84
Chapter 6.	Concluding Remarks	85
6.1.	Conclusion	85
6.2.	Future Work	87
References		88

## Chapter 1

### Introduction

#### 1.1 Background

One of the most important aspects of ship structural design is the ability to predict accurately the ultimate strength of ship's hull girder when subjected to longitudinal bending. A ship's hull may suffer collision or grounding damages, which may threaten safety of ships and surrounding environment as shown in Fig 1.1. In order to enhance the structural safety of ships and reduce the risks, the International Maritime Organization (IMO, 2009) has required in Goal Based Standard for New Ship Construction (GBS) to consider the residual strength of the hull girder in specified damage conditions as one of the functional requirements for the structural rules for bulk carriers and tankers. Also, the ISSC (2006, 2009) discusses the issue of ship collision and grounding which is related to ship structure.



(a) Grounding



(b) Collision

Fig. 1.1 Ship accidents

Many studies have been performed on the estimate of the accidental loads and damages and the assessment of the residual hull girder strength after damages. Pedersen (1994) presented a mathematical modeling to estimate the contact pressure between the

grounded ship and the sea bottom. The grounded contact force was compared to the force which would crush the forward bottom of the ship. The sectional bending moment due to grounding was determined and compared to the ultimate hull girder strengths. The model experiments and full-scale controlled grounding experiments were also performed to validate the mathematical model.

Paik et al (1998) developed a rapid procedure to identify the possibility of hull girder failure after collision and grounding damages based on the closed-form formulae of the ultimate hull girder strength and section modulus after the damages. Wang et al. (2000) proposed a similar approach based on the section modulus. The predicted residual strength was compared with the results by Idealized Structural Unit Method (Paik et al, 1996). Soares et al (2008) evaluated the ability of simplified structural analysis methods based on the Smith's formulation to predict the ultimate strength of damage ship's hull. Toh et al (2012) developed simplified calculation program to calculate the ultimate strength in intact and damage condition and the reduction of hull girder ultimate strength is investigated. The calculation result of simplified method is compared to the FE result for both intact and damage condition.

Ohtsubo et al (1994) showed the experimental and numerical work on the ship structural damages due to collision and grounding. This was one of the first attempts to apply the explicit Finite Element Method codes, such as LS-DYNA and DYTRAN, to the collision and grounding problems of ships. Ozguc et al (2005) investigated the collision resistance and residual strength of single skin and double skin bulk carriers subjected to damages. Lee et al (2008) calculate the ultimate strength with collision damage using LS-DYNA and compared with the experiment results. It is found that the ultimate strength is reduced as a damage size increased as expected. Notaro et al. (2010)

carried out full nonlinear FE assessments of hull girder capacity in intact and damage conditions. The effects of several influences factors such as model extend and complexity, damage representations and model imperfections are investigated on the different vessels. It was found that the effect of damage extent in vertical direction is more critical than in longitudinal direction, and the damage varies the location of the neutral axes including higher stresses in proximity of the damage areas. The various probability levels are considered for the damage extent estimation.

As introduced above, the approaches to predict the residual longitudinal strength of a ship hull girder can be basically categorized as follows:

- (1) Closed-form equation with assumed stress distribution at collapse
- (2) Section modulus approach based the critical member strength
- (3) Smith's method
- (4) Finite element method

Method (1) is a very simple but its accuracy depends on the assumption of stress distribution. Progressive collapse behavior accompanied by the post-ultimate capacity of buckled members cannot be correctly reflected in the estimate. (Caldwell, Paik-Mansour).

Method (2) has been employed in ship classification rules, as typically found in the Single Step Ultimate Capacity Method in IACS/CSR-T (2006). This method is also useful for design but applicable only for the collapse under sagging condition, in which the collapse of deck stiffened panel immediately leads to a hull girder collapse.

Method (3), the Smith method, subdivides a hull girder cross section into the longitudinal elements composed of a stiffener and attached plating, which are assumed to act independently. Assuming that the cross section remains plane and considering the nonlinear load-end shortening behaviors of the elements, the bending moment-curvature

relationship of the cross section is obtained. The translation of neutral axis of the cross section due to the progressive failure of structural elements is considered. The ultimate hull girder bending capacity is defined as the peak value of the bending moment-curvature relationship of the cross section. This method has been widely applied to the progressive bending collapse analysis of a hull-girder cross section (Yao and Nikolov, 1992). It is also adopted in IACS/CSR-T for oil tankers and IACS/CSR-B for bulk carriers as a name of Simplified Method Based on an Incremental-iterative Approach (IACS, 2012).

Method (4), FEM, is a most versatile and generalized approach to know the nonlinear collapse behavior of ships structures. Because of the recent advances in computational capabilities, many applications of the nonlinear Finite Element Analysis have been made for the estimate of damages and the residual strength after the damages, particularly for the purpose of validation of the simplified approaches as mentioned above. As design and assessment tools, however, more simplified methods are still needed.

Amongst the four approaches, Smith's method is the most practical and rational approach for the ultimate strength analysis of a ship hull girder in longitudinal bending. The IACS Harmonized Common Structural Rules for bulk carriers and tankers employs this method for the estimate of the residual hull girder strength, which is one of the functional requirements specified in the IMO/GBS. This study put its focus on the application of the Smith's method to the residual strength assessment of the damaged ships.

When a hull-girder cross section is symmetric with respect to the centerline and subjected to pure vertical bending moment, the neutral axis for vertical bending is always

horizontal and moves only vertically during the progressive collapse behavior. However, when the cross section is asymmetrically damaged due, for example, to a collision, the neutral axis rotates. Both rotation and translation need to be taken into account during the progressive collapse behavior even when only a vertical bending moment is applied, and the problem needs to be treated as a biaxial bending one. Previous studies using the Smith's method on the ultimate strength of hull girders under biaxial thrust (Ozguç and Barltrop, 2008) and the residual strength of damaged hulls (Fang and Das, 2004; Hussein and Guedes Soares, 2009; Choung et al, 2011) consider the rotation and translation of neutral axis in a reasonable way. However, they employ a trial and error approach to detect the position of neutral axis. More easy approach to detect the position of neutral axis is demanded.

In the draft IACS/CSR-H, the residual strength of ship hull girder with collision damage is calculated neglecting the effect of rotation of the neutral axis first and then it is reduced by 10% as the effect of the rotation of the neutral axis. This 10 % reduction is not reasonable, since the reduction ratio depends on the location and extent of the damage in the cross section. More rational reduction rate should be employed in the classification rules.

The effect of the rotation of the neutral axis on the residual hull girder strength depends not only on the damage extent in the cross section but also on the longitudinal extent of the damage. This is because the deformation due to the rotation of the neutral axis at the damaged part is constrained by the adjacent intact part of the hull girder. In order to take such a constraining effect of the intact part into account, the hull girder model including both intact and damaged parts needs to be solved. One possible strategy is to combine the Smith's method (nonlinear moment-curvature relationship) and the ordinary beam finite

element. By connecting the beam elements having intact and damaged cross sections, the constraining effects mentioned above may be considered. This nonlinear beam finite element model is effective for any collapse simulation of a damaged ship hull girder predominantly in bending.

## **1.2 Objective of the Present Study**

Based on the background and motivations in the foregoing section, the primary objective of the present study is to develop a rational and simplified method to estimate the residual hull girder strength of asymmetrically damaged ships considering the effect of rotation of the neutral axis.

Two types of the progressive collapse analysis methods of a hull girder based on the Smith's method are developed. One is the extension of the HULLST developed by Yao and Nikolov (1992) to the hull girder cross section with damages. The other is the combination of the HULLST and the beam finite element model to facilitate the residual strength analysis of a multi-frame space model, including a hold model or a whole ship. In the former method, the incremental formulation of the biaxial bending-moment curvature relationship is presented with an explicit expression of the neutral axis that shifts and rotates. The latter method allows the consideration of the constraining effect offered by the intact part on the damaged part and also the effect of the localization of the plastic deformation at the damaged part on the whole hull girder behavior. Using the proposed methods, the reduction rate of the residual strength of asymmetrically damaged ships due to the rotation of the neutral axis is examined and compared with the value specified in the draft CSR-H.

Concerning the residual strength under the sagging condition, another simplified method using the section modulus considering the rotation of the neutral axis due to damages is proposed as an alternative to the Single Step Ultimate Capacity Method in IACS/CSR-T. Finally, a series of nonlinear Finite Element Analysis is performed for the purpose of validation of the proposed simplified method and also for investigating the effect of the damage more accurately.

### **1.3 Organization of the Dissertation**

The dissertation consists of six chapters. In Chapter 1 explain about the background and the objective of the present study is briefly described.

In chapter 2, the study focuses on the incremental formulation of the progressive bending collapse behavior of ship's hull girder with damages is presented based on the Smith's method. The biaxial bending moment-curvature relationship is expressed in terms of the tangential modulus following the original formulation by Smith (1977). The explicit expressions of the position of the neutral axis for cumulative values of the stress and that for strain increments are given. Solution procedures for several loading patterns including the post ultimate strength behavior under the prescribed biaxial moment loading are presented. The proposed formulation is applied to the residual strength analysis of bulk carriers and tanker having collision damages at the side structures. Particular focuses are placed on the influence of the rotation of neutral axis on the residual hull girder strength and solution procedures to obtain the residual strength including the case of biaxial bending. The progressive collapse analysis of hull girder with collision damages is performed using the Smith's method considering the biaxial

bending behavior. The program code HULLST, developed by Yao and Nikolov (1992), is used with some modifications in the formulation and solution procedures. The solution procedure consists of four cases.

CASE 1 is Hull girder under pure vertical bending moment, the vertical curvature is increased under the condition of horizontal bending moment is constraint. In this case, the rotation of neutral axis is considered by allowing the horizontal curvature.

CASE 2 is Hull girder under vertical bending moment with vertical curvature is increased under the condition of horizontal curvature is constrained. This case shows that the rotation of neutral axis is not taken into account.

CASE 3 is Hull girder under prescribed biaxial curvatures. The residual strength can be found by tracing vertical and horizontal bending moment curves, and

CASE 4 is Hull girder under proportional biaxial moments. Biaxial bending moments are applied to the cross section with a constant ratio of vertical and horizontal bending moment. One of the curvatures, horizontal or vertical curvature is chosen as a controlling parameter.

In Chapter 3 also deals with progressive collapse analysis of ship hull girder with and without collision damage. The program called Beam-HULLST is employed to investigate collapse behavior due to asymmetric damage position under longitudinal bending moment. Basically this program is advanced of beam theory corresponds to Smith's method performed in HULLST with some modifications in the formulations and procedures. The stress-strain formulation in HULLST is introduced into Beam-HULLST.

The simplified approach to estimate the residual hull girder strength of asymmetrically damaged ships is introduced in Chapter 4. Further the advance material from the Chapter 2, and it also discusses the influence of the rotation of the neutral axis

on the residual hull girder strength of asymmetrically damaged ships under longitudinal bending. Progressive collapse analysis of the damaged cross section is performed applying the Smith's method for the biaxial bending problem. An explicit expression of the location of the neutral axis including its rotation is given as a function of biaxial curvatures. The procedures of the progressive collapse analysis of the cross section under biaxial bending are presented for several loading and constraint conditions. A series of progressive collapse of bulk carriers and double hull tanker having collision damages at the side structures is performed. The case study is focused on the sagging condition by implementing simple formulae to estimate the residual strength and the reduction rate due to rotation of the neutral axis are proposed using the elastic cross sectional properties and critical member strength. The effectiveness of the formulae is examined through a comparison with the progressive collapse analysis.

Chapter 5 is validation of the collapse behavior of ship's hull obtained by HULLST and Beam-HULLST with FEM analysis. A single hull bulk carrier with Panamax type is observed as an object of the ship. Fully cross section of the single hull bulk carrier is taken to represent the real ship condition. The model is simply supported at the fore and aft cross section which is assumed to be rigid. The longitudinal bending moments are applied at the both ends of the model. The damage extend is assumed to be placed at one side shell of the structure closed to the deck part. The side shell damage is created simply by a rectangular opening, neglecting any welding residual stress and no crack extension is considered. To achieve a better balance of efficiency and accuracy, the FEM analysis is divided into three phases. In the phase one, the relatively fast rotational velocity of loading is given both ends of the model within the elastic range. Then, in phase two, the rotational velocity is stopped, giving the global damping coefficient in

order to eliminate the vibration. In the phase three, to minimize the dynamic effect, the relatively slow rotational velocity is imposed to the model until the ultimate strength is attained. The analysis condition is determined by the trial and error approach.

In Chapter 6, the concluding remarks are given together with future improvements of the proposed method to be done.

## **Chapter 2**

### **Method of Progressive Collapse Analysis**

#### **2.1 Introduction**

The ultimate longitudinal bending strength is the most fundamental strength to ensure the safety of ships not only in the intact but also in the damage condition. In conjunction with this, when a hull girder cross section is symmetric with respect to the centerline and subjected to pure vertical bending moment, the neutral axis is always horizontal and moves only vertically during the progressive collapse behavior. On the other hand, when the cross section is damaged at asymmetric positions, the neutral axis rotates. Both rotation and translation need to be taken into account and the problem needs to be treated as a biaxial bending problem.

In this chapter, an incremental formulation of the progressive bending collapse behavior of ship hull girder with damages is presented based on the Smith's method. The biaxial bending moment-curvature relationship is expressed in term of the tangential moduli following the original formulation by Smith (1977). The explicit expressions of the position of neutral axis for cumulative values of stress and that for stress increment are given. Solution procedures for several loading patterns including the post ultimate strength behavior under prescribed biaxial moment loading are presented. The proposed formulation is applied to the residual strength analysis of bulk carriers and a tanker having collision damages at the side structures.

## 2.2 Cross-Sectional Force and Deformation Relationship

As a general case, damage due to collision or grounding is assumed to be formed at an asymmetric position of a hull girder cross section as shown in Fig.2.1. The  $y$  and  $z$  coordinates with the origin at the bottom keel are defined as shown in Fig.2.1. Assuming that the cross section remains plane, the axial strain  $\varepsilon_i(y_i, z_i)$  at the  $i$ -th structural element caused by the horizontal curvature  $\phi_H$  and  $\phi_V$  can be expressed as

$$\varepsilon_i(y_i, z_i) = \varepsilon_0 + y_i \phi_H + z_i \phi_V \quad (2.1)$$

Where  $\varepsilon_0$  is the axial strain at the origin O. The axial stress  $\sigma_i$  corresponding to the axial strain  $\varepsilon_i$  is given by the average stress-average strain relationship calculated in advance for the individual elements as illustrated in Fig.2.2. The average stress-average strain relationship with consideration of buckling and yielding is generally a nonlinear function of strain and here expressed as

$$\sigma = f_i(\varepsilon) \quad (2.2)$$

where  $f_i(0) = 0$

The axial force  $P$ , the vertical bending moment  $M_V$ , and the horizontal bending moment  $M_H$  can be obtained by integrating axial stresses over the intact part of the cross section as

$$P = \sum_{i=1}^N \sigma_i A_i \equiv 0 \quad (2.3)$$

$$M_H = \sum_{i=1}^N \sigma_i y_i A_i \quad (2.4)$$

$$M_V = \sum_{i=1}^N \sigma_i z_i A_i \quad (2.5)$$

Where  $N$  is the number of intact elements and  $A_i$  is a cross section of the  $i$ -th element.

An essential condition for the progressive collapse analysis of the hull girder under longitudinal bending is to satisfy the zero-axial force condition of Eq. (2.3). Substituting Eq. (2.1) and (2.2) into Eq. (2.3)~(2.5), a set of nonlinear simultaneous equations with respect to axial strain  $\varepsilon_0$  and curvatures  $\phi_H$  and  $\phi_V$  is obtained. By solving these equations, the relationship between cross-sectional forces and deformations can be obtained. The location of neutral axis in the  $y$ - $z$  plane is given by the following equation of a straight line:

$$\varepsilon_0 + y_i \phi_H + z_i \phi_V = 0 \quad (2.6)$$

### 2.3 Incremental Relationship of Biaxial Bending Moment and Curvature

To solve the nonlinear Eq. (2.3)~(2.5), an incremental approach is employed. Denoting the tangential stiffness obtained as a slope of the average stress-average strain relationship of the  $i$ -th element by  $D_i$  (Fig.2.2), the incremental relationship of axial stress and strain can be expressed as

$$\Delta\sigma = D_i \Delta\varepsilon \left( D_i = \frac{df_i}{d\varepsilon} \right) \quad (2.7)$$

Using Eq. (2.1) and (2.7), the incremental form of Eq. (2.3)~(2.5) can be given by

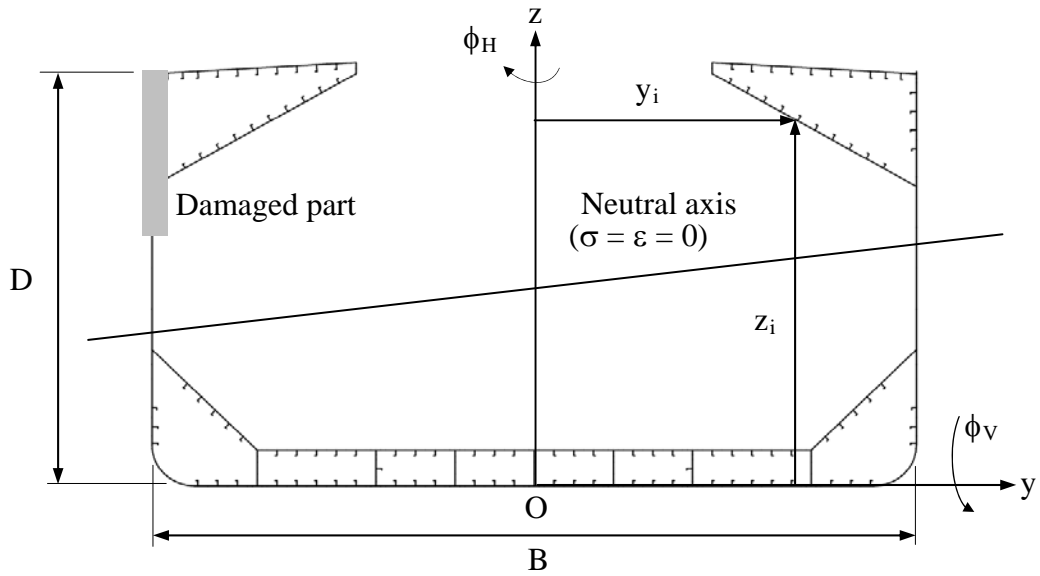


Fig. 2.1 Cross section with damage

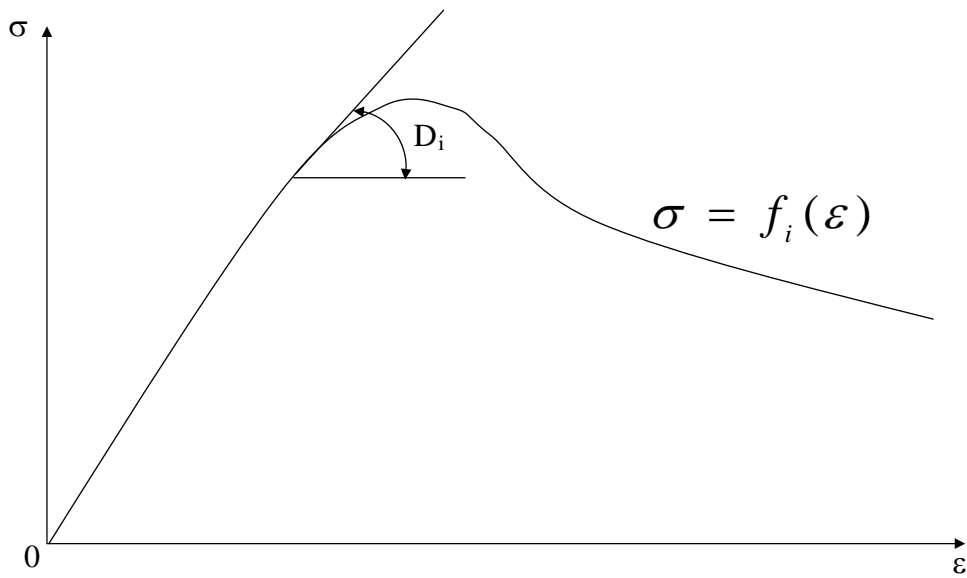


Fig. 2.2 Average stress-average strain relationship of a structural element

$$\begin{Bmatrix} \Delta P = 0 \\ \Delta M_H \\ \Delta M_V \end{Bmatrix} = \begin{bmatrix} \bar{D}_{AA} & \bar{D}_{AH} & \bar{D}_{AV} \\ \bar{D}_{HA} & \bar{D}_{HH} & \bar{D}_{HV} \\ \bar{D}_{VA} & \bar{D}_{VH} & \bar{D}_{VV} \end{bmatrix} \begin{Bmatrix} \Delta \varepsilon_0 \\ \Delta \phi_H \\ \Delta \phi_V \end{Bmatrix} \quad (2.8)$$

Where

$$\begin{aligned}
 \bar{D}_{AA} &= \sum_{i=1}^N D_i A_i, & \bar{D}_{AH} &= \bar{D}_{HA} = \sum_{i=1}^N D_i y_i A_i \\
 \bar{D}_{HH} &= \sum_{i=1}^N D_i y_i^2 A_i, & \bar{D}_{AV} &= \bar{D}_{VA} = \sum_{i=1}^N D_i z_i A_i \\
 \bar{D}_{VV} &= \sum_{i=1}^N D_i z_i^2 A_i, & \bar{D}_{HV} &= \bar{D}_{VH} = \sum_{i=1}^N D_i y_i z_i A_i
 \end{aligned} \tag{2.9}$$

The results of the  $n+1$ -th load step are given by adding the increments obtained by Eq. (2.8) to the result of the  $n$ -th load step as

$$\begin{aligned}
 P^{n+1} &= P^n + \Delta P = 0, & \varepsilon_0^{n+1} &= \varepsilon_0^n + \Delta \varepsilon_0 \\
 M_H^{n+1} &= M_H^n + \Delta M_H, & \phi_H^{n+1} &= \phi_H^n + \Delta \phi_H \\
 M_V^{n+1} &= M_V^n + \Delta M_V, & \phi_V^{n+1} &= \phi_V^n + \Delta \phi_V
 \end{aligned} \tag{2.10}$$

The stiffness Eq. (2.8) can be simplified by the formulation with respect to the variables defined for the instantaneous neutral axes as described in the following. The expression of the axial force increment  $\Delta P$  of Eq. (2.8) can be rearranged in the form:

$$\begin{aligned}
 \Delta P &= \bar{D}_{AA} \Delta \varepsilon_0 + \bar{D}_{AH} \Delta \phi_H + \bar{D}_{AV} \Delta \phi_V \\
 &= \sum_{i=1}^N D_i (\Delta \varepsilon_0 + y_i \Delta \phi_H + z_i \Delta \phi_V) A_i \\
 &= \sum_{i=1}^N D_i \{ \Delta \varepsilon_G + (y_i - y_G) \Delta \phi_H + (z_i - z_G) \Delta \phi_V \} A_i
 \end{aligned} \tag{2.11}$$

Where

$$\Delta \varepsilon_G = \Delta \varepsilon_0 + y_G \Delta \phi_H + z_G \Delta \phi_V \tag{2.12}$$

$y_G$  and  $z_G$  are the coordinates of the point G in Fig.2.3 and  $\Delta \varepsilon_G$  is the axial strain increment at the point G caused by  $\Delta \varepsilon_0$ ,  $\Delta \phi_H$  and  $\Delta \phi_V$ . When  $y_G$  and  $z_G$  are given by

$$y_G = \frac{\left( \sum_{i=1}^N y_i D_i A_i \right)}{\left( \sum_{i=1}^N D_i A_i \right)} \quad (2.13)$$

$$z_G = \frac{\left( \sum_{i=1}^N z_i D_i A_i \right)}{\left( \sum_{i=1}^N D_i A_i \right)} \quad (2.14)$$

Eq. (2.11) can be simply expressed as

$$\Delta P = \left( \sum_{i=1}^N D_i A_i \right) \Delta \varepsilon_G \quad (2.15)$$

Eq. (2.15) means that under pure longitudinal bending, i.e. when  $\Delta P = 0$ , no axial strain is produced at the point G for any combination of horizontal and vertical curvature increments. The coordinates  $(y_G, z_G)$  therefore give the centre position of instantaneous neutral axes for stress increments as shown in Fig.2.3.

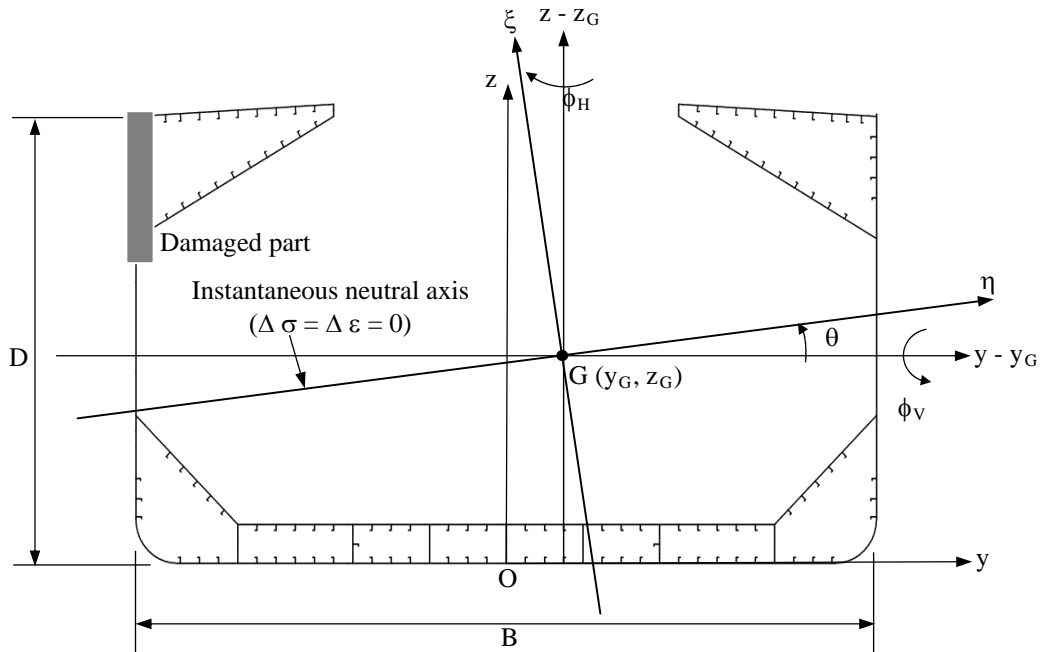


Fig. 2.3 Instantaneous neutral axes for the analysis of incremental relationship of bending moment and curvature

By replacing  $y_i$  and  $z_i$  in Eq. (2.9) by  $(y_i - y_G) + y_G$  and  $(z_i - z_G) + z_G$ , respectively, and using  $\Delta\varepsilon_G$  of Eq. (2.12), (2.8) and (2.9) can be given in the form

$$\begin{Bmatrix} \Delta P = 0 \\ \Delta M_H \\ \Delta M_V \end{Bmatrix} = \begin{bmatrix} D_{AA} & 0 & 0 \\ 0 & D_{HH} & D_{HV} \\ 0 & D_{VH} & D_{VV} \end{bmatrix} \begin{Bmatrix} \Delta\varepsilon_G \\ \Delta\phi_H \\ \Delta\phi_V \end{Bmatrix} \quad (2.16)$$

Where

$$\begin{aligned} D_{AA} &= \sum_{i=1}^N D_i A_i, & D_{HV} &= D_{VH} = \sum_{i=1}^N D_i (y_i - y_G)(z_i - z_G) A_i \\ D_{HH} &= \sum_{i=1}^N D_i (y_i - y_G)^2 A_i, & D_{VV} &= \sum_{i=1}^N D_i (z_i - z_G)^2 A_i \end{aligned} \quad (2.17)$$

Using the coefficients of Eq. (2.17), the incremental relationship of the biaxial bending moments and curvatures can be given by

$$\begin{Bmatrix} \Delta M_H \\ \Delta M_V \end{Bmatrix} = \begin{bmatrix} D_{HH} & D_{HV} \\ D_{VH} & D_{VV} \end{bmatrix} \begin{Bmatrix} \Delta\phi_H \\ \Delta\phi_V \end{Bmatrix}, \quad (2.18)$$

irrespective of the shape of cross section, distribution of tangential stiffness  $D_i$ , the location and damage extent.

The rotation of the instantaneous neutral axes, i.e. principle axes for increment of curvature and bending stress, can be obtained in the following way. The  $\eta - \zeta$  coordinate with the origin at point G is defined as shown in Fig.2.3. The axial strain increment at point  $i$  expressed by the curvature increments  $\Delta\phi_\eta$  and  $\Delta\phi_\zeta$  in  $\eta$  and  $\zeta$  directions, respectively, is given by

$$\Delta\varepsilon_i(\eta_i - \zeta_i) = \zeta_i \Delta\phi_\eta + \eta_i \Delta\phi_\zeta \quad (2.19)$$

The bending moment increments about  $\eta$  and  $\zeta$  axes are

$$\begin{aligned}\Delta M_\eta &= \sum_{i=1}^N \zeta_i \Delta \sigma_i A_i = \left( \sum_{i=1}^N D_i \zeta_i^2 A_i \right) \Delta \phi_\eta + \left( \sum_{i=1}^N D_i \zeta_i \eta_i A_i \right) \Delta \phi_\zeta \\ \Delta M_\zeta &= \sum_{i=1}^N \eta_i \Delta \sigma_i A_i = \left( \sum_{i=1}^N D_i \zeta_i \eta_i A_i \right) \Delta \phi_\eta + \left( \sum_{i=1}^N D_i \eta_i^2 A_i \right) \Delta \phi_\zeta\end{aligned}\quad (2.20)$$

When  $\eta$  and  $\zeta$  are the principle axes with respect to the bending moment and curvature increments, the coupled term in Eq. (2.20) must be zero, i.e.

$$\sum_{i=1}^N D_i \zeta_i \eta_i A_i = 0 \quad (2.21)$$

Substituting the following relationship of the coordinate transformation

$$\begin{aligned}\eta &= (y - y_G) \cos \theta + (z - z_G) \sin \theta \\ \zeta &= (z - z_G) \cos \theta + (y - y_G) \sin \theta\end{aligned}\quad (2.22)$$

to Eq. (2.21), the rotation angle  $\theta$  is obtained as follows:

$$\theta = \frac{1}{2} \tan^{-1} \frac{2D_{HV}}{D_{HH} - D_{VV}} \quad (2.23)$$

For this direction of instantaneous neutral axes, the incremental relationship of the biaxial bending moments and curvatures can be further simplified as

$$\begin{Bmatrix} \Delta M_\eta \\ \Delta M_\zeta \end{Bmatrix} = \begin{bmatrix} D_{\eta\eta} & 0 \\ 0 & D_{\zeta\zeta} \end{bmatrix} \begin{Bmatrix} \Delta \phi_\eta \\ \Delta \phi_\zeta \end{Bmatrix} \quad (2.24)$$

Where

$$D_{\eta\eta} = \sum_{i=1}^N D_i \zeta_i^2 A_i, \quad D_{\zeta\zeta} = \sum_{i=1}^N D_i \eta_i^2 A_i \quad (2.25)$$

It should be noted that  $y_G, z_G$  and  $\theta$  vary at each incremental step depending on the spread of buckling and yielding. The relationship between bending moment and curvature increments may be calculated either by Eq. (2.8), (2.18) or (2.24). The Eq. (2.24) is the most simplified expression, but to deal with the bending moment and

curvatures about the vertical axes, Eq. (2.18) is the most convenient. In the present work, Eq. (2.18) is used hereafter.

Smith (1977) employed the pure vertical approach without iteration in each load step, taking the sufficiently small increment of curvature. When an incremental-iterative approach is applied to obtain the convergence of solutions in each load step until the acceptable level of accuracy is achieved, the increment of curvatures are expressed as the sum of sub-increments within the load step as

$$\begin{Bmatrix} \Delta\phi_H \\ \Delta\phi_V \end{Bmatrix} = \sum_{r=1}^m \begin{Bmatrix} \Delta\phi_H^{(r)} \\ \Delta\phi_V^{(r)} \end{Bmatrix} \quad (2.26)$$

The sub-increments  $\Delta\phi_H^{(r)}$  and  $\Delta\phi_V^{(r)}$  at the 1st iteration step ( $r=1$ ) are given by equation 18. For subsequent iteration steps, they are obtained by the equation

$$\begin{Bmatrix} \Delta M_H^e - \Delta M_H^i \\ \Delta M_V^e - \Delta M_V^i \end{Bmatrix} = \begin{bmatrix} D_{HH}^{(r)} & D_{HV}^{(r)} \\ D_{VH}^{(r)} & D_{VV}^{(r)} \end{bmatrix} \begin{Bmatrix} \Delta\phi_H^{(r)} \\ \Delta\phi_V^{(r)} \end{Bmatrix} \quad (2.27)$$

Where the left end side is the unbalanced moment between externally applied moment to the cross section and the internal moment is calculated from the biaxial stress.

It is generally recommended to use the pure incremental approach with sufficiently small increment rather than the incremental-iterative approach, since in the progressive collapse behavior unloading may take place in the collapse element due to the shift and rotation of neutral axes. When unloading occurs, Eq. (2.2) must be changed to that for unloading behavior. The present work uses pure incremental approach without Eq. (2.26) and (2.27). Once the curvature increments  $\Delta\phi_H$  and  $\Delta\phi_V$  at the current load step are obtained, the axial strain increment  $\Delta\varepsilon_0$  can be calculated by Eq. (2.12)

considering  $\Delta\varepsilon_G = 0$ . Substituting the cumulative values of  $\phi_H$ ,  $\phi_V$  and  $\varepsilon_0$  into Eq. (2.6), the position of neutral axis is determined.

## 2.4 Solution Procedures

The incremental form of bending moment-curvature relationship, Eq. (2.18), can be applied to the residual strength analysis of a hull girder under following loading and/or constraint conditions:

### CASE 1: Hull girder under pure vertical bending moment

The vertical bending moment is applied to the cross section with no constraint on the horizontal curvature. In this case, the horizontal curvature as well as the vertical curvature is induced under the condition of  $M_H = 0$ . The incremental equation to be solved is

$$\begin{Bmatrix} 0 \\ \Delta M_V \end{Bmatrix} = \begin{bmatrix} D_{HH} & D_{HV} \\ D_{VH} & D_{VV} \end{bmatrix} \begin{Bmatrix} \Delta\phi_H \\ \Delta\phi_V^0 \end{Bmatrix} \quad (2.28)$$

Where the superscript '0' indicates a prescribed value. The solutions are

$$\Delta\phi_H = -\frac{D_{HV}}{D_{HH}}\Delta\phi_V^0, \quad \Delta M_V = \left( D_{VV} - \frac{D_{VH}D_{HV}}{D_{HH}} \right) \Delta\phi_V^0 \quad (2.29)$$

$\Delta\phi_H$  Indicates that the horizontal curvature is induced by the vertical bending moment when the damage is at the asymmetric positions. The residual strength is calculated from the peak value of  $M_V - \phi_H$  curve.

### CASE 2: Hull girder under vertical bending moment, with horizontal curvature constraint

The vertical curvature  $\phi_V$  is increased under the condition of  $\phi_H = 0$ . Only vertical curvature is increased, and thus no rotation of the neutral axis takes place. This loading condition can be simulated by increasing the vertical curvature  $\phi_V$  under the condition of  $\phi_H = 0$ , that is,

$$\begin{Bmatrix} \Delta M_H \\ \Delta M_V \end{Bmatrix} = \begin{bmatrix} D_{HH} & D_{HV} \\ D_{VH} & D_{VV} \end{bmatrix} \begin{Bmatrix} 0 \\ \Delta \phi_V^0 \end{Bmatrix} \quad (2.30)$$

The solutions are

$$\Delta M_H = D_{HV} \Delta \phi_V^0, \quad \Delta M_V = D_{VV} \Delta \phi_V^0 \quad (2.31)$$

$\Delta M_H$  is a reaction moment to constraint the horizontal curvature. The residual strength is calculated from the peak value of  $M_V - \phi_H$  curve. Comparing Case 1 and Case 2, the influence of the rotation of the neutral axis on the residual vertical bending strength can be examined.

### CASE 3: Hull girder under prescribed biaxial curvatures

The vertical and horizontal curvatures are applied to the cross section with the prescribed ratio of  $\Delta \phi_H / \Delta \phi_V$ .

$$\begin{Bmatrix} \Delta M_H \\ \Delta M_V \end{Bmatrix} = \begin{bmatrix} D_{HH} & D_{HV} \\ D_{VH} & D_{VV} \end{bmatrix} \begin{Bmatrix} \Delta \phi_H^0 \\ \Delta \phi_V^0 \end{Bmatrix} \quad (2.32)$$

The residual strength can be found by tracing  $M_V - M_H$  curve.

Case 2 is the special case of Case 3 where  $\Delta \phi_H^0 / \Delta \phi_V^0 = 0$ . Because of the progressive collapse of structural elements and the resulting change in the stiffness parameters  $D$ , the bending moment ratio  $M_V / M_H$  changes nonlinearly even when the applied curvature ratio  $\Delta \phi_H / \Delta \phi_V$  is constant, as shown in Fig. 4. The residual strength is

obtained by detecting the  $M_V$ - $M_H$  point at the maximum distance from the origin, as shown by the hollow circle in Fig. 4.

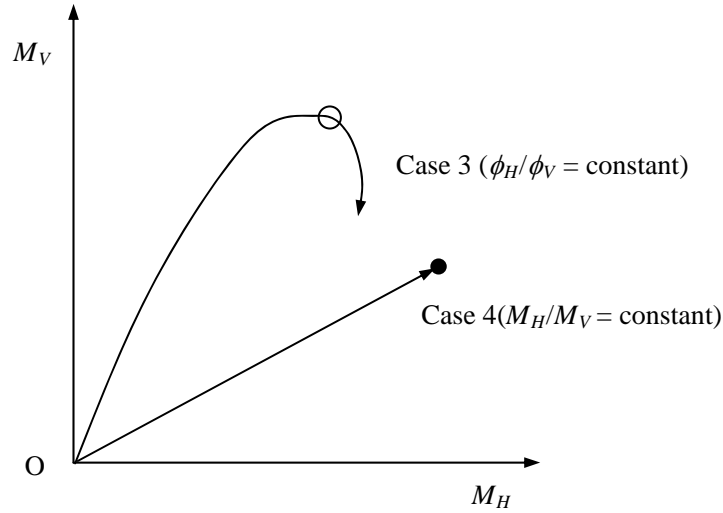


Fig. 2.4 Loci of the biaxial bending moment.

#### CASE 4: Hull girder under proportional biaxial moments

Biaxial bending moments are applied to the cross section with a constant ratio of  $M_V$  and  $M_H$ . One of the curvatures,  $\phi_H$  or  $\phi_V$ , is taken as a controlling parameter. For example, when  $\phi_V$  is employed

$$\begin{Bmatrix} \alpha \Delta M_V \\ \Delta M_V \end{Bmatrix} = \begin{bmatrix} D_{HH} & D_{HV} \\ D_{VH} & D_{VV} \end{bmatrix} \begin{Bmatrix} \Delta \phi_H \\ \Delta \phi_V^0 \end{Bmatrix} \quad \therefore \alpha = \frac{M_H}{M_V} \quad (2.33)$$

The solutions are

$$\Delta M_V = \frac{\Delta M_H}{\alpha} = \frac{D_{HH} D_{VV} - D_{HV}^2}{D_{HH} - \alpha D_{VH}} \Delta \phi_V^0$$

$$\Delta \phi_H = \frac{\alpha D_{VV} - D_{HV}}{D_{HH} - \alpha D_{VH}} \Delta \phi_V^0 \quad (2.34)$$

When the prescribed ratio of  $\Delta M_H/\Delta M_V$  is constant,  $M_V$  and  $M_H$  change linearly as shown in Fig. 4. The residual strength can be directly obtained by the peak value of  $M_V$  or  $M_H$ . The reduction of the post ultimate capacity can be also calculated. The complicated procedures of detecting the ultimate capacity, required in Case 3 or in the incremental-iterative approach using secant-moduli<sup>11)</sup>, are not needed.

The analysis procedures for all the analysis cases can be summarized as

- (1) Subdivided the cross-section into elements composed of stiffener and attached plating.
- (2) Derive the average stress-average strain relationship of individual elements, Eq. (2.2), considering the influence of buckling and yielding.
- (3) Derive the tangential axial stiffness of individual elements  $D_i$ , Eq. (2.7), from the average stress-average strain curve at the present strain.
- (4) Calculate the centre position of instantaneous neutral axis  $y_G$  and  $z_G$ , Eq. (2.13) and (2.14).
- (5) Evaluate the flexural stiffness of the cross section with respect to the instantaneous neutral axis, Eq. (2.18).
- (6) Calculate the unknown increments in individual elements from the curvature and/or bending moment under specified condition, Eq. (2.28)~(2.34).
- (7) Calculate the strain increment in individual elements from the curvature increment, and their stress increments using the slope of average stress-average strain curve.

- (8) Add the obtained increments of curvature, bending moment as well as strains and stresses in the elements to their cumulative values, Eq. (2.1) and (2.10).
- (9) Calculate the position of neutral axis for the cumulative values of stress and strain, Eq. (2.6).
- (10) Proceed to the next incremental step.

## 2.5 Example Calculation and Discussion

Progressive collapse analysis of hull girders with collision damage is performed using the Smith's method considering the biaxial bending behavior. The program code HULLST, developed by Yao and Nikolov (1992), is used with some modification in the formulation and solution procedures. Two single hull bulk carriers and one double hull oil tanker are taken as the subject ships as shown in table.2.1.

Table 2.1 Subject ships

Ship	B1	B4	T4
L (mm)	217,000	219,000	234,000
B (mm)	32,236	32,240	44,000
D (mm)	18,300	19,900	21,200
Design criteria	Pre-IACS UR	IACS CSR-B	IACS CSR-T

The damage of the upper part of side shell due to collision is assumed. The vertical damage extent is taken as 10%, 20%, 40% and 70% of the depth D for both bulk carrier and tanker. The horizontal damage extent is taken as B/16, and the same value is assumed for all damaged cases. In the Draft Harmonized Common Structural Rules for bulk carriers and tankers (IACS 2013), the specified damage extent is 70% of depth D

and B/16. Some smaller values of the damage depth are considered for the purpose of comparison. The damaged cross sections of Ships B1, B4 and T4 are respectively illustrated in Figs. 2.5, 2.6 and 2.7. The finite elements in the damaged area are completely removed assuming the complete loss of stiffness and strength. For the double hull tanker, only outer side shell is assumed to be damaged.

Vertical bending moment and vertical curvature relationship obtained for the Ships B1, B4 and T4 with 70% damage are shown in Figs. 2.8~2.10. CASE 1 considers the rotation of neutral axis and CASE 2 does not. It is found that CASE 2 generally gives larger ultimate strength than CASE 1 because the horizontal curvature is constrained. The effect is largest in Ship B1, smaller in Ship B4, and almost negligible in Ship T4. For Ship B1, CASE 1 strength is 7.3% smaller than CASE 2 in sagging and 7.8% in hogging.

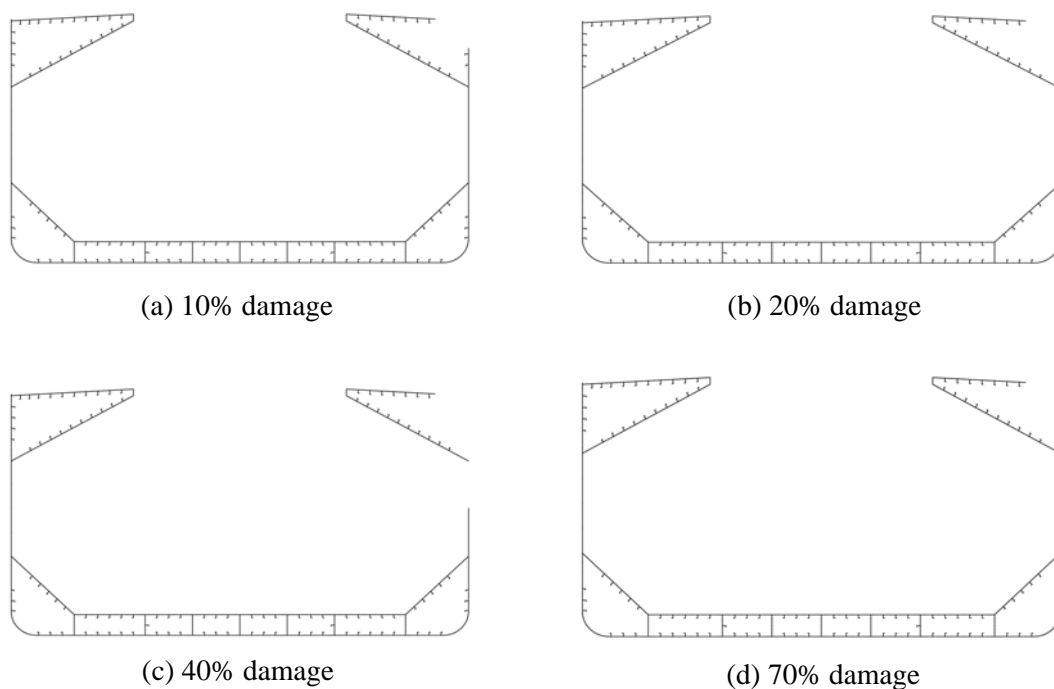


Fig. 2.5 Single Hull Bulk Carrier (Ship B1)

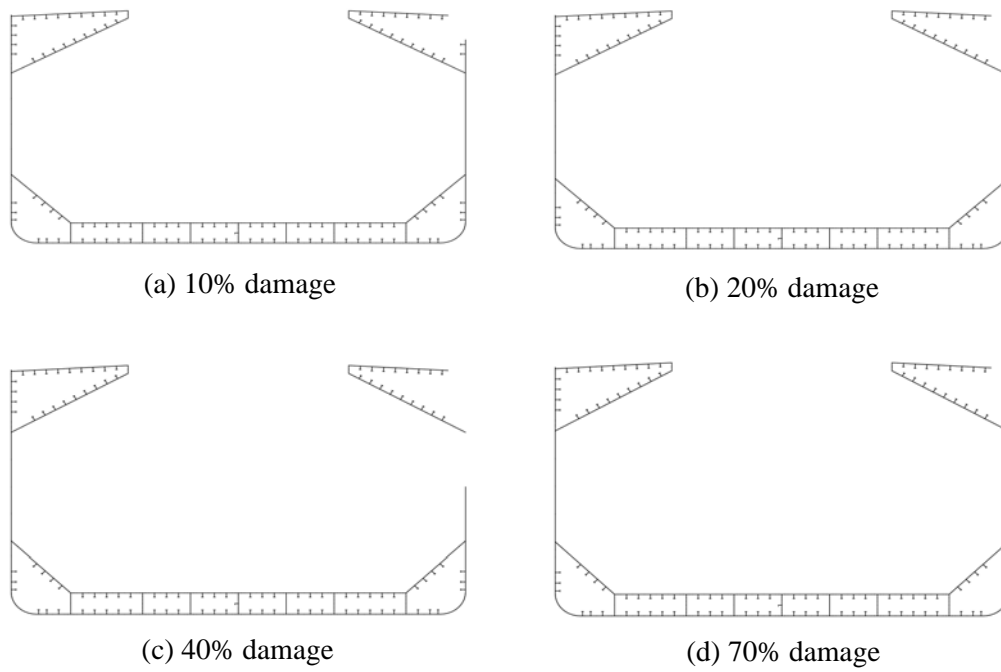


Fig. 2.6 Single Hull Bulk Carrier (Ship B4)

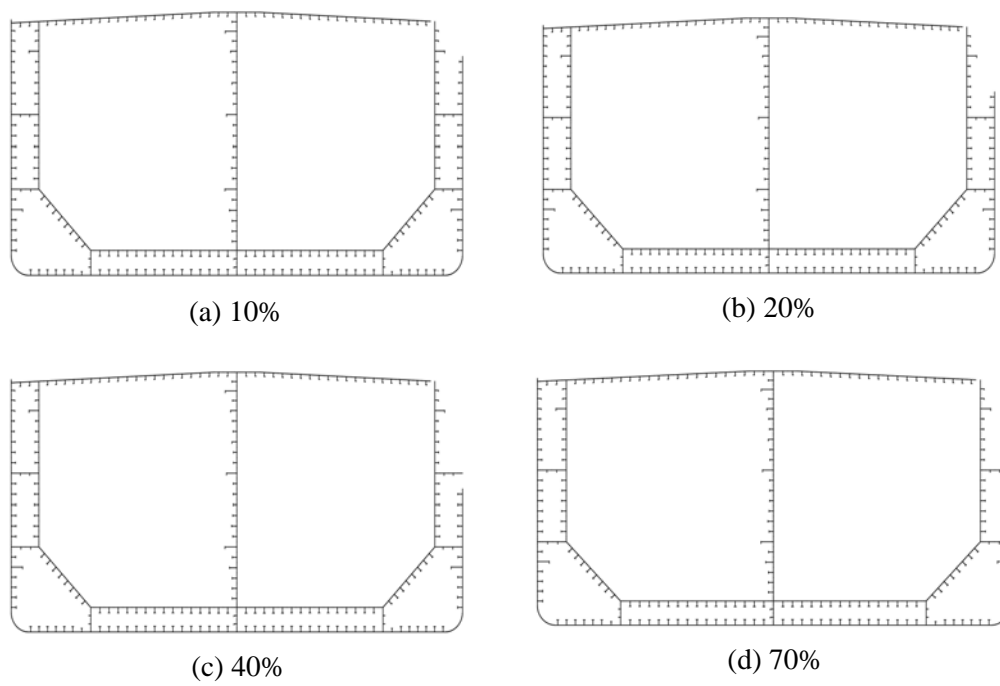


Fig. 2.7 Double Hull Oil Tanker (Ship T4)

The difference between B1 and B4 may be related to that of the depth to breadth ratio, scantlings etc. More systematic analyses are needed to draw general conclusions. According to the result of T4, the effect of rotation of neutral axis on the ultimate longitudinal bending strength is small when only the outer shell is damaged.

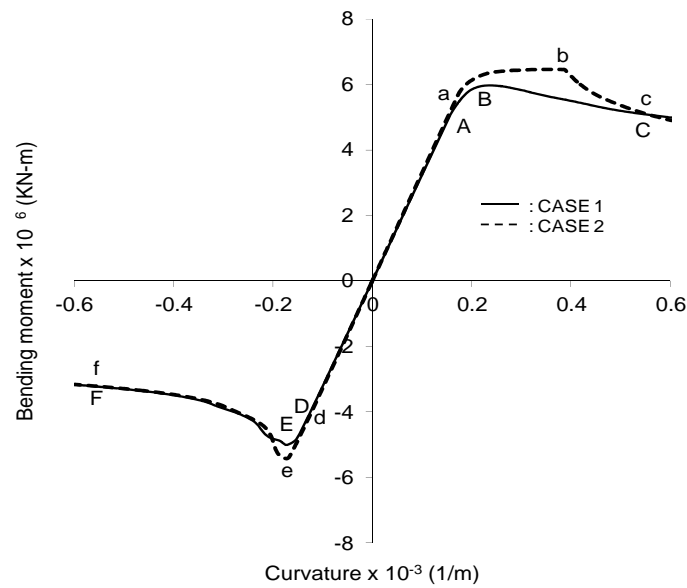


Fig. 2.8 Vertical bending moment-vertival curvature relationship (Ship B1, 70% damage)

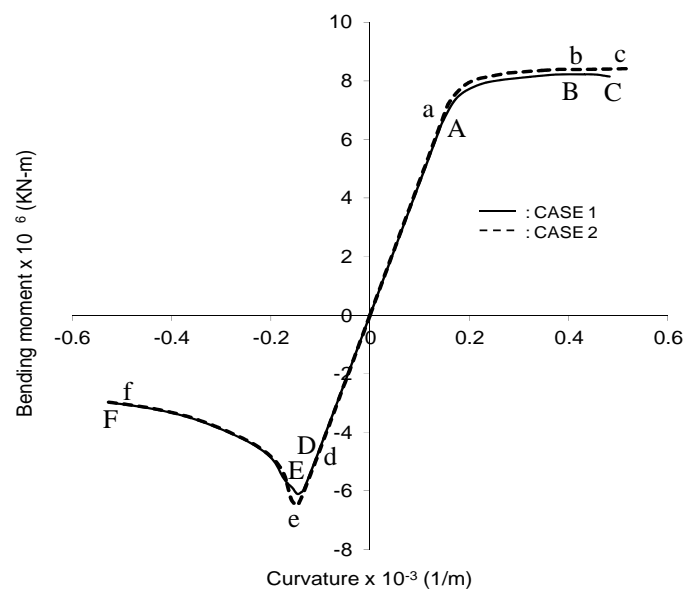


Fig. 2.9 Vertical bending moment-vertival curvature relationship (Ship B4, 70% damage)

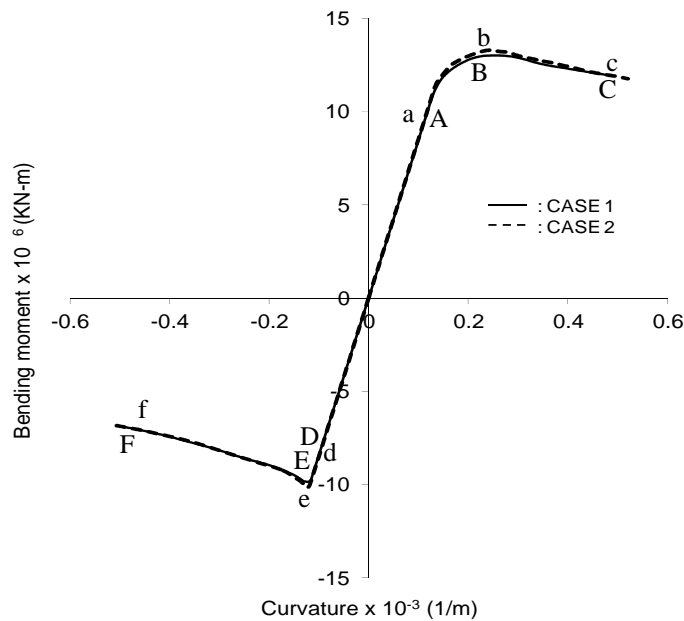


Fig. 2.10 Vertical bending moment-vertival curvature relationship (ShipT4, 70%Damage)

Figs. 2.11~2.13 show the stress distribution of Ship B1, Ship B4 and Ship T4 with 70% damage obtained by CASE 1 analysis. The results at the points A to F in Figs. 2.8~2.10 are plotted, together with the neutral axis. The triangles in the Figures indicates the collapse elements in tension and the circles those in compression. In the hogging condition (A~C), yielding occurs at the deck part of the damage side first and spreads to the undamaged side. Then, buckling takes place at the bottom part of the undamaged side, and the ultimate bending moment is attained. The load carrying capacity of the bottom members, which fail in buckling, decreases beyond their ultimate strength as illustrated in Fig. 2.2. To satisfy the equilibrium condition of the axial force for a whole cross section, the stress at the deck side also decreases. Correspondingly, the neutral axis moves upward at the undamaged side.

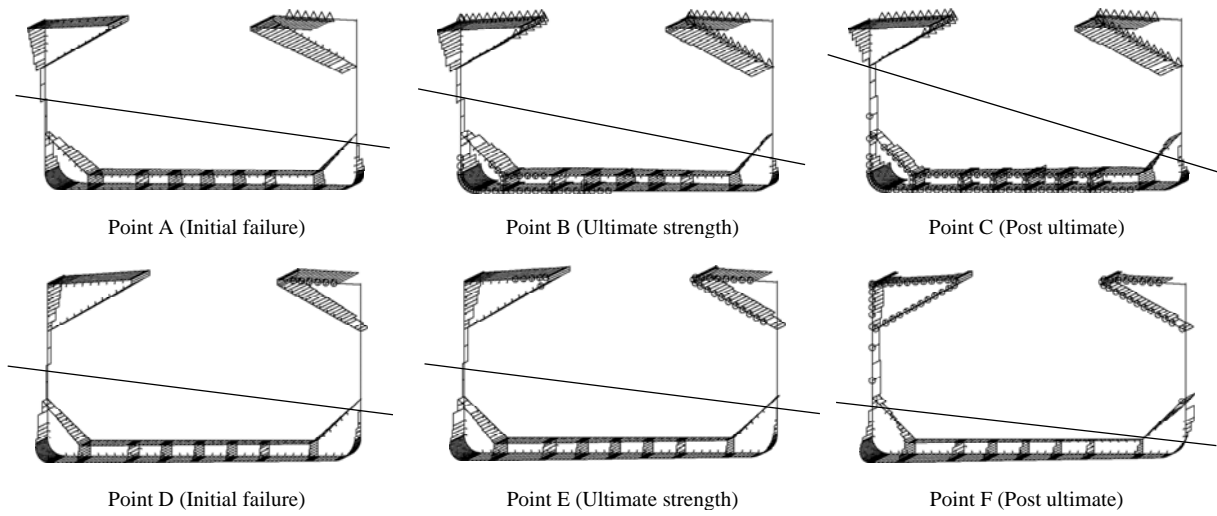


Fig. 2.11 Stress distribution and neutral axis (Ship B1, 70% damage, CASE 1)

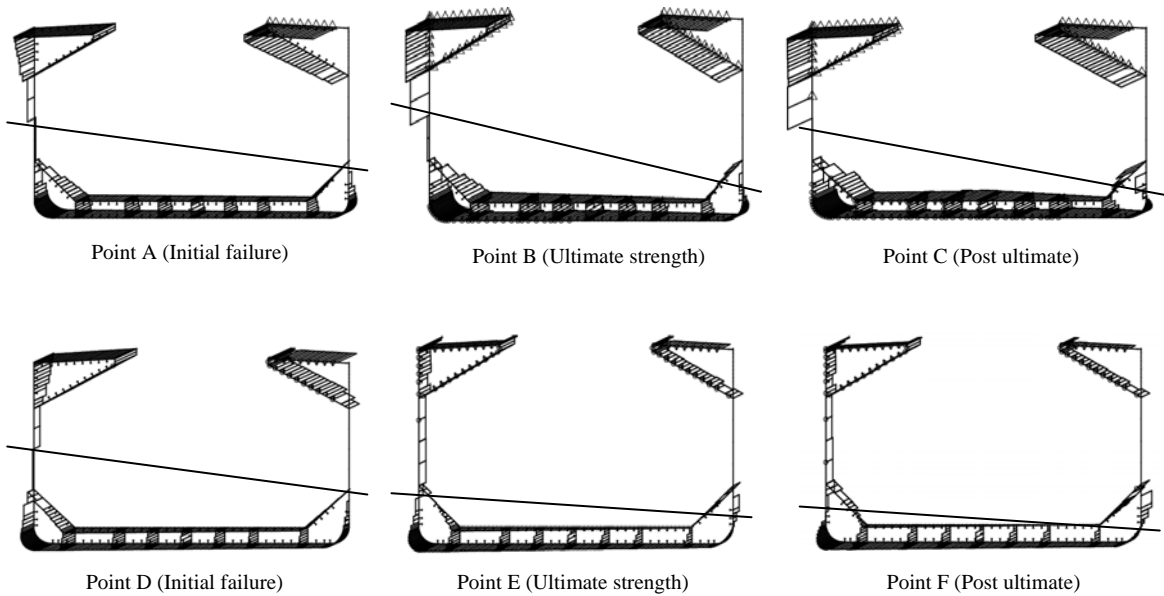


Fig. 2.12 Stress distribution and neutral axis (Ship B4, 70% damage, CASE 1)

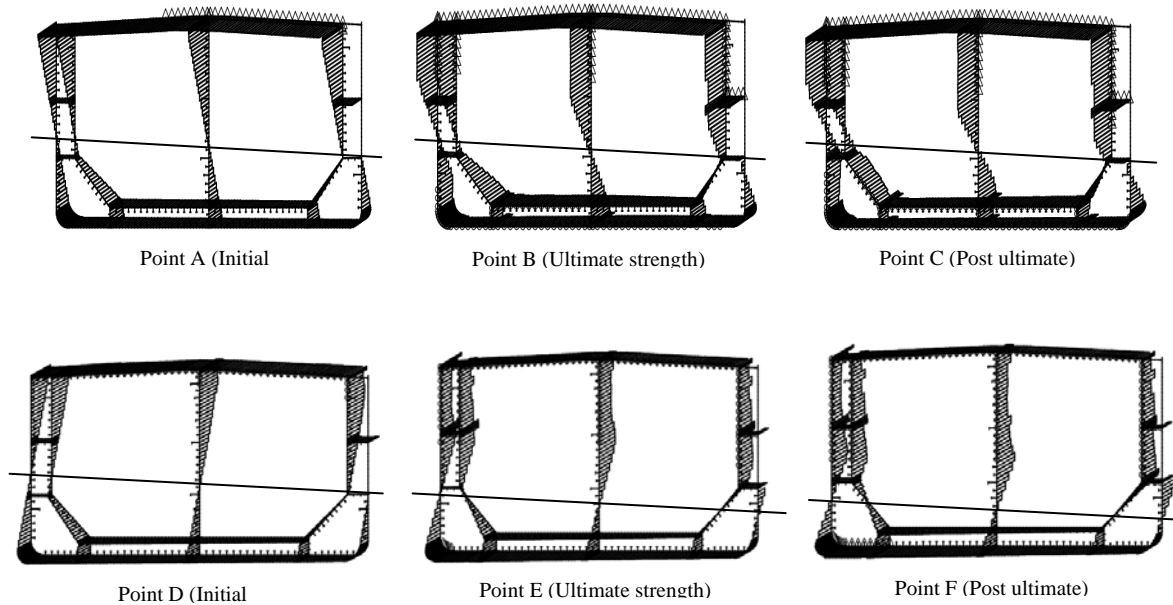


Fig. 2.13 Stress distribution and neutral axis (Ship T4, 70% damage, CASE 1)

In the sagging condition (D~F), buckling occurs at the deck of the damaged side first and spreads to the undamaged side. Due to reduction of load carrying capacity at the deck part, neutral axis moves downward. No yielding occurs at the bottom part.

Figs. 2.14~2.16 show the stress distribution obtained by CASE 2 analysis. Since the rotation of the neutral axis is not considered, the stress distribution and the spread of failures are symmetric with respect to the centerline. In hogging condition (a~c), the ultimate bending moment capacity is attained when the upper part of the cross section is almost fully yielded and the bottom part reached the ultimate compressive strength (point b). Beyond point b, the load carrying capacity of the buckled bottom part decreases, leading to the elastic unloading at a whole upper part. This is reason why the bending moment capacity rapidly decreases beyond point b in Fig. 2.8. Such a behavior is not observed in CASE 1. The significant difference in the calculated collapse and unloading behaviors again shows that the rotation of neutral axis needs to be taken into account. It

is also should be noted that since the elastic unloading of the yielded region often takes place in the progressive collapse behavior of a hull girder, in particular in post-ultimate behaviors, the incremental formulation is needed for this kind of analysis.

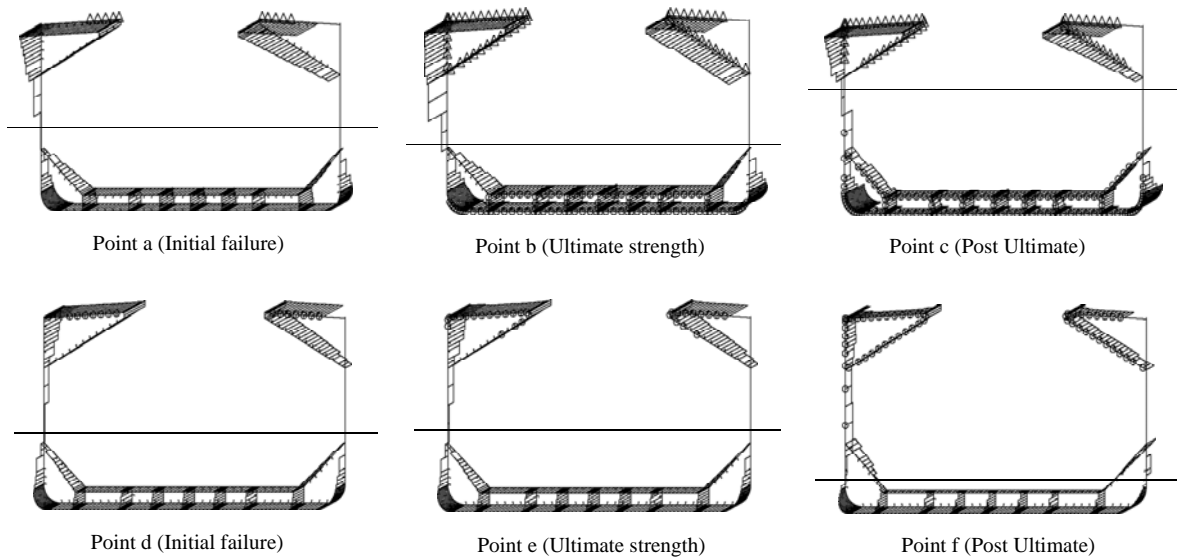


Fig. 2.14 Stress distribution and neutral axis (Ship B1, 70% damage, CASE 2)

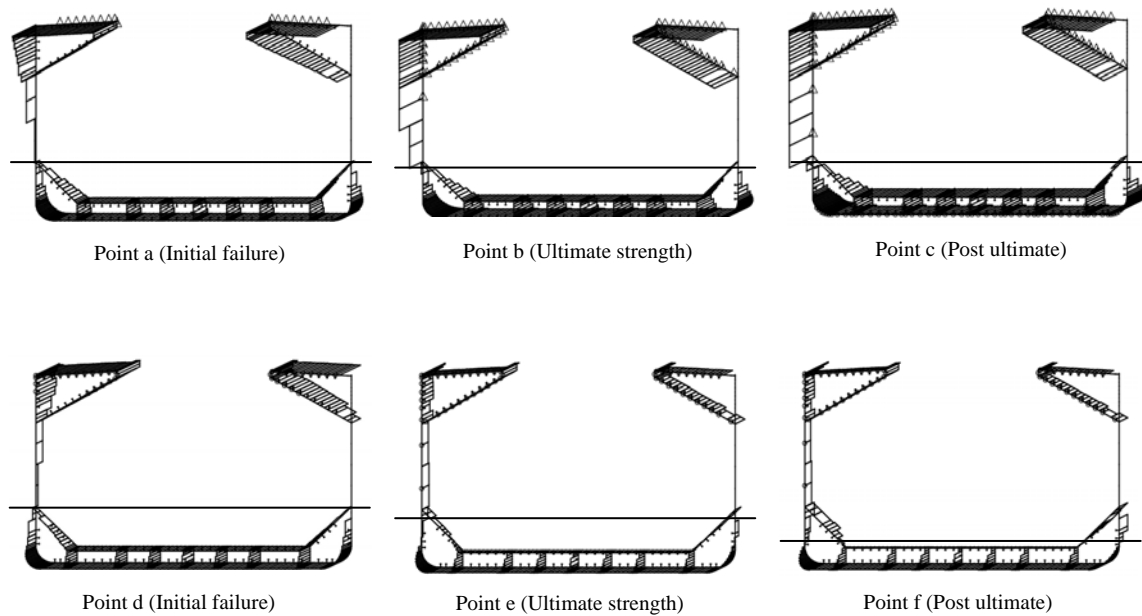


Fig. 2.15 Stress distribution and neutral axis (Ship B4, 70% damage, CASE 2)

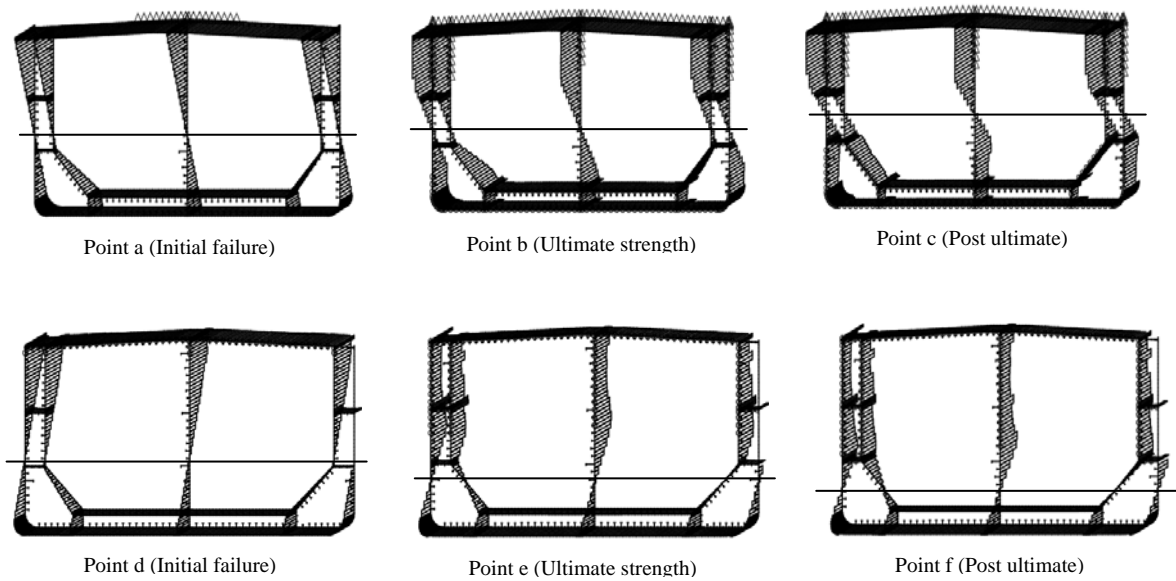
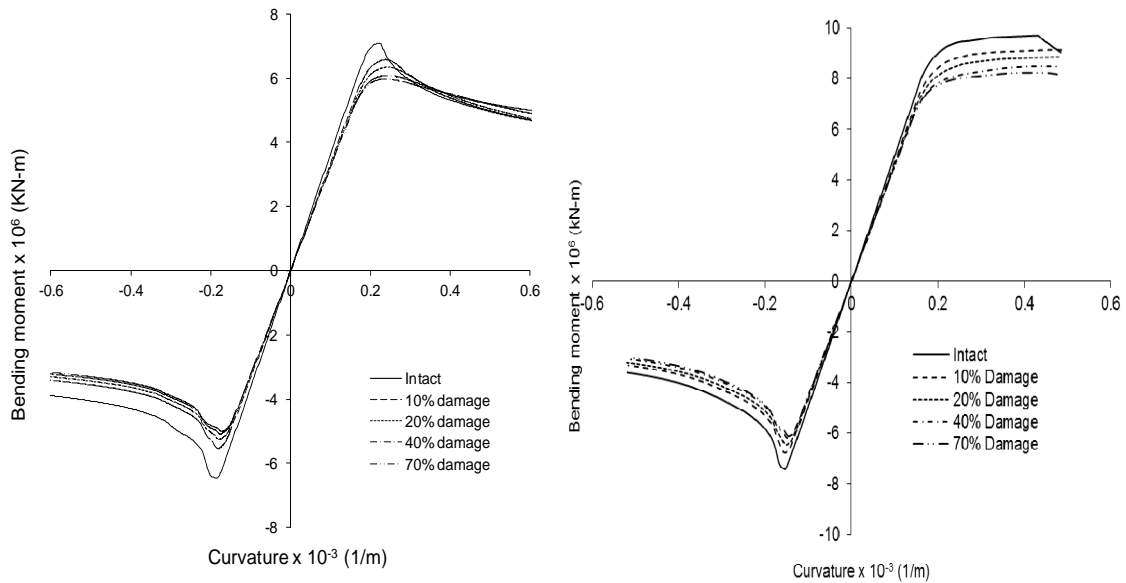


Fig. 2.16 Stress distribution and neutral axis (Ship T4, 70% damage, CASE 2)

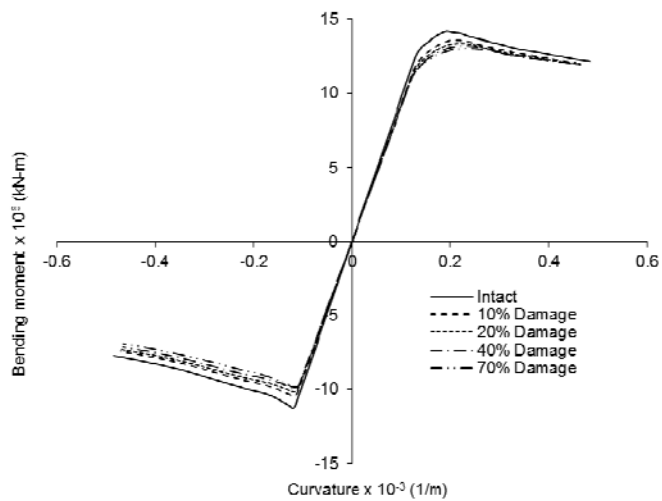
Comparing with the bulk carriers, the rotation of neutral axis has no significant effect to the ultimate bending moment compared to CASE 2 for the case of double hull oil tanker. This may be caused by the inner hull which can resist the rotation of neutral axis if the damage takes place at the outer shell only.

The bending moment-curvature relationship of Ship B1, Ship B4 and Ship T4 obtained for the different damage extents are summarized in Fig. 2.17. The results of CASE 1 analysis are shown. The residual strength is significantly reduced by the 10% damage near the deck part. The effect of further extent of the damage toward bottom direction is less significant than 10% damage. As to the effect of the rotation of neutral axis, further study is necessary according to the damage extent, including the case of damage of both inner and outer side shells of a double-hull oil tanker.



(a) Ship B1, CASE 1

(b) Ship B4, CASE 1



(c) Ship T4, CASE 1

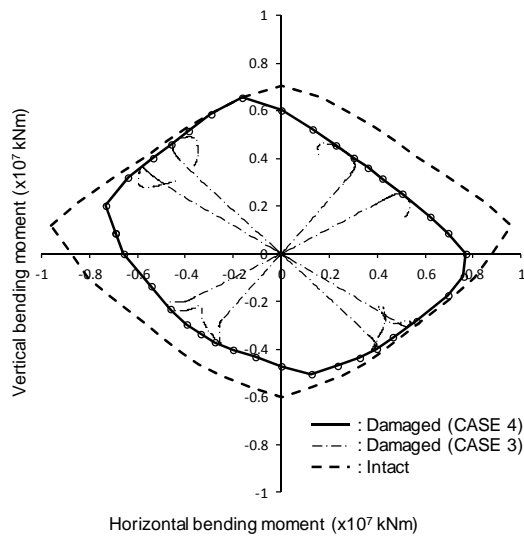
Fig. 2.17 Effect of damage extent on the residual hull girder strength

After ships suffered the damage due to collision, grounding, flooding and heeling may take place, and the hull girder is subjected to biaxial bending, the ultimate strength interaction relationship under biaxial bending moment is therefore necessary for the

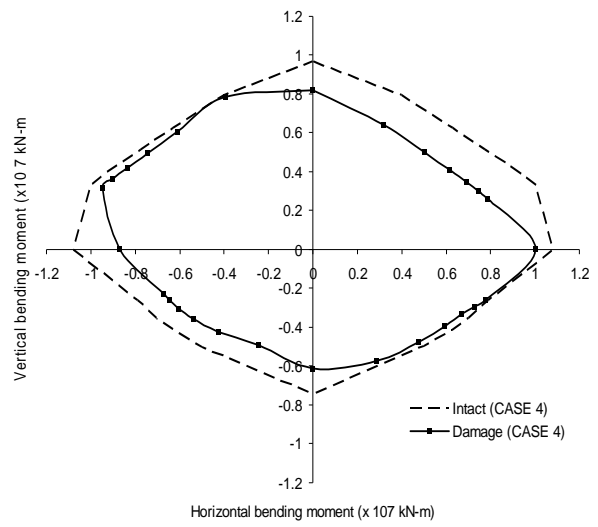
residual strength assessment of damage hull girders. There are two basic approaches to obtain the ultimate interaction curves; one is the proportional curvature method where  $\Delta\phi_H^0 / \Delta\phi_V^0$  is constant in CASE 3 and the other is the proportional moment method where  $\Delta M_H / \Delta M_V$  is constant in CASE 4. Both methods were applied to Ship B1 with 70% damage as an example. The moment loading method is applied with 70% damage in Ship B4 and Ship T4.

The ultimate strength interaction curve obtained by CASE 4 analysis is plotted by solid line in Fig. 2.18. The horizontal and vertical moments are increased proportionally as shown by arrow. On the other hand, the chain dotted lines show the horizontal/vertical moment paths for different curvature ratio obtained by CASE 3 analysis. The biaxial moment ratio varies along the path with the change of tangential stiffness of the cross section. It is found that the solid curve gives the accurate envelope the horizontal/vertical moment paths and both analysis methods give the almost identical ultimate strength interaction curve. CASE 4 is considered to be more useful for the calculation of the ultimate strength interaction curve and strength assessment, since the applied moment ratio can be easily controlled.

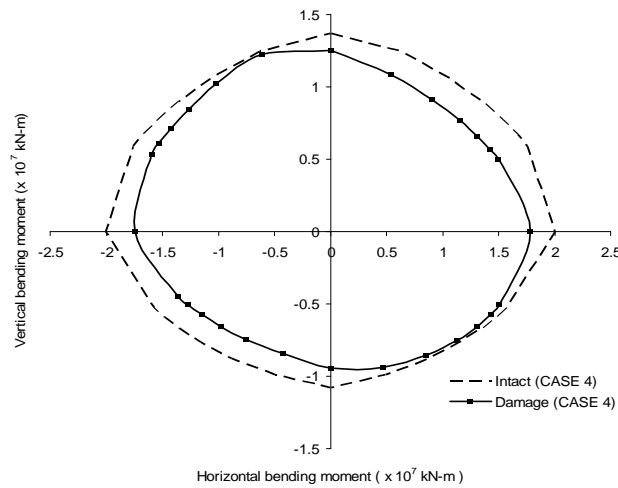
The dashed line in Fig. 2.18 shows the ultimate strength interaction curve of the intact cross section. The reduction of the ultimate strength due to damage is found to be larger when the bending stresses due to biaxial moment act in the same direction at the damage cross region.



(a) Ship B1



(b) Ship B4



(c) Ship T4

Fig. 2.18 Vertical and horizontal bending moment interaction diagram curve

## 2.6 Conclusion

Residual strength analysis of bulk carriers and a tanker with collision damages has been performed using the newly presented incremental formulation of biaxial bending collapse behavior of ship's hull girder based on the Smith's method. The explicit

expressions of the position of the neutral axis including its rotation and some relevant solutions procedures have been given.

The following conclusions can be drawn:

1. For the case of subject ships taken in this study, the effect of rotation of neutral axis on the estimate of the residual hull girder strength is about 8% at maximum for bulk carriers and almost negligible for a tanker having outer shell damage.
2. Tangential stiffness formulation considering the rotation of neutral axis and the elastic unloading of collapsed elements should be used for the rational estimate of the progressive collapse behavior of a ship's hull girder.
3. Ultimate strength interaction relationship obtained by applying the proportional biaxial moment is in good agreement with that is predicted by applying the proportional biaxial curvature.

## **Chapter 3**

# **Progressive Collapse Analysis using Beam Finite Element**

### **3.1 Introduction**

To avoid a collapse of the ship' hull under normal circumstances, design rules given by classification societies define a maximum stress level which should not be exceeded under the prescribed extreme loading condition or alternately a minimum elastic section modulus required. These have proven to be effective for intact ships in normal seas and loading conditions. However, their applicability to assess the survivability of ships in accidental situation, e.g. collision or grounding damage, is uncertain due to the interacting effects of local yielding, buckling or rupture as well as due to the loading on the hull. In this regard, the ultimate strength is a better basis for safety assessment as well as design, because it can define the true ultimate limit state.

The progressive collapse behavior of an asymmetrically damaged cross section under longitudinal bending moment, investigated in Chapter 2, corresponds to the collapse behavior of a hull girder having a damage of large length and subjected to uniform bending moment at the damaged part. In more general case, however, the damage length is limited and thus the effect of the rotation of the neutral axis due to an asymmetric damage is confined and constrained by the intact part. In addition, the loading condition may change both in magnitude and distribution after the damage, especially when heeled angle increases due to flooding. One strategy to consider such a limited damaged length and the change in the external load distributions on the hull

girder is to idealize the whole or part of hull girder using beam finite elements and the damage effect is introduced to some particular elements. For the rapid judgment of a survivability of damaged hull girder in emergency, a simplified and efficient approach such as a beam model is required.

From this view point, a method of the progressive collapse analysis of a ship hull girder with asymmetric damages is developed using the beam finite element and introducing the Smith approach to each element, and the program code Beam-HULLST is developed. The constraining effect of the intact parts on the damaged part where the neutral axis rotates and the effect of localization of the plastic deformation at the damaged part on the collapse behavior of a whole ship are examined.

## **3.2 Fundamentals of Thin-Walled Beam**

It has been proven practice to use simple beam theory to analyze the progressive collapse behavior of ship hull girder under longitudinal bending. Many experiments have confirmed that the bending behavior of ships agrees quite well with the beam theory. The hull girder of cross section represents the bending strength of the primary hull structure. This means that the calculation of hull girder cross section is very important for the ship design. Structural members that are continues in longitudinal direction are included in the calculation of cross section. The members are divided into plates and stiffeners with attached plating. Smith's methods has been widely employed to handle this procedure.

The formulation in Beam-HULLST is based on the thin-walled beam theory. Here, the fundamental theory of thin-walled beam element including the torsion effect as a general case. The coordinate system is defined as shown in Fig.3.1. The x- and y-axes are

defined on the beam cross section and the z-axis is parallel to the beam axis. The origin of the coordinate system is located at the gravity center of the cross section. The s-coordinate is defined along the mid-thickness line.

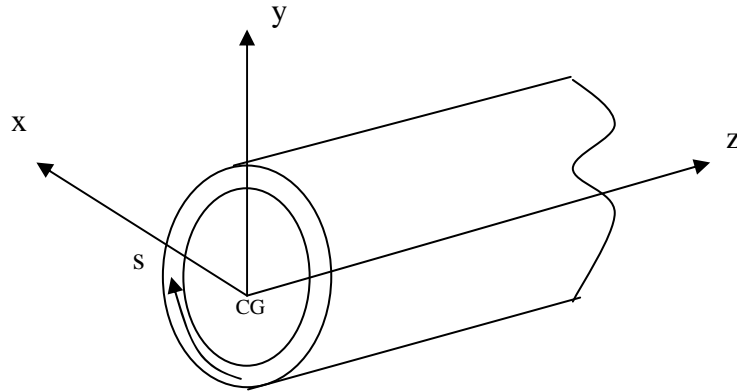


Fig.3.1 Coordinate system of a thin walled beam

Assuming that the cross section remains undistorted during deformation, the displacement  $U$ ,  $V$  and  $W$  in the  $x$ ,  $y$  and  $z$  directions at the coordinate  $(x, y, z)$  can be expressed as

$$U(x, y, z) = u_s(z) - (y - y_s)\theta(z) \quad (3.1)$$

$$V(x, y, z) = v_s(z) + (x - x_s)\theta(z) \quad (3.2)$$

$$W(x, y, z) = w(z) - x u_s'(z) - y v_s'(z) + \omega_{ns}(x, y)\theta'(z) \quad (3.3)$$

where  $u_s$  and  $v_s$  are the displacements at the shear center in  $x$  and  $y$  direction and  $w$  is the displacement at the gravity center in  $z$  direction.  $\theta$  is the rotation angle about the shear center.  $x_s$  and  $y_s$  are  $x$  and  $y$  coordinates of the shear center.  $\omega_{ns}$  is the warping function about the shear center. A prime (') denotes differentiation with respect to the  $z$ -coordinate.

The strains based on the displacements of Eq. (3.1) and (3.2) can be expressed as

$$\varepsilon_z = w' - x u_s'' - y v_s'' + \omega_{ns} \theta'' \quad (3.4)$$

$$\begin{aligned} \gamma_{sz} &= \gamma_{xz} \frac{\partial x}{\partial s} + \gamma_{yz} \frac{\partial y}{\partial s} \\ &= \left\{ \frac{\partial \omega_{ns}}{\partial s} - (y - y_s) \frac{\partial x}{\partial s} + (x - x_s) \frac{\partial y}{\partial s} \right\} \theta' \end{aligned} \quad (3.5)$$

where  $\varepsilon_z$  is the strain in the z-axis direction.  $\gamma_{sz}$  is the shear strain in the sz plane. The stress and strain relationship can be expressed as

$$\begin{pmatrix} \sigma_z \\ \tau_{sz} \end{pmatrix} = \begin{bmatrix} d_{11} & d_{12} \\ d_{21} & d_{22} \end{bmatrix} \begin{pmatrix} \varepsilon_z \\ \gamma_{sz} \end{pmatrix} \quad (3.6)$$

where  $\sigma_z$  is the axial stress and  $\tau_{sz}$  is the shear stress in the sz plane.  $d_{ij}$  gives a stress-strain relationship. In the present work, the ship cross section is modeled by thin-walled beam. Hence,  $d_{ij}$  corresponds to the stiffness of segmented members which consist of plate and stiffened plate where it also depends on the yielding and buckling.

For the case of finite element formulation, a beam element  $ij$  is considered and it is divided in z direction as shown in Fig.3.2. The length of the element is denoted by  $l$ .

$\{u_s\}$  is the nodal displacement vector at the shear center, consisting of the translation in x direction and its derivative with respect to z (denote by ') as

$$\{u_s\}^T = [u_{si}, u_{si}', u_{sj}, u_{sj}'] \quad (3.7)$$

where the subscript  $i$  means the node  $i$ . Similarly, other nodal displacements can be expressed as

$$\{v_s\}^T = [v_{si}, v_{si}', v_{sj}, v_{sj}'] \quad (3.8)$$

$$\{\theta_s\}^T = [\theta_i, \theta_i', \theta_j, \theta_j'] \quad (3.9)$$

$$\{w\}^T = [w_i, w_j] \quad (3.10)$$

$$\{d\}^T = [\{u_s\}, \{v_s\}, \{\theta\}, \{w\}] \quad (3.11)$$

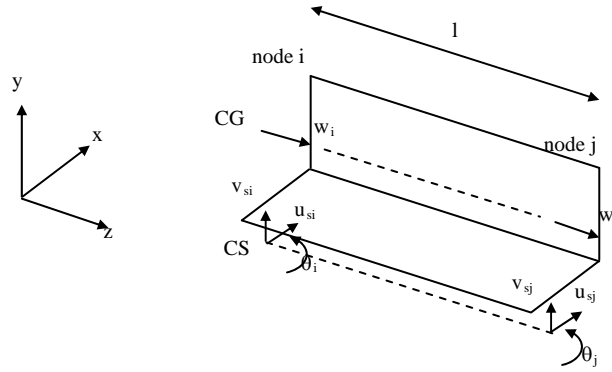


Fig.3.2 Beam element ij

where  $\{v_s\}$  is the nodal displacement vector at shear center in y direction,  $\{\theta\}$  is the torsion angle about shear center and torsion rate, and  $\{w\}$  is the axial displacement at the gravity center.

Correspondingly, the nodal forces are defined as

$$\{F_u\}^T = [F_{xi}, M_{yi}, F_{xj}, M_{yj}] \quad (3.12)$$

$$\{F_v\}^T = [F_{yi}, M_{xi}, F_{yj}, M_{xj}] \quad (3.13)$$

$$\{F_\theta\}^T = [T_i, B_i, T_j, B_j] \quad (3.14)$$

$$\{F_w\}^T = [F_{zi}, F_{zj}] \quad (3.15)$$

$$\{F\}^T = [\{F_u\}, \{F_v\}, \{F_\theta\}, \{F_w\}] \quad (3.16)$$

where  $\{F_u\}$  and  $\{F_v\}$  are the shear forces and bending moments,  $\{F_\theta\}$  the torsion moment and bi-moment about the axis at the shear center, and  $\{F_w\}$  the axial force. The axial displacement  $w(z)$  is interpolated linearly within the element and the horizontal and vertical deflections  $u_s(z)$ ,  $v_s(z)$  and torsion angle  $\theta(z)$  by cubic polynomials. Using the

nodal displacement and nodal coordinates, the displacement functions can be expressed as a function of nodal displacement in the form

$$\begin{aligned} u_s(z) &= [A_c(z)]\{u_s\} & , & & v_s(z) &= [A_c(z)]\{v_s\} \\ \theta(z) &= [A_c(z)]\{\theta\} & , & & w(z) &= [A_L(z)]\{w\} \end{aligned} \quad (3.17)$$

where

$$[A_c(z)] = \begin{bmatrix} 1 & z & z^2 & z^3 \\ -\frac{3}{l^2} & \frac{2}{l} & \frac{3}{l^2} & \frac{2}{l} \\ \frac{2}{l^3} & \frac{1}{l^2} & -\frac{2}{l^3} & \frac{1}{l^2} \end{bmatrix}$$

$$[A_L(z)] = \begin{bmatrix} 1 & z \\ -\frac{1}{l} & \frac{1}{l} \end{bmatrix}$$

Substituting Eq. (3.17) into Eq. (3.4) and (3.5), the axial and shear strain can be expressed as

$$\begin{pmatrix} \varepsilon_z \\ \gamma_{sz} \end{pmatrix} = \begin{bmatrix} [B_1] & -x[B_2] & -y[B_3] & \omega_{ns}[B_2] \\ 0 & 0 & 0 & g(s)[B_3] \end{bmatrix} \{d\} \quad (3.18)$$

where

$$[B_1] = \frac{d}{dz}[A_L] \quad , \quad [B_2] = \frac{d^2}{dz^2}[A_c] \quad , \quad [B_3] = \frac{d}{dz}[A_c]$$

$$g(s) = \frac{\partial \omega_{ns}}{\partial s} - (y - y_s) \frac{\partial x}{\partial s} + (x - x_s) \frac{\partial y}{\partial s}$$

Applying the principle of virtual work to the stress and strain increment, the incremental form of the stiffness equation is derived in the form

$$\{\Delta F\} = [K]\{\Delta d\} \quad (3.19)$$

where the stiffness equation  $[K]$  is given by

$$[K] = \int_V \begin{bmatrix} d_{11}[B_1] & -xd_{11}[B_{12}] & -yd_{11}[B_{12}] & \omega_{ns}d_{11}[B_{12}] \\ -xd_{11}[B_{21}] & x^2d_{11}[B_2] & xyd_{11}[B_2] & -x\omega_{ns}d_{11}[B_2] \\ -yd_{11}[B_{21}] & xyd_{11}[B_2] & y^2d_{11}[B_2] & -y\omega_{ns}d_{11}[B_2] \\ \omega d_{11}[B_{21}] & -x\omega_{ns}d_{11}[B_2] & -y\omega_{ns}d_{11}[B_2] & \omega_{ns}^2d_{11}[B_2] + g^2d_{22}[B_3] \end{bmatrix} \quad (3.20)$$

In case of the elastic cross section with uniform material properties, the stress-strain relationship of Eq. (3.6) at the arbitrary point is given by  $d_{11} = E$ ,  $d_{22} = G$ ,  $d_{12} = d_{21} = 0$ , where  $E$  is young's modulus and  $G$  is shear modulus. In the progressive collapse analysis,  $d_{ij}$  must be changed considering buckling and yielding. In this study, the buckling and yielding of stiffened panel under axial load is predominantly considered in the residual strength assessment. As a most simple approach, the interactive term is ignored, i.e.  $d_{ij} = 0$  ( $i \neq j$ ), and the axial stiffness  $d_{11}$  is calculated by HULLST and the shear stiffness is set as  $d_{22} = G$  before the ultimate strength and  $d_{22} = 0$  beyond the ultimate strength. More rational formulation of  $d_{ij}$  is needed in future including the effect of shear failure.

### 3.3 Method of Analysis

Progressive collapse analysis of hull girders with collision damage is performed using the beam finite elements in which the Smith's method is implemented for the calculation of the axial stress-strain relationship of the plate and stiffened panel members.

The procedure of the progressive collapse analysis using thin-walled elastic beams in this study is summarized as follow:

1. Ship hull girder cross section is idealized by the beam elements.

2. Following the Smith's method, the cross section of each beam element is divided into plate and stiffened plate as shown in Fig.3.3.
3. Elastic stiffness matrix of beam elements is calculated using Eq. (3.20).
4. Progressive collapse analysis is performed by applying prescribed force or curvature at the beam nodes.

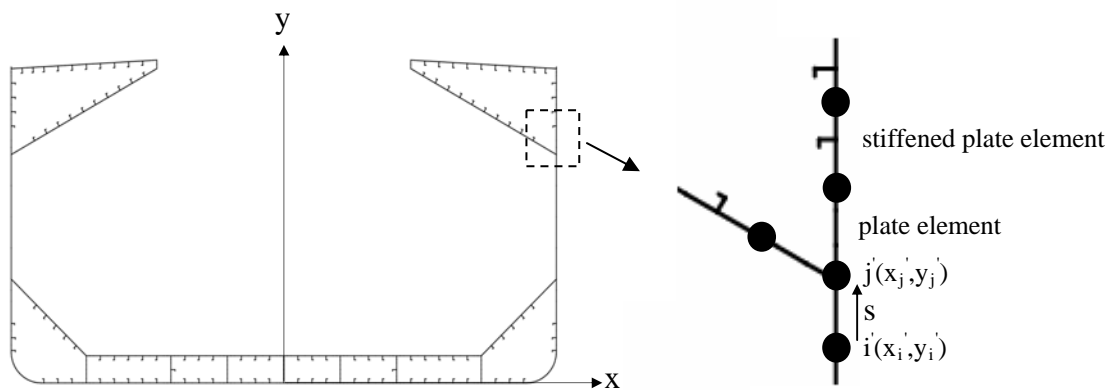


Fig. 3.3 Element division on the cross section

Two types of beam models are employed as shown in Fig. 3.4 One is the one frame-space model and the other the five frame-space model. The damage length is assumed to be one frame-space length in both models. 70% damage is assumed in one side of the cross section. The analysis of the one-frame space model corresponds to the progressive collapse analysis of the damaged cross section obtained by HULLST. On the other hand, the five frame space model includes the damaged part partially, and thus the constraining effect of the intact part on the deformation of the damaged part due to the rotation of the neutral axis can be considered.

The boundary condition for the beam models is shown in Fig. 3.5. The forced rotation angles about horizontal axis are applied at the both-end nodes in the opposite

directions. To allow for the shift of the neutral axis during the progressive collapse, the longitudinal translation at one end is fixed and the other end set free under the condition of zero axial loads. In addition, the rotation about the vertical axis as well as about the horizontal axis is allowed at both ends to consider an occurrence of the horizontal curvature under vertical bending moment due to the rotation of the neutral axis the damaged part (Case 1). For the one frame space model, the analysis with the rotation about vertical axis fixed (Case 2) is also performed for comparison purpose.

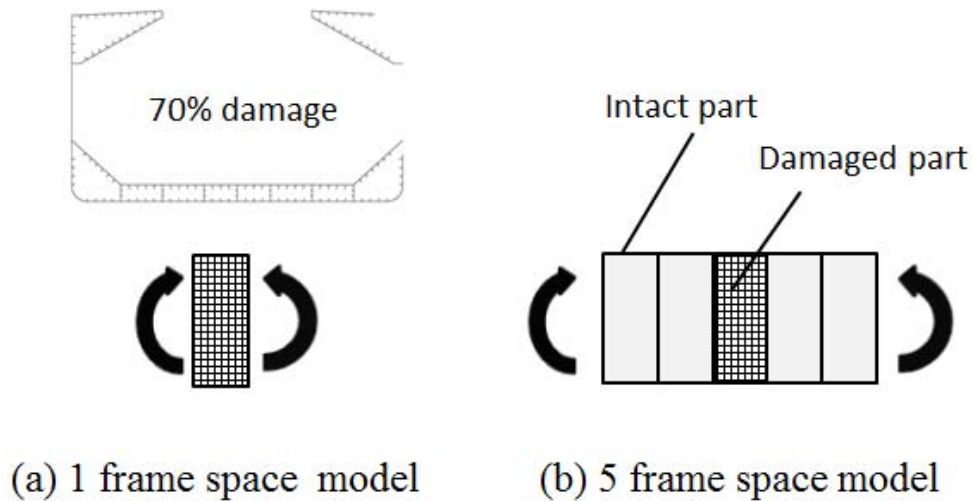


Fig. 3.4 Beam-HULLST model for analysis

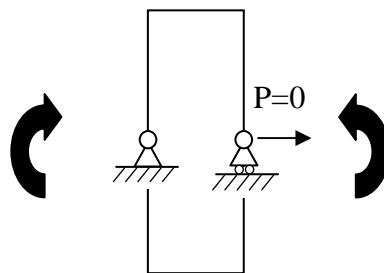


Fig. 3.5 Boundary condition

### 3.4 Case Studies

Two single hull bulk carriers, B1 and B4, shown in 2.5 are taken as the subject ship. The damage is located at asymmetric position on the side shell of the hull girder cross section. The vertical damage extent is taken for investigation the ultimate strength as 70% of ship depth. The horizontal damage extent is taken  $B/16$  and it is kept constant for all damage cases.

The vertical bending moment and vertical curvature relationships obtained by HULLST and those by Beam-HULLST with one frame space model are compared in Fig. 3.6. As shown, the two analysis methods give almost identical results. The reasonable agreement between two programs has been obtained. It is again found that the case 2 analysis that constrains the rotation of the neutral axis slightly overestimate the ultimate strength.

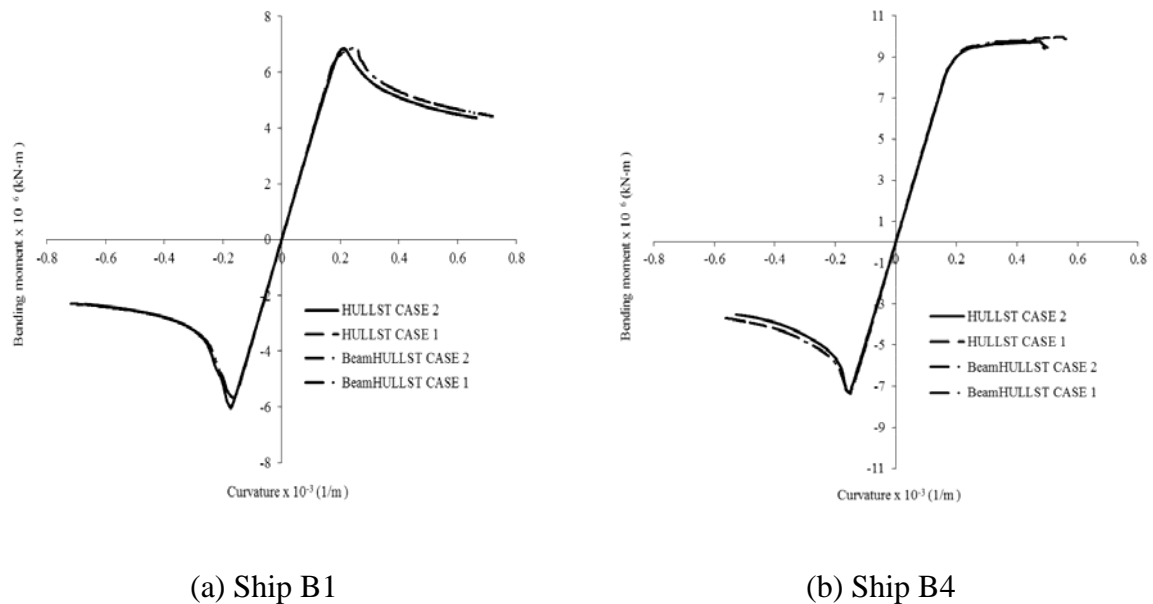


Fig. 3.6 Moment-Curvature relationship for intact of Ship B1, B4 and T4

Figure 3.7 shows the bending moment–curvature relationships of a single-side Panamax-size Bulk carrier (Ishibashi et al, 2008) obtained by the Beam-HULLST. The three-hole model of the subject ships is shown in Fig.3.8. The structural member dimensions are determined based on the IACS/CSR-B. Fig. 3.7 compares the results obtained by the one frame-space model and the five frame-space model. The average curvature was calculated by dividing the relative rotation angle between both-end cross sections by the overall length of the model.

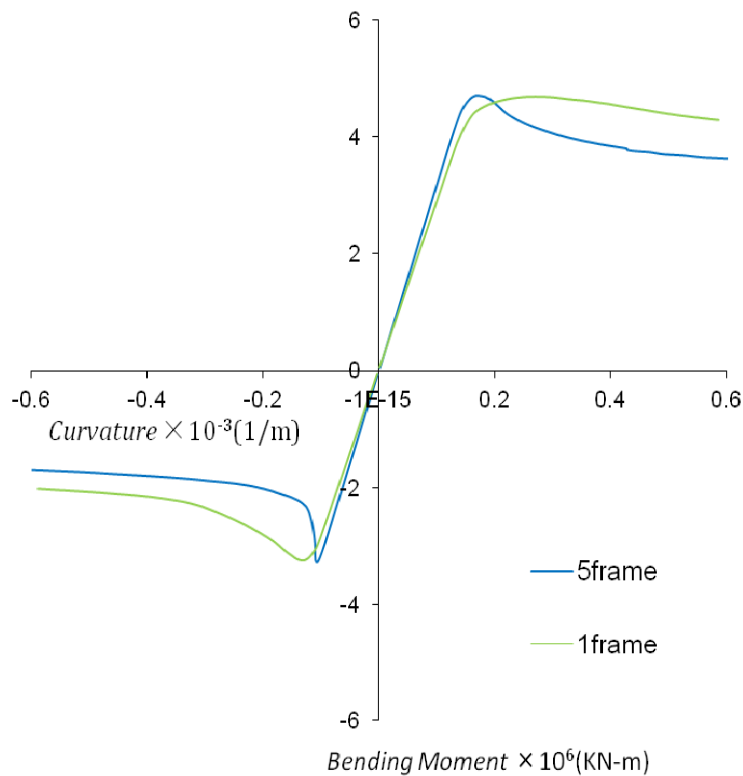


Fig.3.7 Bending moment-average curvature relationship of a panama-size bulk carrier obtained by Beam-HULLST using the one frame-space model and the five frame-space model.

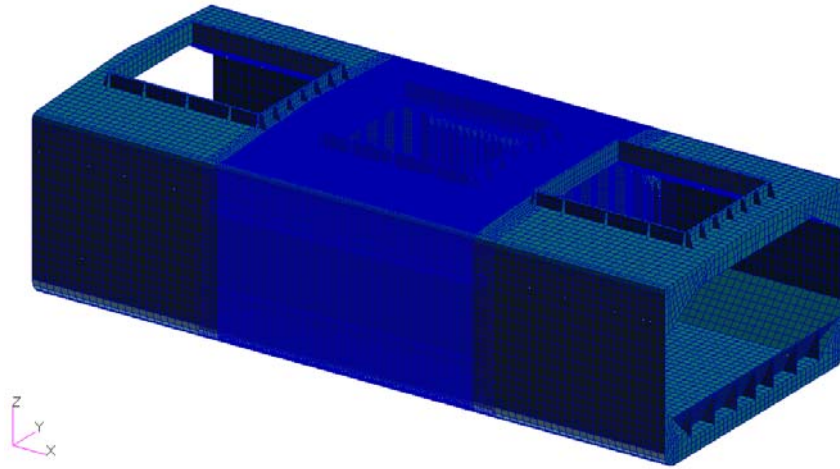


Fig. 3.8 Three-hold model of Paramax-size bulk carrier

It is found that the five frame-space model consisting of one damaged frame space at the middle and the intact frame space for the rest part gives slightly larger ultimate strength than that obtained by the one frame space model. This is because the effect of the rotation of the neutral axis at the damaged part is constrained by the presence of the intact part. The reduction of the residual strength due to the rotation of the neutral axis is found to be further smaller than that specified in the IACS draft rule.

It is also found from Fig. 3.7 that the bending moment capacity beyond the ultimate strength of the five frame-space model decreases more rapidly than that of the one-frame-space model. This is because of localization of the plastic deformation at the damaged cross section and the simultaneous unloading in the rest part of the model. As shown, the collapse of the damaged ship takes place in more brittle manner (sudden drop of the capacity) than that predicted by the bending moment-curvature relationship of the cross section as obtained by HULLST. This suggests the need for the Beam-HULLST model that can deal with the behavior of the whole hull girder.

## **3.5 Conclusion**

Residual strength analysis of bulk carriers and a tanker with collision damages has been performed using Beam-HULLST, the following conclusions are:

1. It has been confirmed that the progressive collapse behavior obtained by the Beam-HULLST using one beam element almost coincides with the result by HULLST for a cross section.
2. The influence of the rotation of the neutral axis at the asymmetrically damaged cross section is reduced by the presence of the adjacent intact parts. The reduction rate of the residual hull girder strength should be smaller than that found in the analyses of Chapter 2 for a cross section
3. The localization of the plastic deformation at the damaged part and the simultaneous unloading at the rest part of the hull girder has a significant influence on the post-ultimate strength behavior of the hull girder. The Beam-HULLST that can handle this effect is effective for the risk assessment of the damaged hull girder in the damaged condition.

## **Chapter 4**

# **Simple Formula of Residual Hull Girder Strength under Sagging Condition**

### **4.1 Introduction**

The aim of the present work is basically two-fold; one is to investigate the influence of the rotation of the neutral axis on the residual hull girder strength of asymmetrically damaged ships, and the other to develop the practical methods to predict the residual hull girder strength and behavior including the effect of the rotation of the neutral axis.

Two effective methods for the progressive collapse analysis of the damaged hull girder are presented in the foregoing chapters. As to the sagging condition, it is well recognized that the ultimate hull girder strength is almost attained when the primary deck members in longitudinal compression reached their ultimate strength. This forms a basis of the Single Step Ultimate Capacity Method in the existing IACS/CSR-T. The similar behaviors have been observed in the present HULLST and Beam-HULLST analyses.

As a simple practical approach to estimate the residual hull girder strength of asymmetrically damaged ships in the sagging condition, a simple closed formula of the residual hull girder strength is proposed. Its effectiveness is examined through a comparison with the result of the progressive collapse analysis.

## 4.2 Basic Assumption

The following assumption is made for the prediction of the residual hull girder strength under the sagging condition:

- (1) The ultimate sagging strength is attained when a stiffened panel element at the specified location (hereafter called ‘critical element’) reached the ultimate strength.
- (2) The hull girder cross section is elastic until the failure of the critical member.
- (3) The ultimate strength of the critical member is predicted from the average axial stress and average axial strain relationship calculated by HULLST (Yao and Nikolov).

## 4.3 Estimation of the Residual Hull Girder Strength and Neutral Axis Effects

In the elastic cross section, the bending stress at the  $i$ -th element (see Fig.4.1),  $\sigma_i$ , is expressed as

$$\sigma_i = E\{(y_i - y_G)\phi_H + (z_i - z_G)\phi_V\} \quad (4.1)$$

where  $E$  is Young’s modulus,  $y_G$  and  $z_G$  the centroid coordinates, and  $\phi_H$  and  $\phi_V$  the horizontal and vertical curvatures, respectively.  $y_G$  and  $z_G$  are given by

$$y_G = \frac{\left( \sum_{i=1}^N y_i D_i A_i \right)}{\left( \sum_{i=1}^N D_i A_i \right)} \quad (4.2)$$

$$z_G = \frac{\left( \sum_{i=1}^N z_i D_i A_i \right)}{\left( \sum_{i=1}^N D_i A_i \right)} \quad (4.3)$$

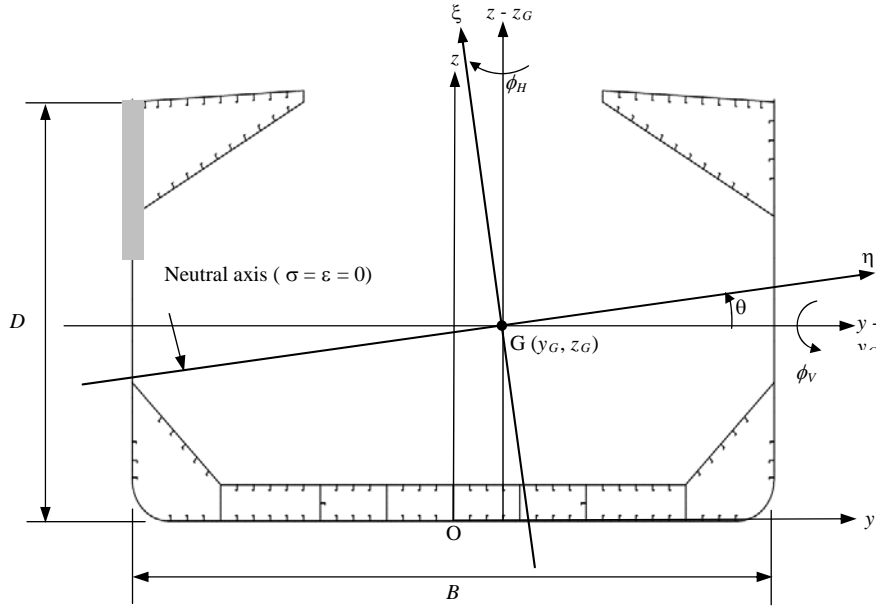


Fig. 4.1 Neutral axes of the elastic hull girder cross section with a symmetric damage

The biaxial moment and curvature relationship is given in the form

$$\begin{Bmatrix} M_H \\ M_V \end{Bmatrix} = \begin{bmatrix} EI_{HH} & EI_{HV} \\ EI_{VH} & EI_{VV} \end{bmatrix} \begin{Bmatrix} \phi_H \\ \phi_V \end{Bmatrix} \quad (4.4)$$

where

$$I_{HV} = I_{VH} = \sum_{i=1}^N (y_i - y_G)(z_i - z_G)A_i, \quad I_{HH} = \sum_{i=1}^N (y_i - y_G)^2 A_i, \quad I_{VV} = \sum_{i=1}^N (z_i - z_G)^2 A_i \quad (4.5)$$

When the vertical bending moment is applied to the cross section with no constraint on the horizontal curvature (Case 1), the horizontal curvature as well as the vertical curvature is induced under the condition of  $M_H = 0$ . The incremental equation to be solved is

$$\begin{Bmatrix} 0 \\ M_V \end{Bmatrix} = \begin{bmatrix} EI_{HH} & EI_{HV} \\ EI_{VH} & EI_{VV} \end{bmatrix} \begin{Bmatrix} \phi_H \\ \phi_V \end{Bmatrix} \quad (4.6)$$

Therefore,

$$\begin{Bmatrix} \phi_H \\ \phi_V \end{Bmatrix} = \frac{1}{E(I_{HH} I_{VV} - I_{HV}^2)} \begin{Bmatrix} -I_{HV} M_V \\ I_{HH} M_V \end{Bmatrix} \quad (4.7)$$

Substituting Eq. (4.7) to Eq. (4.1), the bending stress  $\sigma_i$  is given by

$$\sigma_i = \frac{-(y_i - y_G)I_{HV} + (z_i - z_G)I_{HH}}{(I_{HH} I_{VV} - I_{HV}^2)} M_V \quad (4.8)$$

The terms including the moment of inertia,  $I_{HV}$ , represent the effect of the rotation of the neutral axis.

On the other hand, when the vertical bending moment is applied to the cross section with the horizontal curvature constrained (Case 2), the bending moment are induced under the condition of  $\phi_H = 0$ , that is,

$$\begin{Bmatrix} M_H \\ M_V \end{Bmatrix} = \begin{bmatrix} EI_{HH} & EI_{HV} \\ EI_{VH} & EI_{VV} \end{bmatrix} \begin{Bmatrix} 0 \\ \phi_V \end{Bmatrix} \quad (4.9)$$

Substituting Eq. (4.7) to Eq. (4.1), the bending stress  $\sigma_i$  is given by

$$\sigma_i = \frac{(z_i - z_G)}{I_{VV}} M_V \quad (4.10)$$

Here, it is assumed that the residual hull girder strength in the sagging condition  $M_V^u$  is attained when a critical member at the location of  $(y_C - z_C)$  reached its ultimate strength,  $\sigma_C^u$ , namely for Case 1

$$M_V^u = \frac{I_{HH} I_{VV} - I_{HH}^2}{-(y_C - y_G)I_{HV} + (z_C - z_G)I_{HH}} \sigma_C^u, \quad (4.11)$$

And for Case 2

$$M_V^u|_{\text{CASE2}} = \frac{I_{VV}}{(z_C - z_G)} \sigma_C^u \quad (4.12)$$

Therefore, the reduction rate of the residual strength due to the rotation of the neutral axis in the framework of the proposed approximate approach is given by ratio of Eq. (4.12) to Eq. (4.11) as

$$\frac{M_V^u}{M_V^u|_{CASE2}} = \frac{I_{HH} I_{VV} - I_{HH}^2}{-(y_C - y_G)I_{HV} + (z_C - z_G)I_{HH}} \frac{(z_C - z_G)}{I_{VV}} \quad (4.13)$$

## 4.4 Results and Discussion

The single hull bulk carrier (Ship B1 and Ship B2) and double hull oil tanker (T2) are taken as subject ships to investigate the applicability of the formula of the residual strength, Eq. (4.11), and the reduction ratio of the residual strength due to the rotation of the neutral axis, Eq. (4.13). The vertical damage extent is taken as 10%, 20%, 40% and 70% of ship's depth, while horizontal damage extent is B/16.

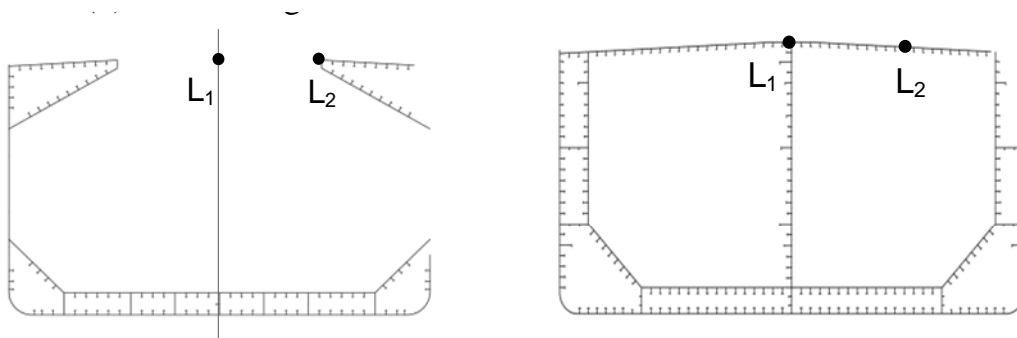


Fig. 4.2 Locations of the critical deck element

The investigation of the residual hull girder strength under sagging condition is performed by taking two locations of the critical deck elements as shown in Fig. 4.2. Ship B1 and Ship B2, the locations of the critical element are L<sub>1</sub> and L<sub>2</sub>, L<sub>1</sub> is located at

the center line and  $L_2$  at the hatch coaming on the damage side. For the case of T2,  $L_1$  is located at the center line and  $L_2$  at the distance of  $B/4$  from the damage side shell. For the location  $L_1$  of bulk carriers, the ultimate strength of the critical element is evaluated by using that of the element at  $L_2$ .

The residual strengths of B1, B2 and T2 obtained for the four different damage extents are summarized in Fig. 4.3. It is found that Eq. (4.11) gives an estimate of the residual strength which is in good agreement with the result of the progressive collapse analysis. For bulk carriers, the critical element at the location  $L_2$  gives a better estimate of the residual strength. This is consistent with the observed collapse behavior in which the ultimate strength is attained when topside tank region of the damage side almost fully failed. The location  $L_1$  cannot well take account of the effect of the horizontal curvature induce by  $M_V$ , resulting in the slight overestimate of the strength. In the case of tankers, the location  $L_1$  gives better estimate of the residual strength than  $L_2$ . This is also consistent with the failure behavior of T2 in which the ultimate strength is attained when the deck part almost fully failed.

Fig. 4.4 shows the comparison the reduction rates of the residual strength due to rotation of the neutral axis obtained by Eq. (4.13) and progressive collapse analysis. The influence of the rotation of the neutral axis is larger for a larger damage extent in general. For the case of the subject ships and damages under consideration, the influence is larger in bulk carriers than in tankers. Eq. (4.13) gives a relatively good estimate of the reduction rate. It can be a good basis of a rational expression of the influence of the rotation of the neutral axis on the reserved hull girder strength, as required in ship structural. More systematic analyses are definitely needed to develop the formula having larger applicability in ship types and damaged cases.

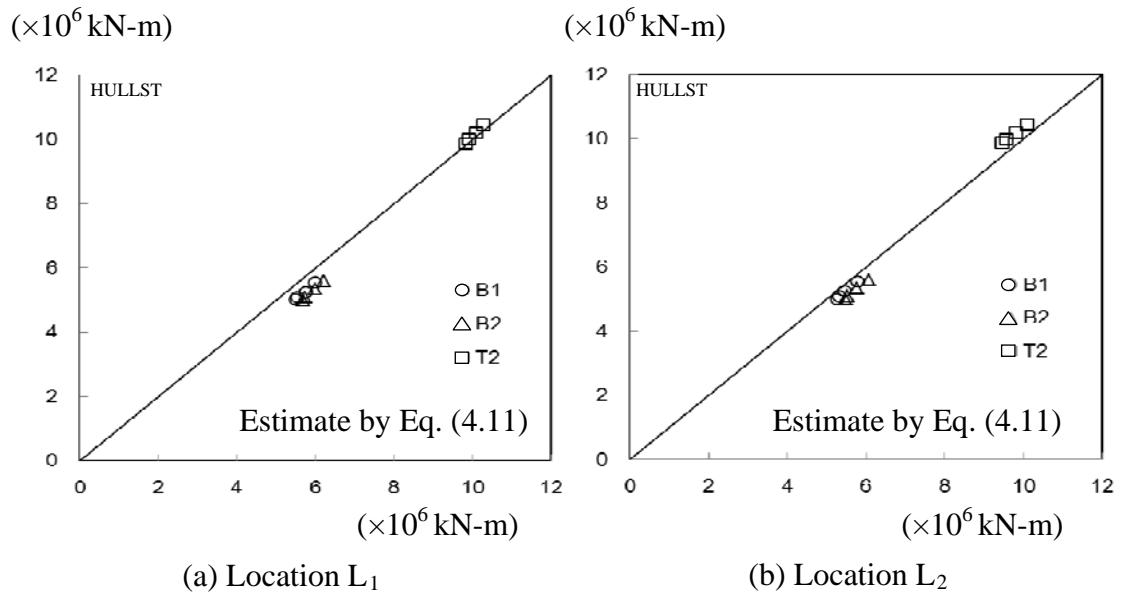


Fig. 4.3 Comparison of residual hull girder strength  $M_V$  between the simplified method and the progress collapse analysis

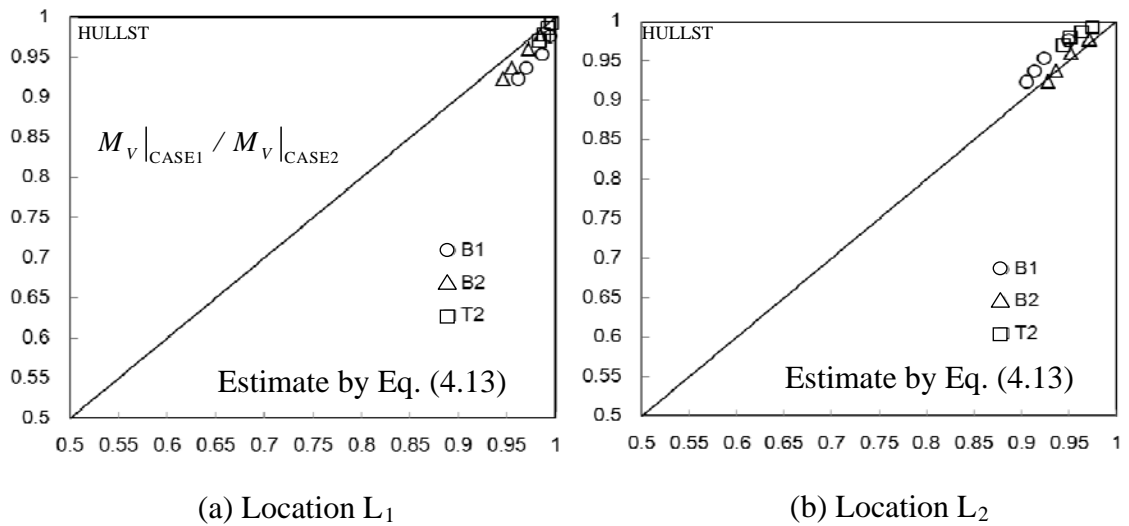


Fig. 4.4 Comparison of reduction ratio of residual hull girder strength due to the rotation of neutral axis between the simplified method and the progress collapse analysis (CASE 1/CASE 2)

## **4.5 Conclusion**

Based on the observation of the progressive collapse behavior of a bulk carrier and tanker with the top-side damage, an attempt is made to estimate the residual hull girder strength in the sagging condition using the elastic cross-sectional properties and critical member strength. A closed formula of the residual strength and that of the reduction ratio of the residual strength due to the rotation of the neutral axis are proposed.

It was found through a comparison with the results of obtained by the progressive collapse analysis that the residual hull girder strength of asymmetrically damaged ships under the sagging bending moment can be predicted by the proposed formulae with a reasonable accuracy.

## **Chapter 5**

# **Finite Element Analysis**

### **5.1 Introduction**

A ship's hull is very complicated stiffened panel structure consisting of structural components such as decks, bottoms, side shells, bulkheads, transverse frames and longitudinals. Although the nonlinear FE method is widely accepted as a reliable tool for the investigation of nonlinear structural behaviors, its applications to the progressive collapse analysis of ship's hull girder have been still limited due to great demand on the computer resources and manpower. Despite these difficulties, the nonlinear FE analysis is believed to be the only available and suitable tool to assess the ultimate hull girder strength with damage under longitudinal bending moment.

A series of Finite Element analysis (FE analysis) is carried out in this chapter to validate the proposed simplified methods of the progressive collapse analysis. The explicit dynamic FEM code, MSC/DYTRAN, is adopted for the assessment of the ultimate hull girder strength of a three-cargo-hold model of a single-side Panamax bulk carrier under longitudinal bending moment with and without damage in the hogging and sagging conditions. An efficient solution procedure is applied; i.e. the bending moment is applied with relatively high speed up to the specified value within the elastic range, then the moment is kept constant until the elastic vibration is damped, and finally the bending moment is applied with a low speed to obtain the ultimate strength and post-ultimate collapse behavior in a quasi-static manner.

## **5.2 Structural Modeling**

The nonlinear explicit FEM code MSC.DYTRAN is employed to analyze the progressive collapse behavior of a bulk carrier. MSC.PATRAN is used as a pre- and post-processor. The Finite Element model generated in the present work is illustrated in Fig. 5.1. This is a Panamax-size bulk carrier with a single side structure. The longitudinal extent of the model covers three cargo holds and two transverse bulkheads with lower stools. In order to investigate the influence the rotation of the neutral axis due to asymmetric damage on ultimate strength, the full breadth of the ship is modeled. The damage is assumed in the middle hold, which is modeled by the finer mesh than both-side holds. A rigid body object, implemented in Dytran, is attached at the both ends of the model, and forced rotation velocity of the same magnitude is applied to the model.

The four-node quadrilateral shell element (Dytran Element code) is used for modeling plate parts and the two-node beam element (Element code) for stiffeners. The fine mesh is employed in the middle hold with the damage and coarse mesh in the end holds.

The material is assumed to be homogenous and isotropic. The strain-hardening effects are not taken into account as a fundamental case. The forward and aft hold does not have stiffener in the bottom and deck part, but have the equivalent inplane stiffness. Main and web frames are not included except transverse. The transverse is attached for both deck and bottom structure.

### 5.3 Analysis Cases

Fig. 5.1 and Fig. 5.2 show the full model and the midship cross section including the dimensions of longitudinal members.

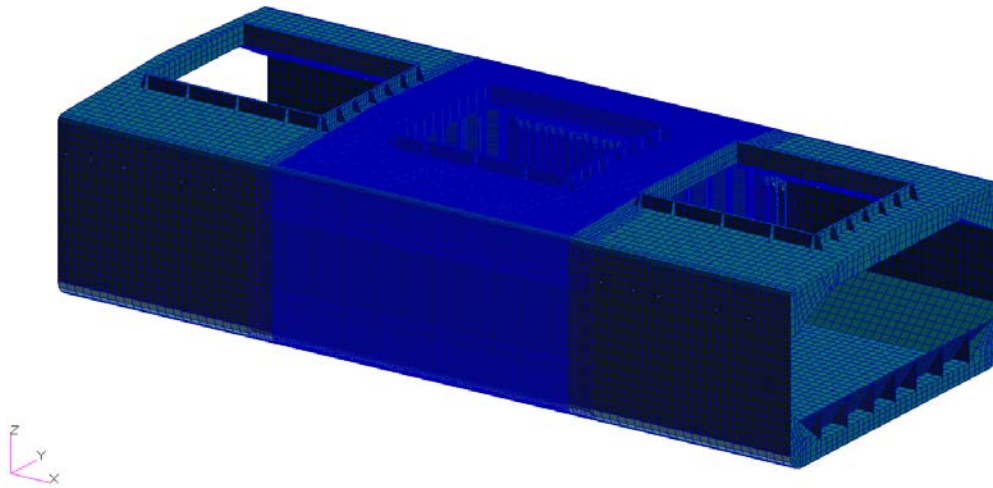


Fig.5.1 Three-cargo-hold of single hull bulk carrier of Panamax model

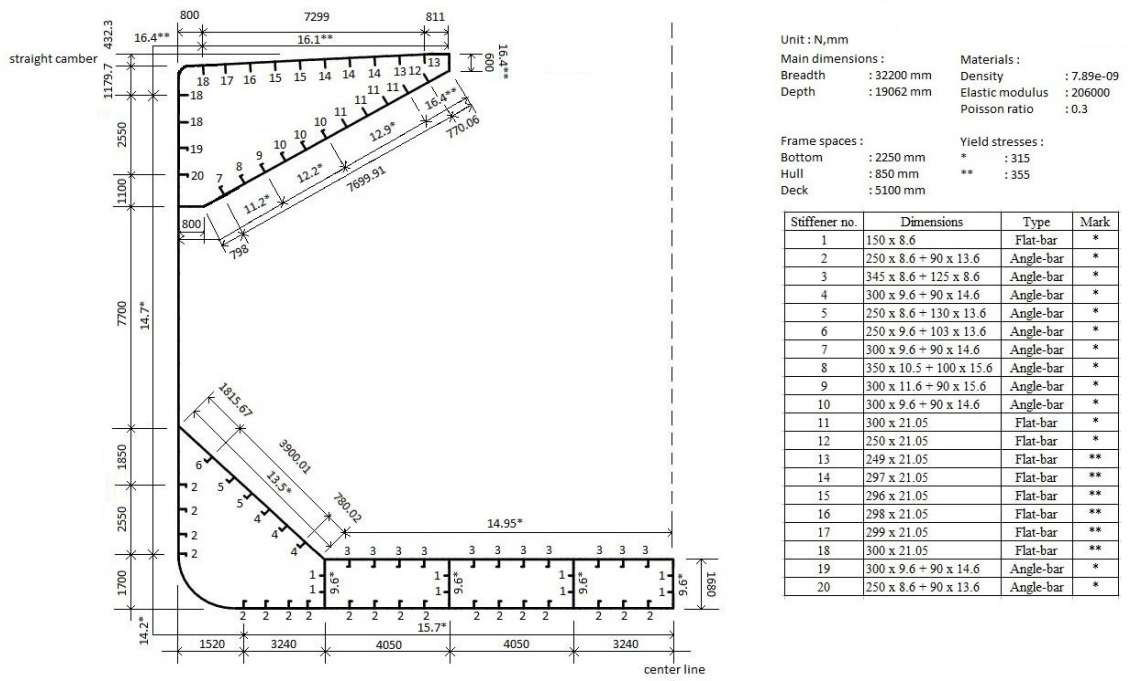


Fig.5.2 Cross section of three-cargo-hold model

The model is simply supported at the fore and aft end cross sections, which are assumed to be rigid. The forced rotations are applied about the horizontal axis at the height of the geometric center of the end intact cross sections. To consider the effect the rotation of the neutral axis at the damage part and resulting occurrence of horizontal deflection and curvature, the rotation about the vertical axis is allowed at both ends of the model (Case 1). The rotation about the longitudinal axis is constrained. The support point of the end cross sections at one end is fixed in the longitudinal direction, while the other end is allowed to move in the longitudinal direction under zero-axial force condition. This allows the shift and rotation of the neutral axis during the process of the progressive collapse.

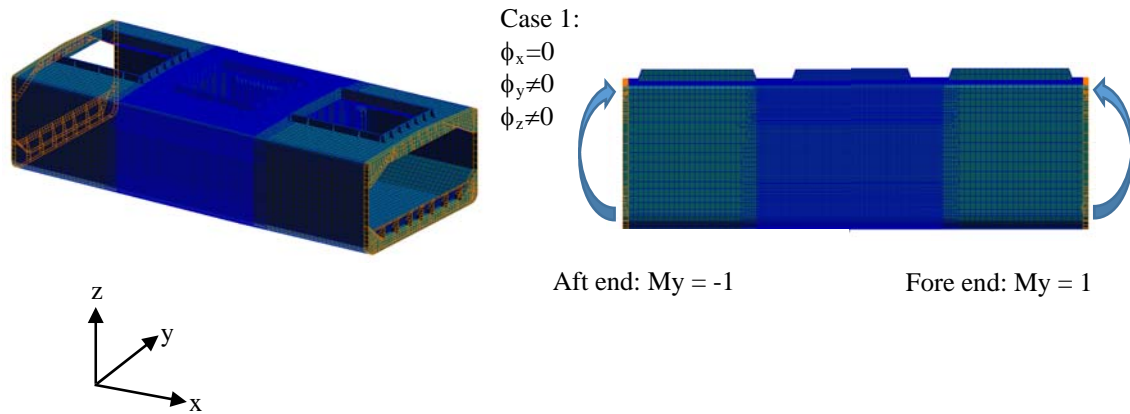


Fig.5.3 Boundary condition (Case 1) and rigid body object

For comparison purpose, the analysis with the forced constraint on the horizontal curvature and therefore that constraining the rotation of the neutral axis is also performed as shown in Fig. 5.4. The translation in the transverse direction (y-direction) is fully constrained at all the nodes on the center plane. An alternative approach is to constrain

the rotation of the cross section about the vertical axis at both ends or at the transverse bulkheads by applying the Multi-Pint Constraint. But here, this simple and over-constraining boundary condition is adopted as an extreme case.

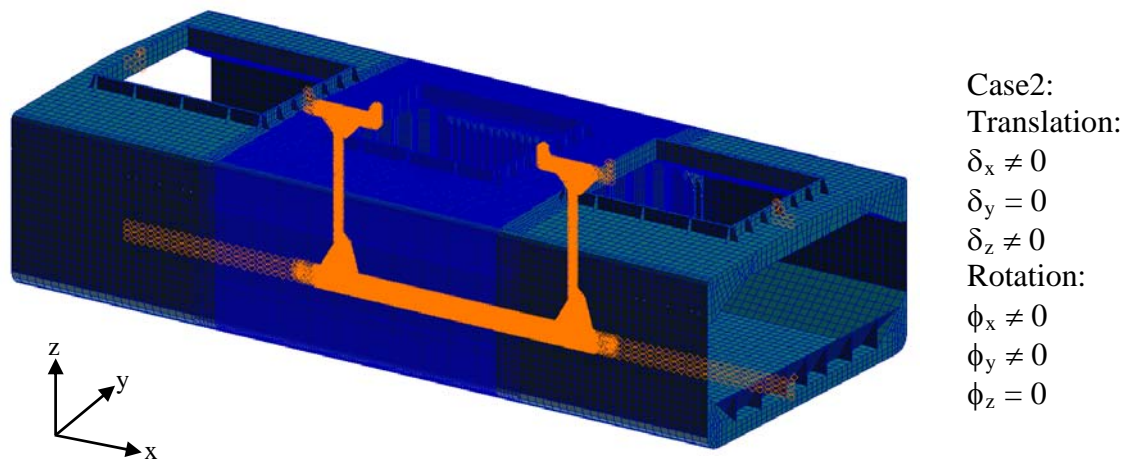


Fig.5.4 Boundary condition (Case 2)

The collision damage is modeled by removing the plate and stiffener elements at the damage region assuming the complete loss of the capacity at the damage part. As the fundamental case, the damage of the one frame-space length is located at the mid-hold part of the central hold. The 20% and 70% damages are shown in Fig.5.5.

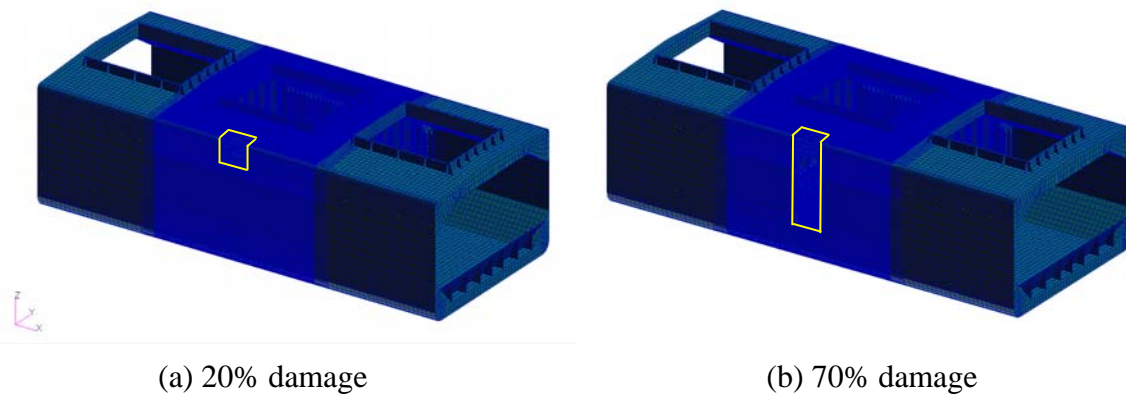


Fig.5.5 Illustration of the collision on the three-hold model

The 20% damage has a dimension of 5100 mm in length and 3939 mm in depth, and the 70% damage 5100 mm in length and 13889 mm in depth. The transversal damage extent is set as B/16 and used for two damage cases. The 70 % damage corresponds to the damage extent specified in the draft IACS/CSR-H.

To achieve a better balance of efficiency and accuracy, the FEM analysis is divided into three phases as described in Fig. 5.5. In the phase one, the relatively fast rotational velocity (0.015 rad/sec) of loading is given both ends of the model within the elastic range. Then in phase two, the rotational velocity is stopped, giving the global damping coefficient 0.0004 in order to eliminate the vibration. In the phase three, to minimize the dynamic effect, the relatively slow rotational velocity (0.002 rad/sec) is imposed to the model until the ultimate longitudinal strength is attained. The analysis conditions were determined by the trial and error approach.

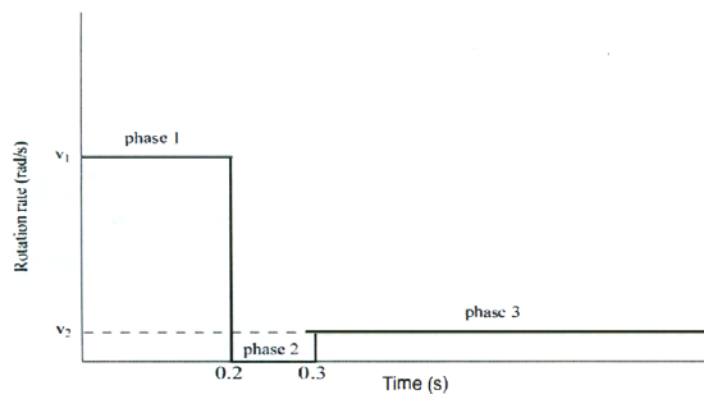


Fig.5.5 Time history of applied rotational velocity (3 hold model)

## 5.4 Intact Condition

The Finite Element Method has been selected as numerical analysis to validate the analytical solution which has been performed by using Smith's method for the

assessment of the residual hull girder strength. The starting point is showing the result of the Finite Element analysis for intact case, then the damage condition is introduced step by step and finally the results are compared to the analytical solution. In all the analyses, the rotational velocity about the horizontal axis is applied as a forced velocity.

Fig.5.6 shows the moment-time and moment-average curvature relationships of the intact hull girder under the hogging condition. Figs. 5.7 and 5.8 show the deformation and stress distribution at and beyond the ultimate strength. At the beginning stage of loading (up to point a'), elastic vibration is observed but it is later damped and thereafter the behavior can be regarded as quasi-static. It is found from Fig. 5.7 that the ultimate strength of the intact hull girder in the hogging condition is attained when the outer bottom part close to the transversal bulkhead is almost failed in compression rather than in the mid-hold area. Beyond the ultimate strength at the point C, all the outer bottom elements near the transversal bulkhead failed and the collapse region extends from the bilge side to the shell. The bending capacity is rapidly decreases. The collapse region is localized and the rest part unloads.

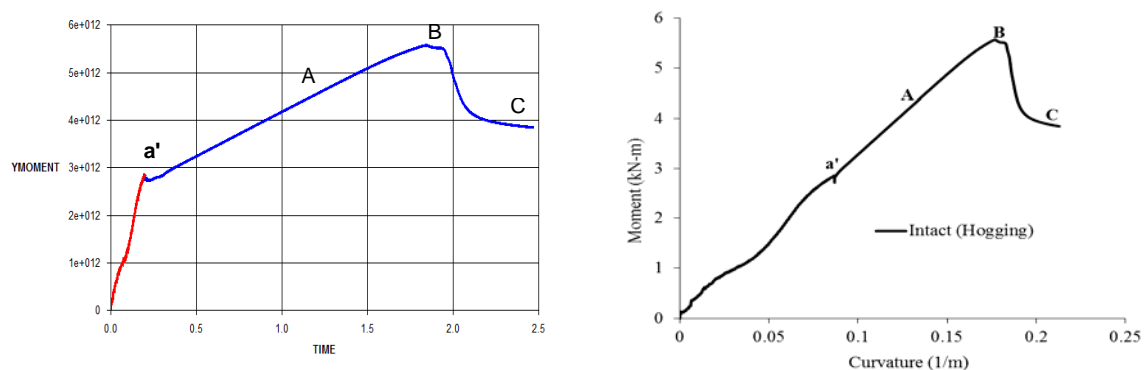
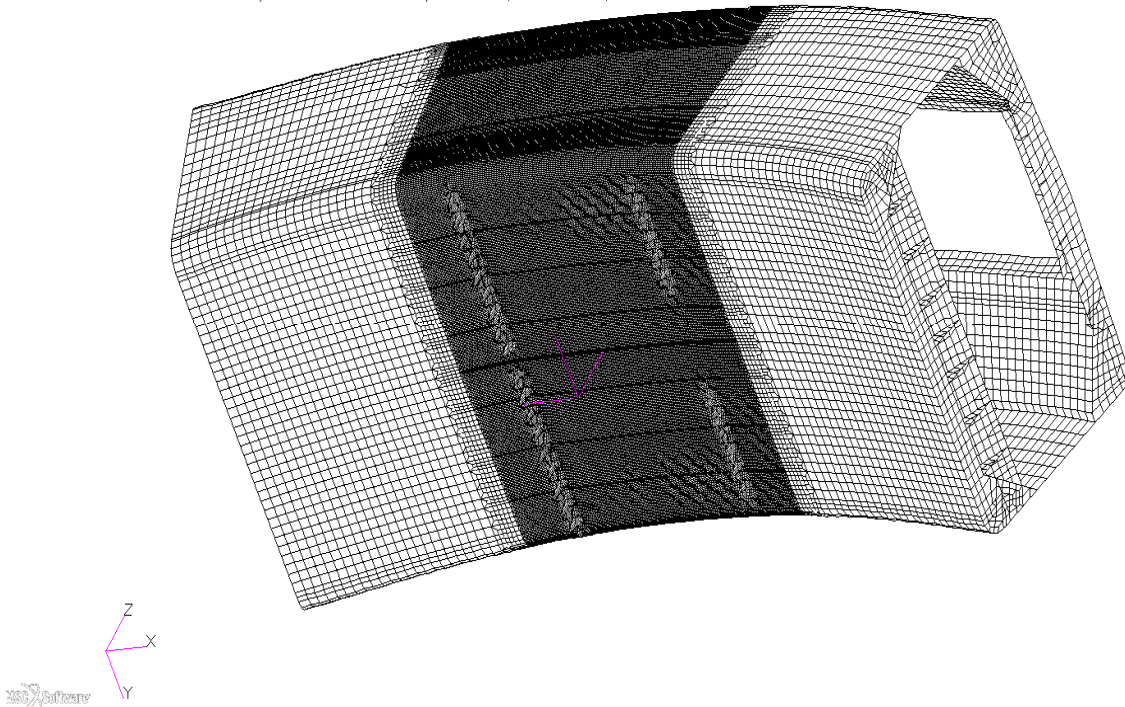


Fig.5.6 Moment-time and moment-curvature relationship (intact-hogging)

Patran 2012 64-Bit 19-May-13 13:30:02

Deform: 3HOLD\_HOGINTACT-T1\_A, A2:Cycle 187509, Time 1.875, Displacement... (NON-LAYERED)



Patran 2012 64-Bit 19-May-13 13:39:23

Fringe: 3HOLD\_HOGINTACT-T1\_A, A2:Cycle 187509, Time 1.875, Stress, T, von Mises, At Middle

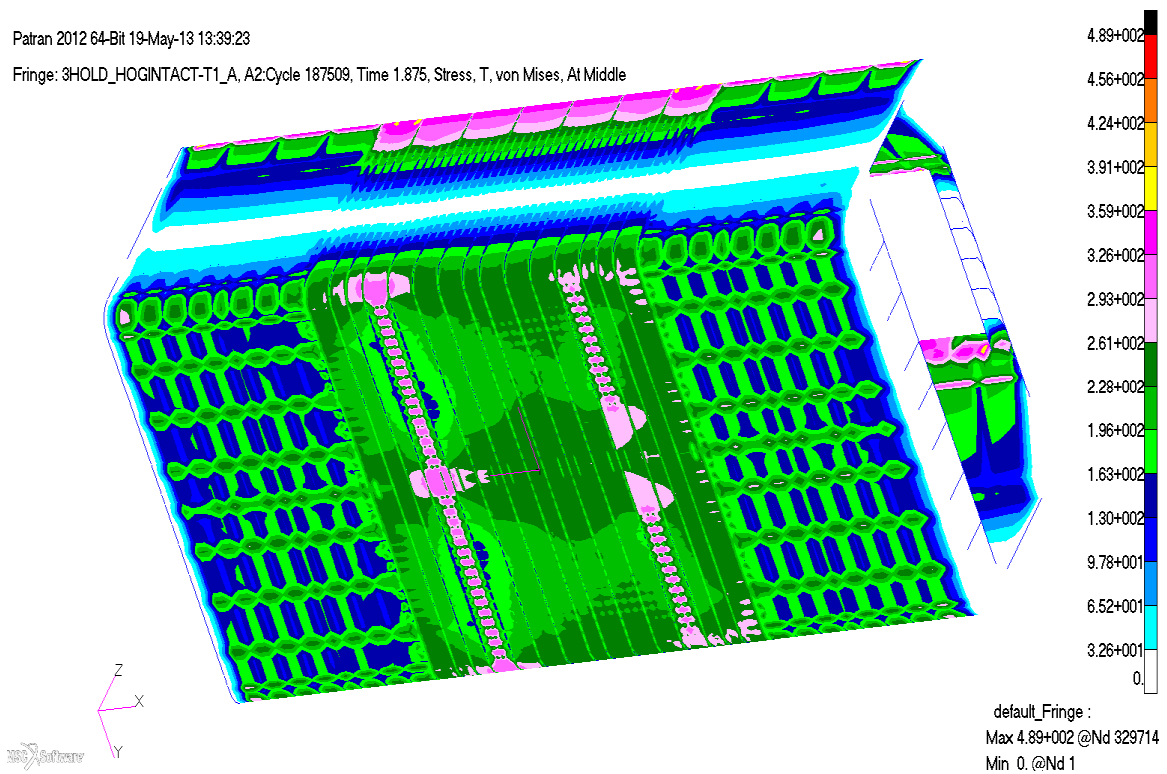
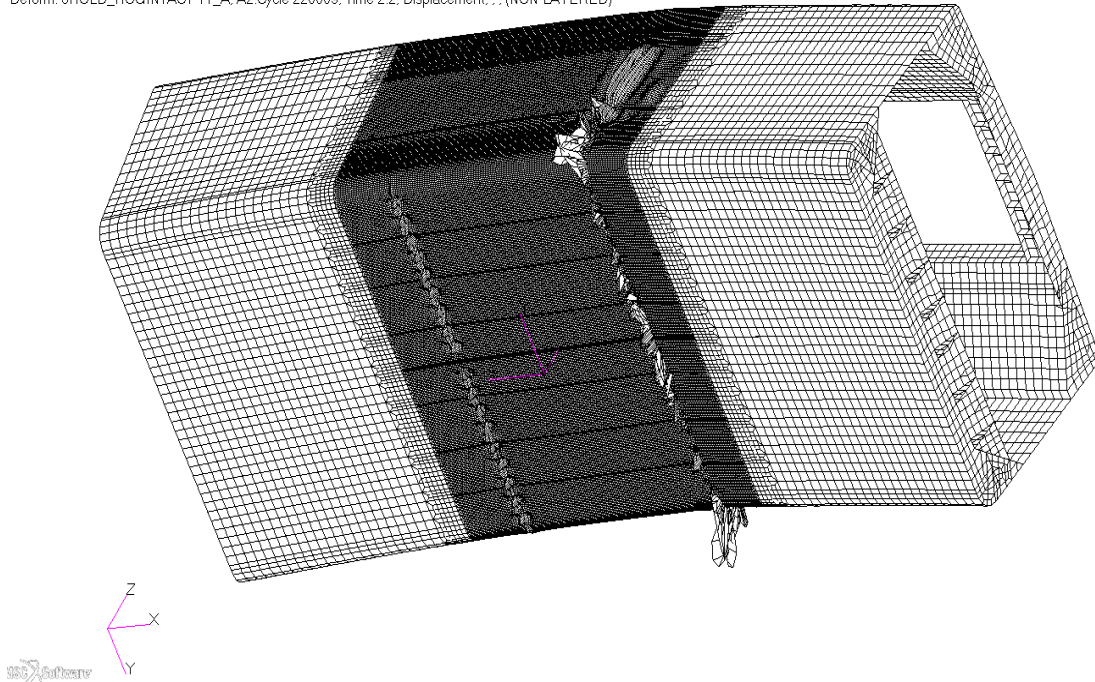


Fig.5.7 Deformation and stress distribution at point B (intact-hogging)

Patran 2012 64-Bit 19-May-13 13:46:57

Deform: 3HOLD\_HOGINTACT-T1\_A, A2:Cycle 220009, Time 2.2, Displacement. . . (NON-LAYERED)



Patran 2012 64-Bit 19-May-13 13:49:00

Fringe: 3HOLD\_HOGINTACT-T1\_A, A2:Cycle 220009, Time 2.2, Stress, T, von Mises, At Middle

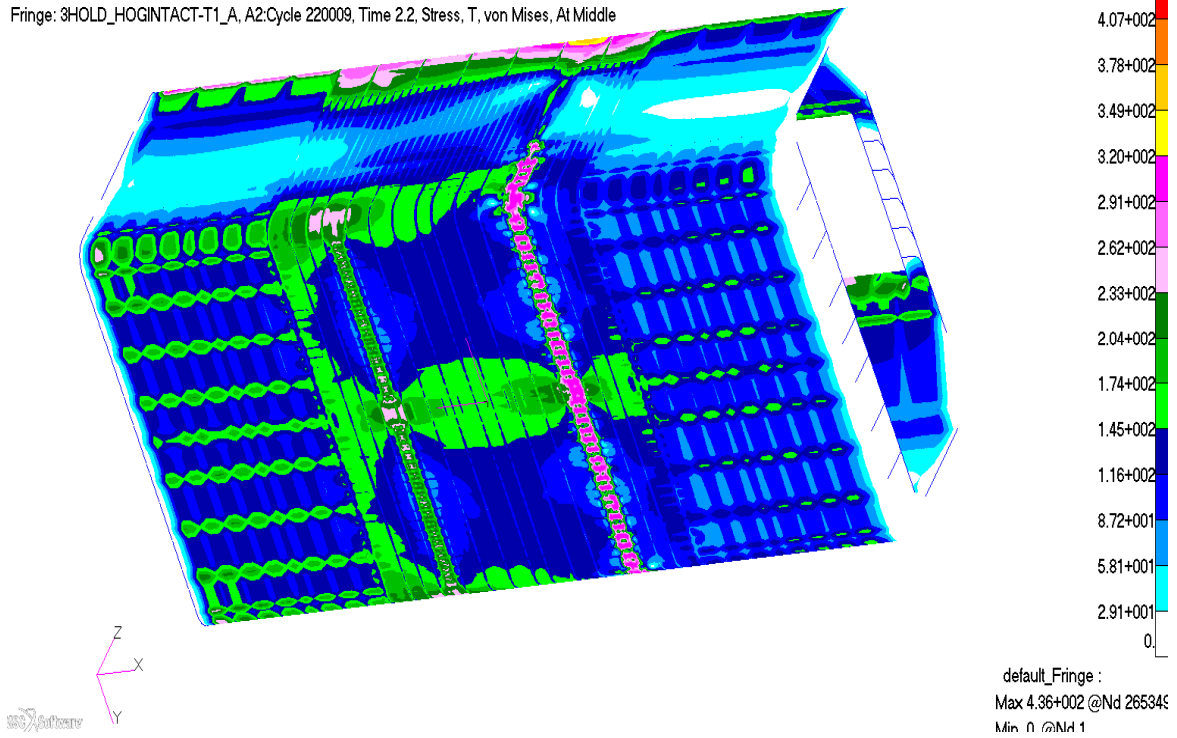


Fig.5.8 Deformation and stress distribution at point C (intact-hogging)

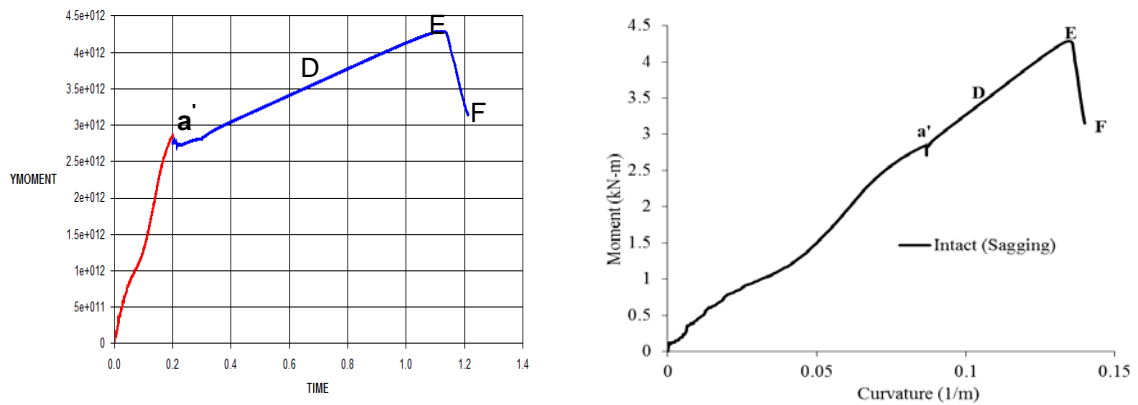


Fig.5.9 Moment-time and moment-curvature relationship (intact-sagging)

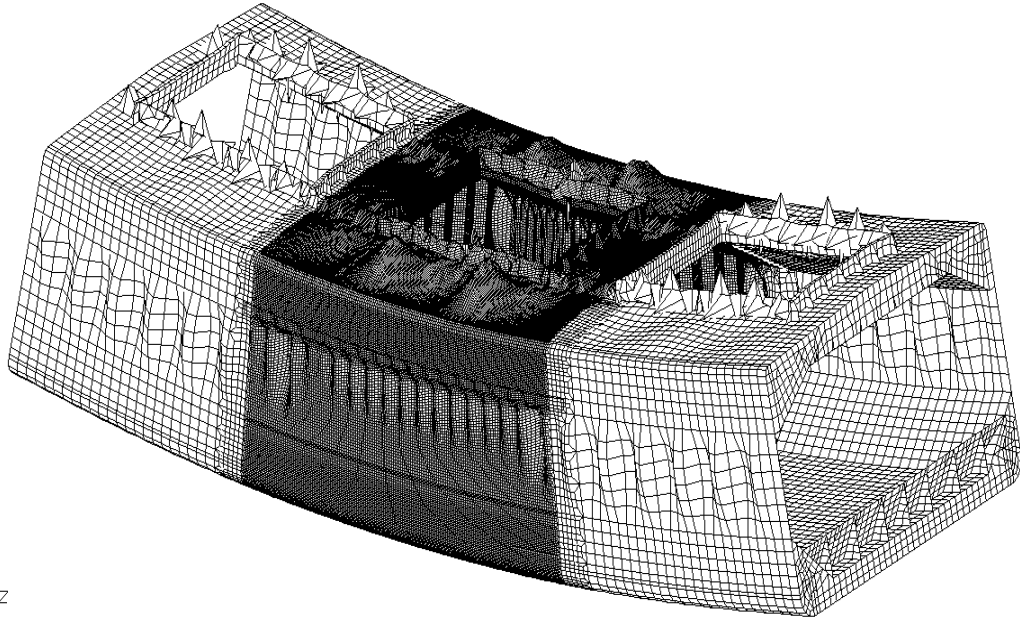
The moment-time and moment-curvature relationships obtained for the intact hull girder under the sagging condition are shown in Fig. 5.9, and the deformation and Mises equivalent stress distributions at and beyond the ultimate strength in Fig 5.10 and 5.11.

In sagging condition, the ultimate strength is attained soon after the structural component in the deck part failed. Although the significant deflection of the hatch coaming is observed, the direct trigger to the collapse of the failure of deck members. Almost no yielding is observed in the bottom part because of the shorter distance from the neutral axis and the reduction of load carrying capacity of the deck members.

After reaching the ultimate strength, the behavior of the model changed gradually in the post ultimate strength. Deformation and stress distribution are shown in Fig. 5.11 where the buckling deformation is localized at the frame space at the mid-ship and the unloading takes place in the rest part. The load carrying capacity beyond the ultimate strength is more rapidly decreases than the hogging case.

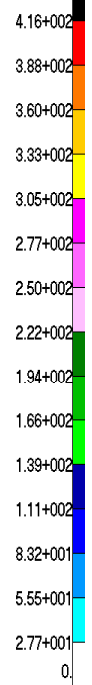
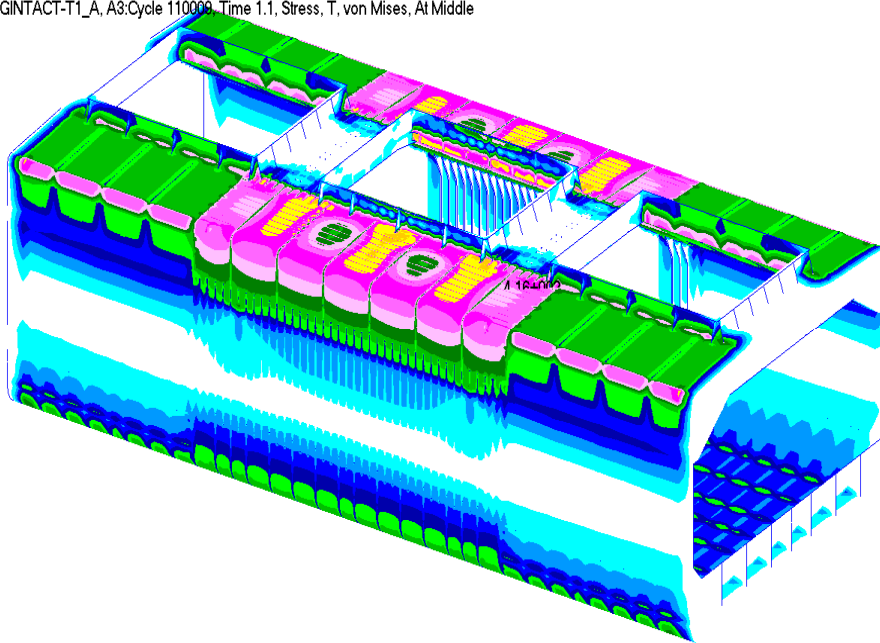
Patran 2012 64-Bit 19-May-13 14:15:00

Deform: 3HOLD\_SAGINTACT-T1\_A, A3:Cycle 110009, Time 1.1, Displacement... (NON-LAYERED)



Patran 2012 64-Bit 19-May-13 14:15:41

Fringe: 3HOLD\_SAGINTACT-T1\_A, A3:Cycle 110009, Time 1.1, Stress, T, von Mises, At Middle



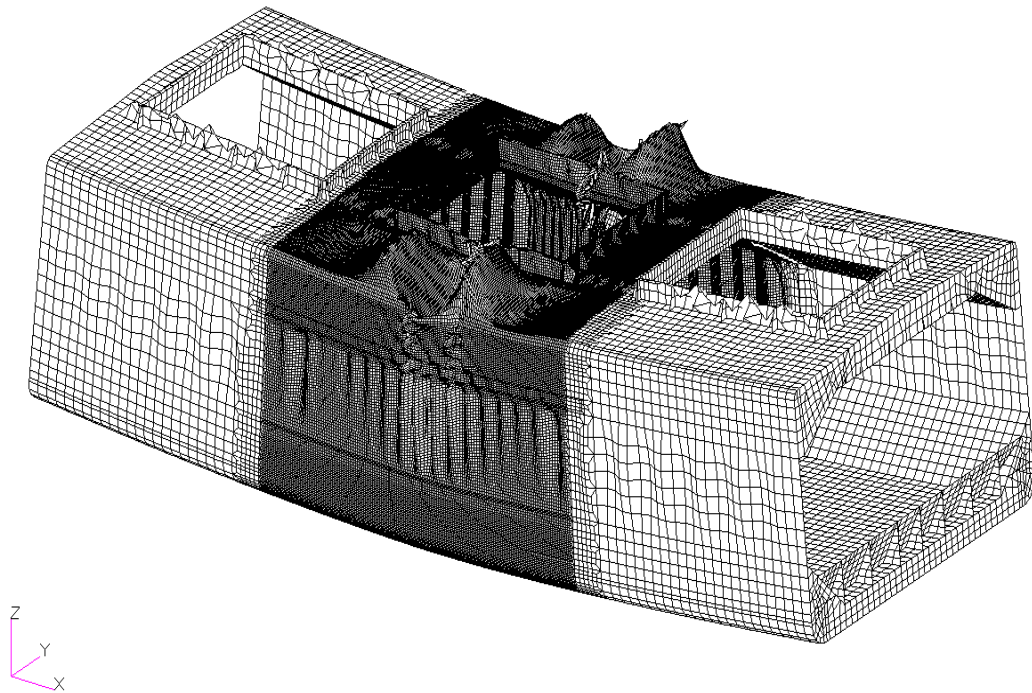
default\_Fringe :  
Max 4.16+002 @Nd 556567  
Min 0. @Nd 1



Fig.5.10 Deformation and stress distribution at point E (intact-sagging)

Patran 2012 64-Bit 19-May-13 14:16:57

Deform: 3HOLD\_SAGINTACT-T1\_A, A3:Cycle 120009, Time 1.2, Displacement... (NON-LAYERED)



Patran 2012 64-Bit 19-May-13 14:17:36

Fringe: 3HOLD\_SAGINTACT-T1\_A, A3:Cycle 120009, Time 1.2, Stress, T, von Mises, At Middle

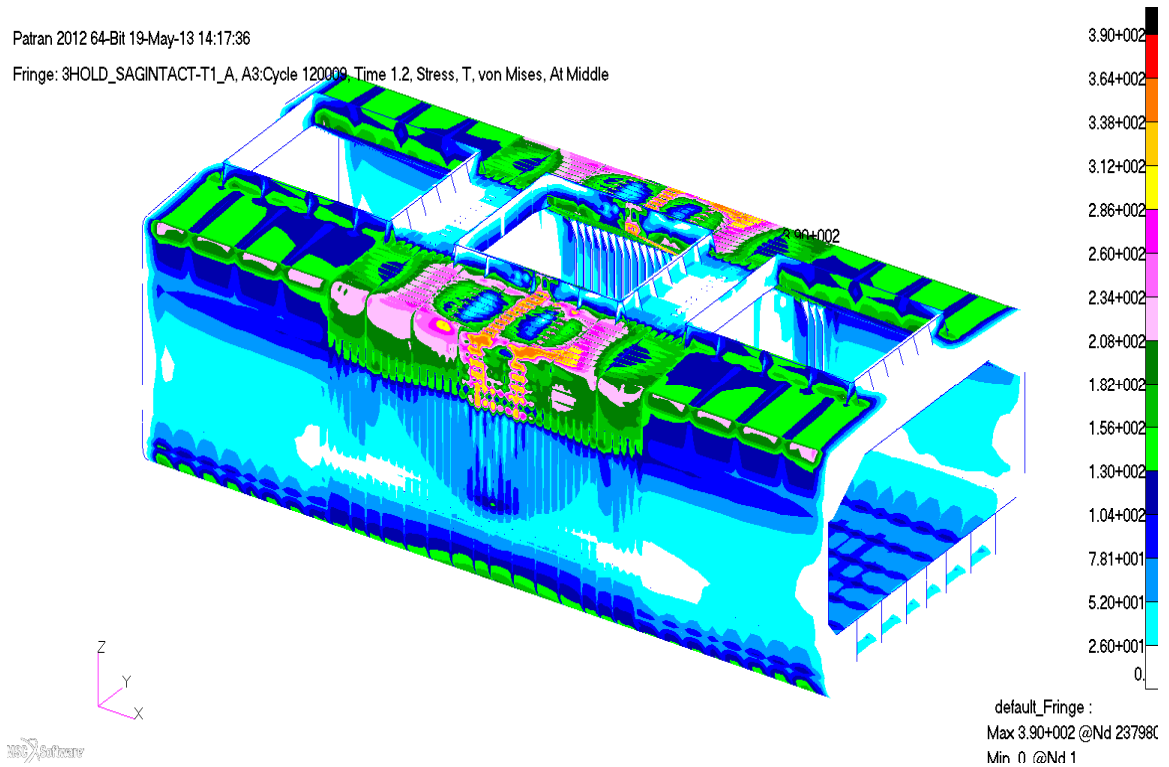


Fig.5.11 Deformation and stress distribution at point F (intact-sagging)

## 5.5 Damaged Condition

### 5.5.1 20% Damage

The moment-time and moment-curvature relationship obtained for the 20% damage are shown in Fig.5.12 and 5.13 for the hogging and sagging condition, respectively. Case 1 considers the rotation of neutral axis and Case 2 does not. Similar to the results obtained by HULLST and Beam-HULLST, Case 2 gives larger ultimate strength than Case 1, because the horizontal curvature is constrained in Case 2. The effect of the constraint is however much smaller than that observed in HULLST analysis.

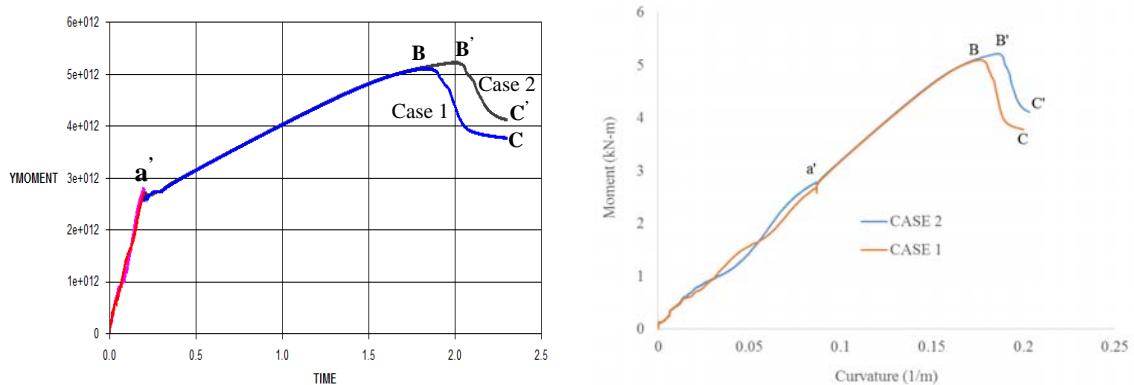


Fig.5.12 Moment-time and moment-curvature relationship (20% damage-hogging)

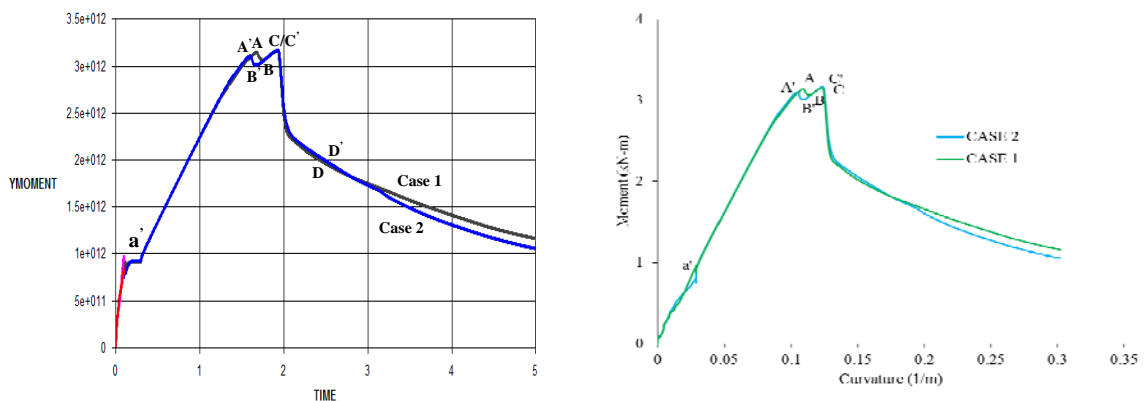
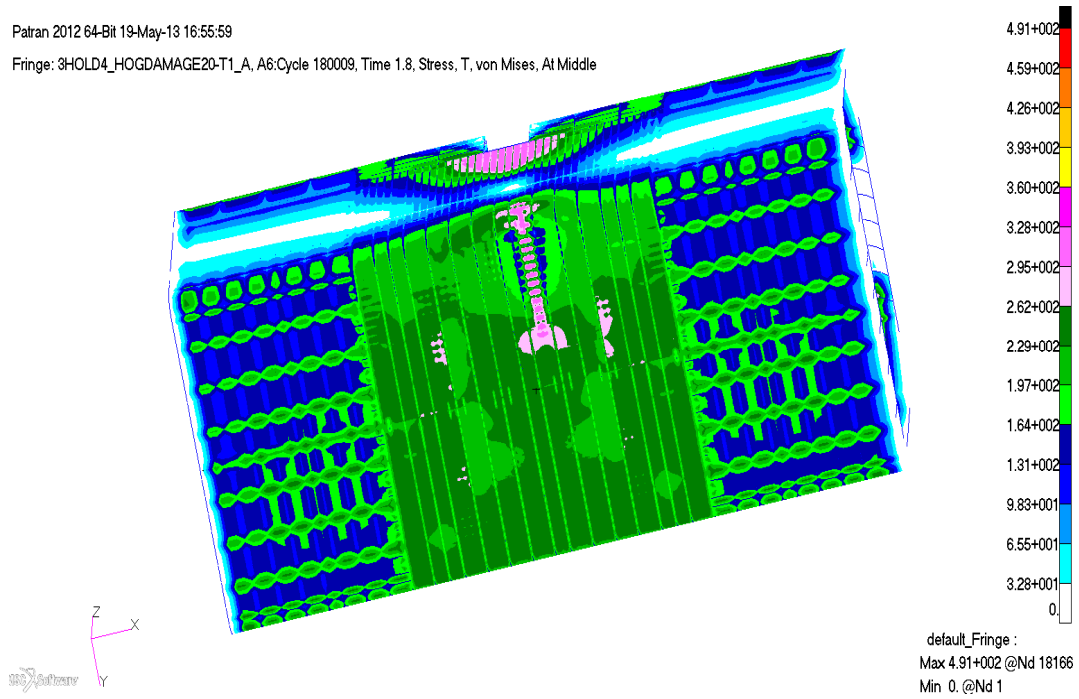


Fig.5.13 Moment-time and moment-curvature relationship (20% damage-sagging)

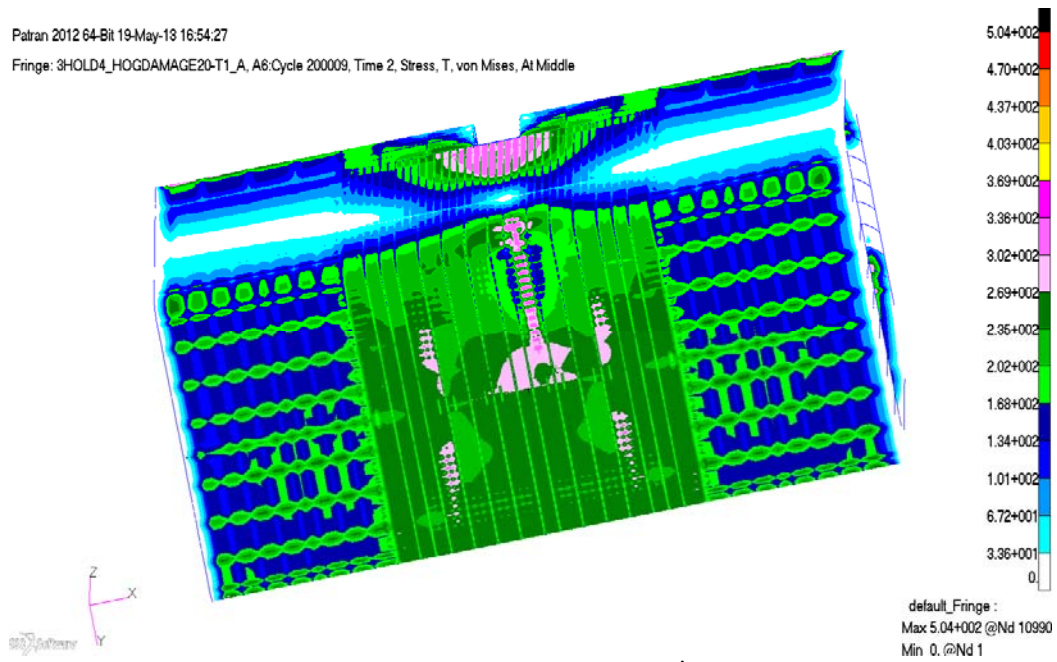
This is probably because the load redistribution more easily takes place in the shell model which is more flexible than the beam model that assumes a rigid and plane cross section. The assumption of 10% reduction of the residual strength assumed in the draft structural rules is again considered to be over-pessimistic.

Two peaks are observed in the moment-curvature relationship in the sagging condition, Fig. 5.13. At the first peak, points A and A', the initial buckling takes place at the deck part on the damaged side. The load carrying capacity once decreases because of the reduction of the post-buckling capacity at the damaged side, but again increases as the internal load is redistributed to the intact side of the deck. After the deck part on the intact side failed in compression, the maximum residual capacity is attained at the points B and B'. It should be noticed in Fig. 5.13 that the initial failure of the deck part on the damaged side takes place earlier in Case 2 than in Case 1. This is probably because of the difference of the deck stress distribution as a result of the constraint on the horizontal curvature in Case 2.

Fig. 5.14 shows the Mises stress distributions at the ultimate strength in the hogging condition. In Case 1, Yielding is spreads in the damaged side of the bottom plate while in Case 2 in the both damaged and intact sides of the bottom plate. This is clearly due to the constraint on the horizontal curvature and this results in the slightly larger ultimate strength than Case 1. Fig. 5.15 shows the Mises stress distributions at the ultimate strength in the sagging condition. Compared to the hogging condition, the difference of the stress distribution between Case 1 and case 2 is small. This is probably because the failure develops in larger area of cross section in the hogging condition than in the sagging condition and over-constraint on the horizontal curvature has a larger effect.

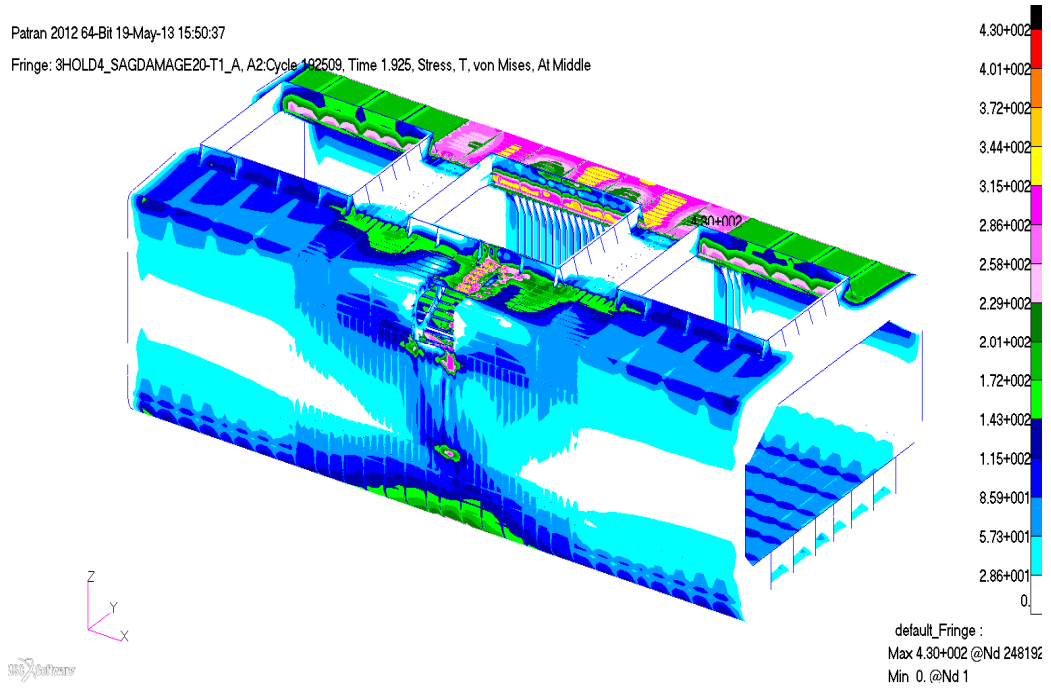


(a) Case 1 (point B)

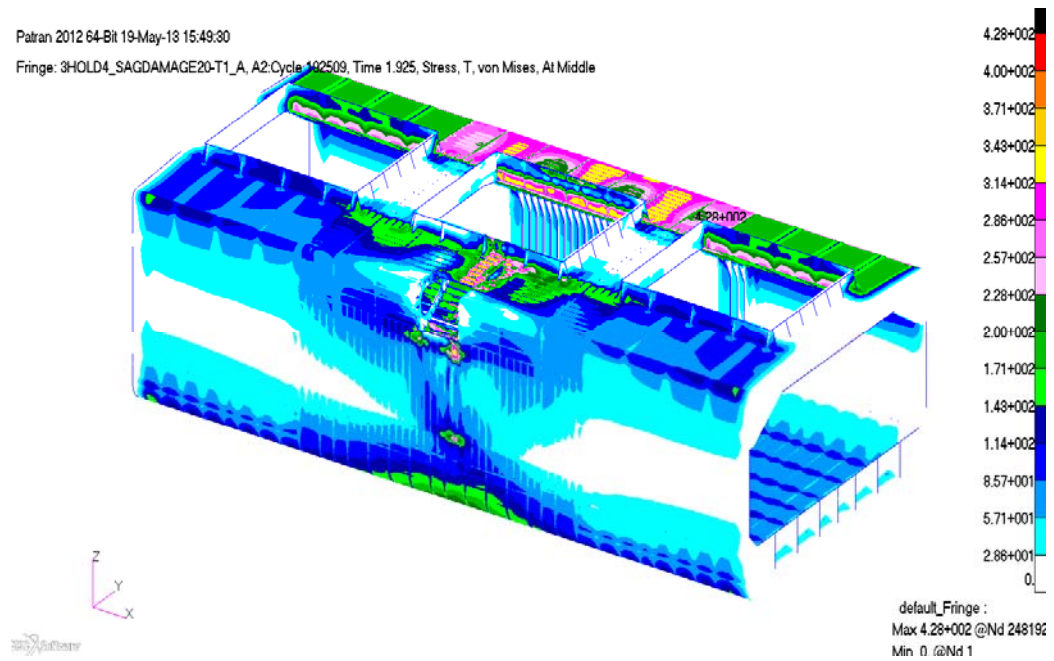


(b) Case 2 (point B)

Fig.5.14 Stress distribution at the ultimate strength (20% damage-hogging)



(b) Case 1 (point C)



(a) Case 2 (point C')

Fig.5.15 Stress distribution at ultimate strength (20% damage-sagging)

### 5.5.2 70% Damage

Fig. 5.16 and 5.17 show the moment-time and moment-curvature relationship for 70% damage case in the hogging and sagging conditions, respectively. The vertical bending moment induces the horizontal curvature in Case 1 while in Case 2 does not. Case 2 gives ultimate strength 1.07% larger than Case 1 in the hogging condition. On the other hand, in the sagging condition, Case 2 is almost same as or even smaller than Case 1. This is partly because of the over-constraint on the horizontal curvature. It is however clear that the effect of the rotation of neural axis obtained by the FE analysis is smaller than that obtained by HULLST and Beam-HULLST, and much smaller than that assumed in the draft structural rules.

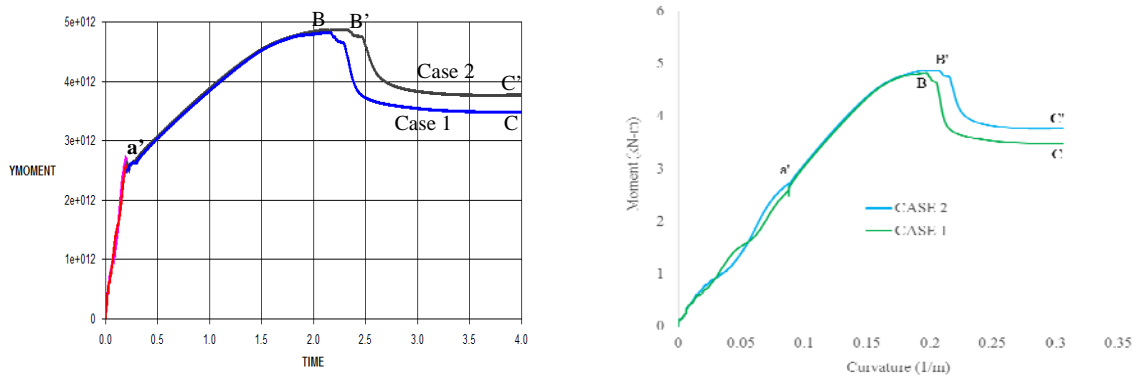


Fig.5.16 Moment-time and moment-curvature relationship (70% damage-hogging)

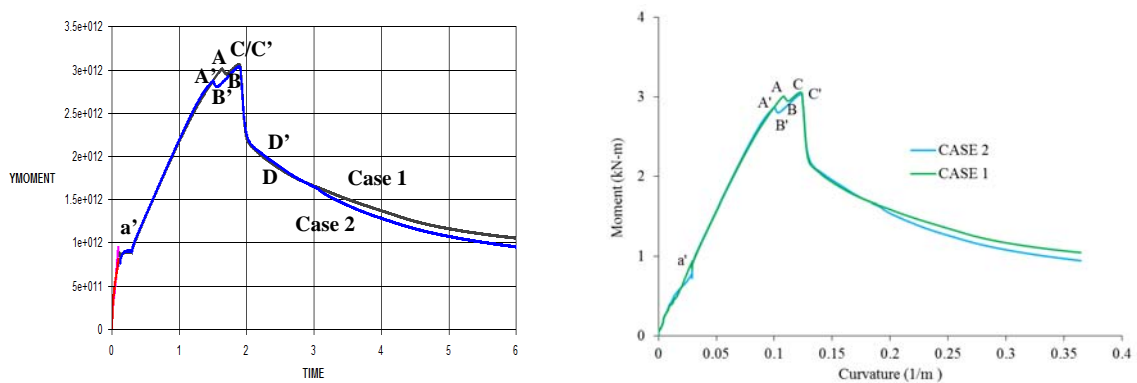
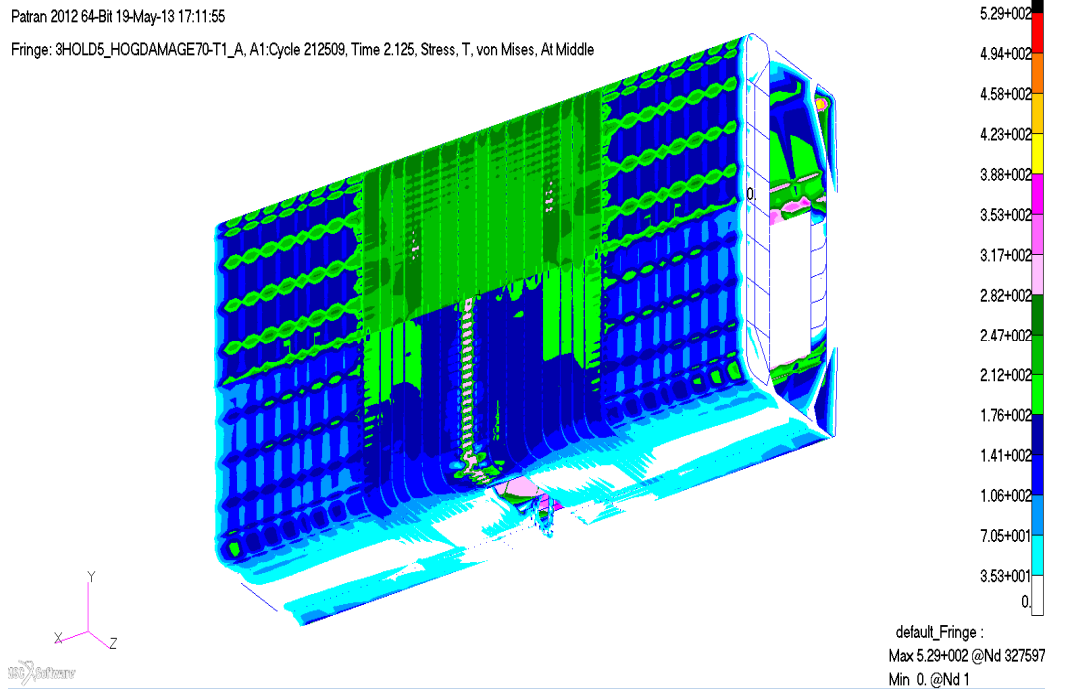
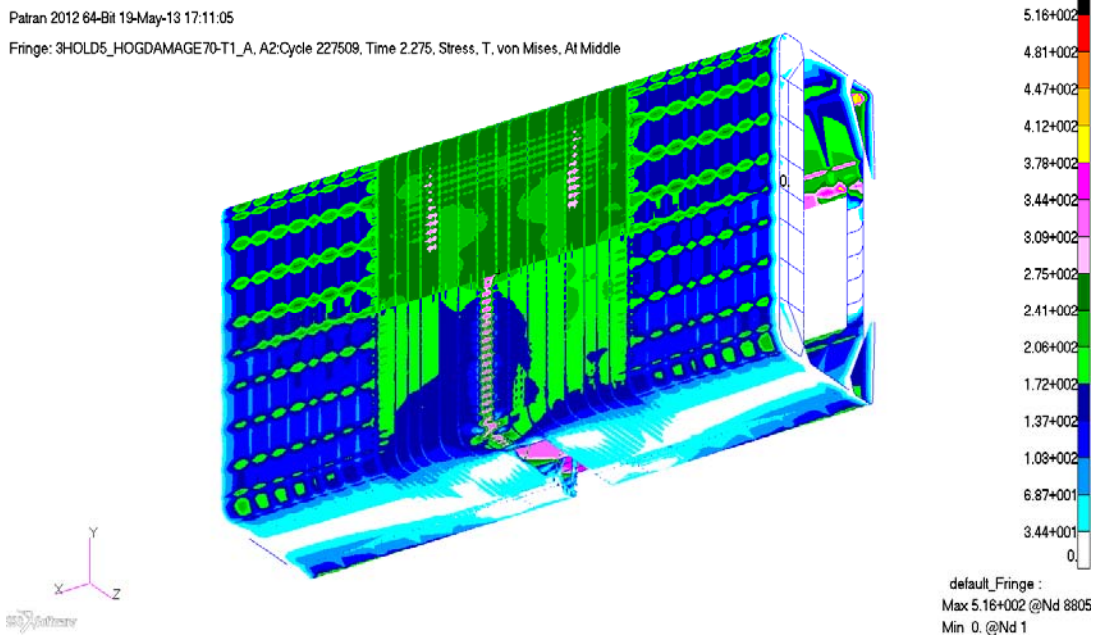


Fig.5.17 Moment-time and moment-curvature relationship (70% damage-sagging)

The deformation and stress distribution at the ultimate strength are shown in Figs. 5.18 and 5.19. The difference of Cases 1 and 2 are almost similar to those of the 20% damage.

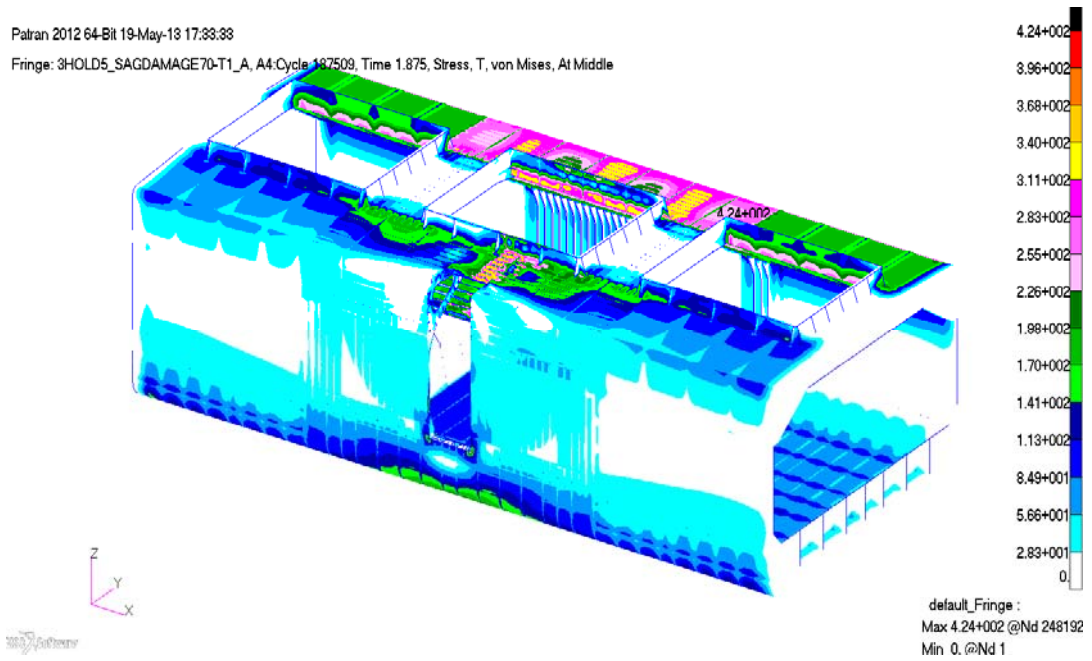


(b) Case 1 (point B)

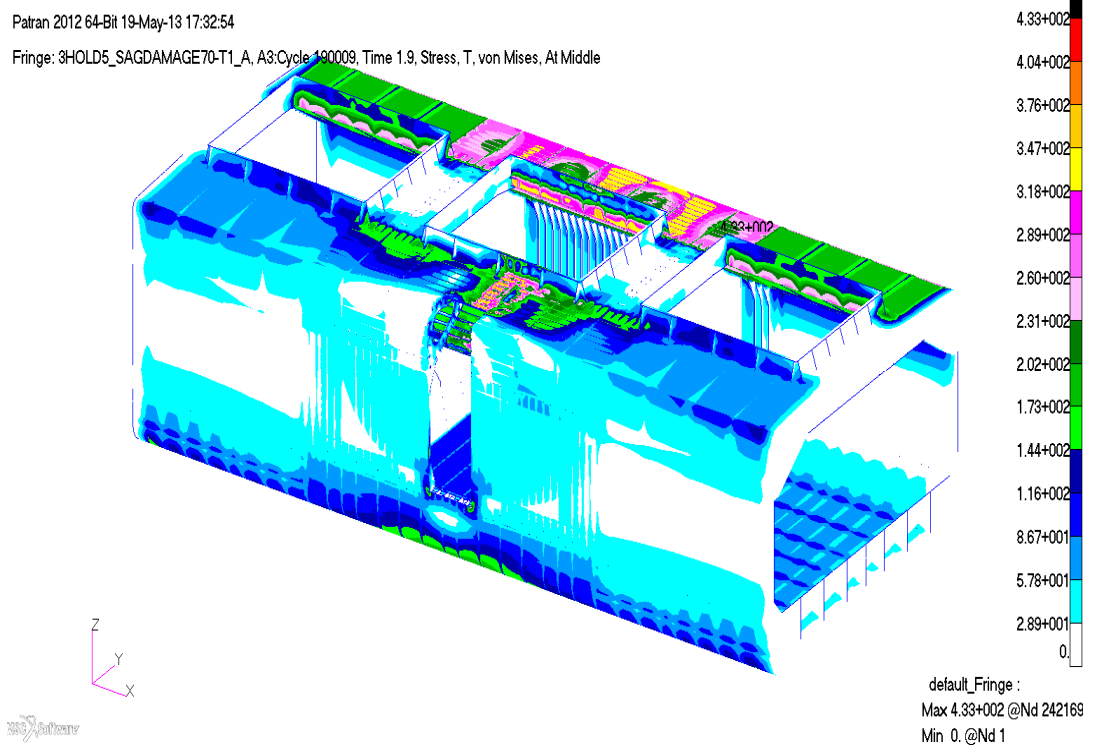


(a) Case 2 (point B')

Fig.5.18 Stress distribution at ultimate strength (70% damage-hogging)



(a) Case 1 (point C)



(b) Case 2 (point C')

Fig.5.19 Stress distribution at ultimate strength (70% damage-sagging)

## 5.6 Comparison of FE Analysis and Smith's Method

To validate the proposed simplified methods based on the Smith's method for the residual hull girder strength analysis, the results obtained by the HULLST and Beam-HULLST are compared with FEM analysis using MSC/DYTRAN. The three-hole model shown in Fig. 5.1 is the target model but the analysis of a partial model is also performed for comparison purpose.

Fig. 5.20 is the relationship between the vertical bending moment and the averaged curvature over the full length of the model for analysis. In the Beam-HULLST analysis, one frame-space model is used, and in FEM the three-hole model. It is confirmed that HULLST and Beam-HULLST gives almost identical bending moment-curvature relationship. The ultimate strength obtained by the HULLST and Beam-HULLST is quite in good agreement with the FEM results. However, the post-ultimate strength behavior obtained by FEM drops much more rapidly than that obtained by the HULLST and the Beam-HULLST for one-frame space model. This is due to the localization of the plastic deformation at the collapsed cross-section and the unloading at the rest part. As the load carrying capacity decreases beyond the ultimate strength at the collapsed cross-section, the rest part unloads and the curvature decreases. The capacity therefore drops with a very small increase in the average curvature for the full length. To make this clearer, the FEM analysis for a one-frame space model has been also performed. The comparison of the results is shown in Fig. 5.21. The HULLST and Beam-HULLST results are in good agreement with the FEM result.

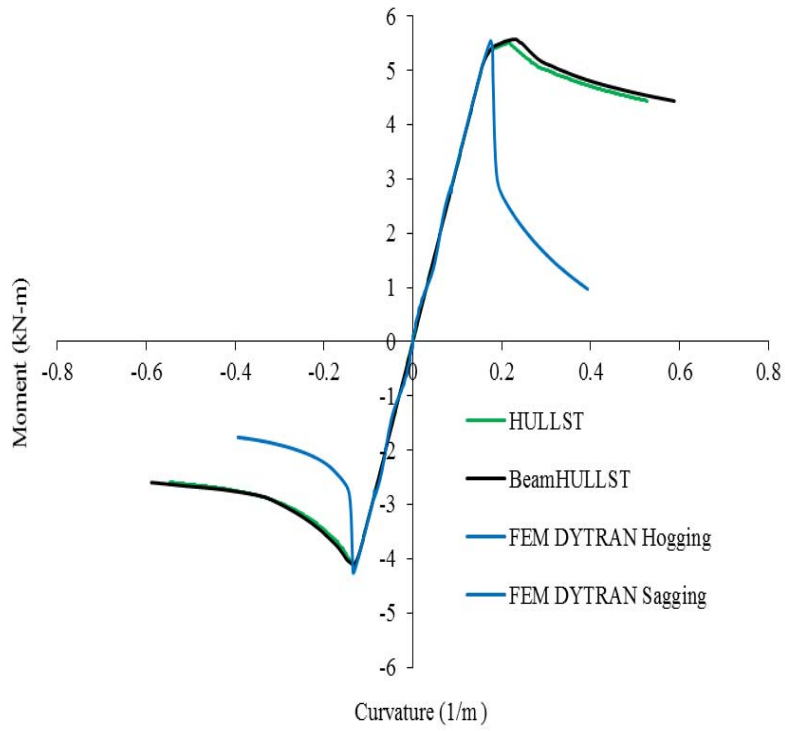


Fig.5.20 Moment-Curvature relationship of three-hold model (Intact condition)

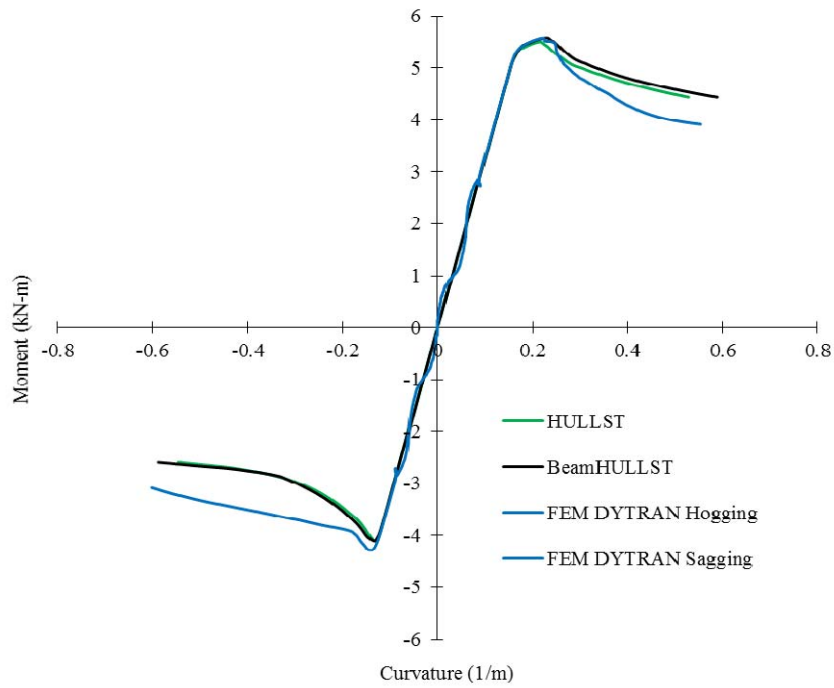


Fig.5.21 Moment-Curvature relationship of one-frame space for (Intact condition)

Figs. 5.22 and 5.23 show the bending-moment and averaged-curvature relationship of the 20% damage model. One frame-space model is used for the Beam-HULLST analysis. On the other hand, the three-holed model is used in FEM analysis in Fig.5.22 and one-frame space model in Fig.5.23. The difference in the post-ultimate strength behavior between the three-holed model and the one frame-space model is due to the localization of plastic deformation as already explained. As to the accuracy of the residual strength (ultimate capacity), HULLST and Beam-HULLST give the prediction that is in good agreement with the FEM results for the hogging condition but significantly underestimate for the sagging condition. This is partly because the effect of the stress concentration due to the damage opening is not taken into account in the Smith's method based on the beam theory and partly because the axial stress-axial strain relationships used in the HULLST and Beam-HULLST analysis assumes the buckling collapse behavior of a continuous stiffened panel and does not consider the free edges at the damaged part. It is recognized that these must be improved for the accurate prediction of the residual hull girder strength using the Smith's method.

Figs.5.24 and 5.25 show the results obtained for the 70% damage. The similar tendency can be found as in the case of 20% damage. The effect of the rotation of the neutral axis can be capture by the HULLST and Beam-HULLST, but the rational modeling of the damage and the buckling/plastic collapse behavior of the members I the damaged part has also a significant impact on the estimate of the residual hull girder strength.

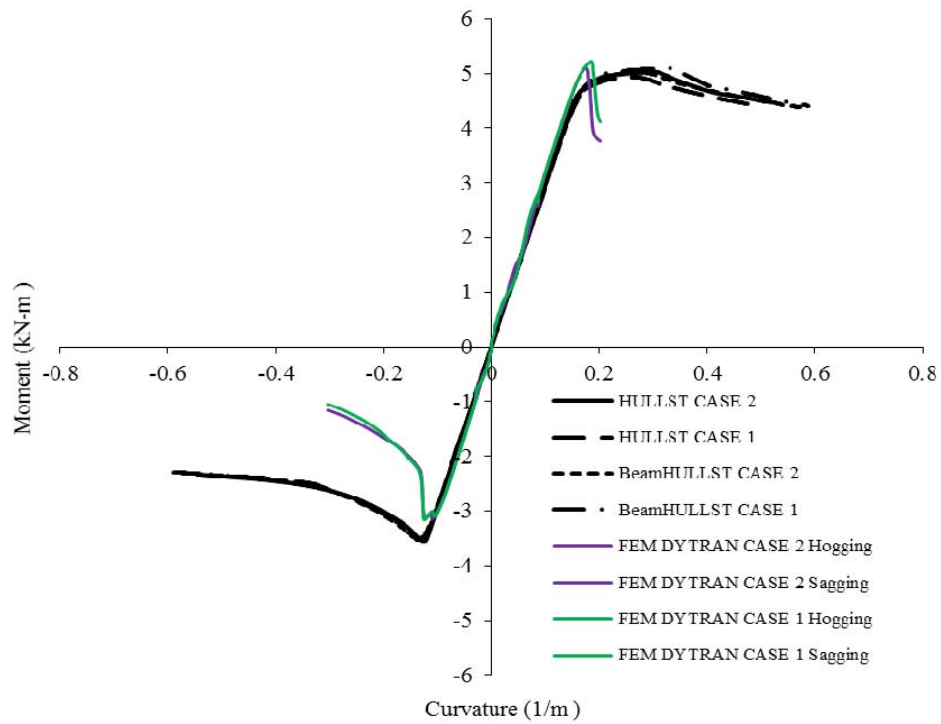


Fig.5.22 Moment-Curvature relationship of three-hold model for 20% damage

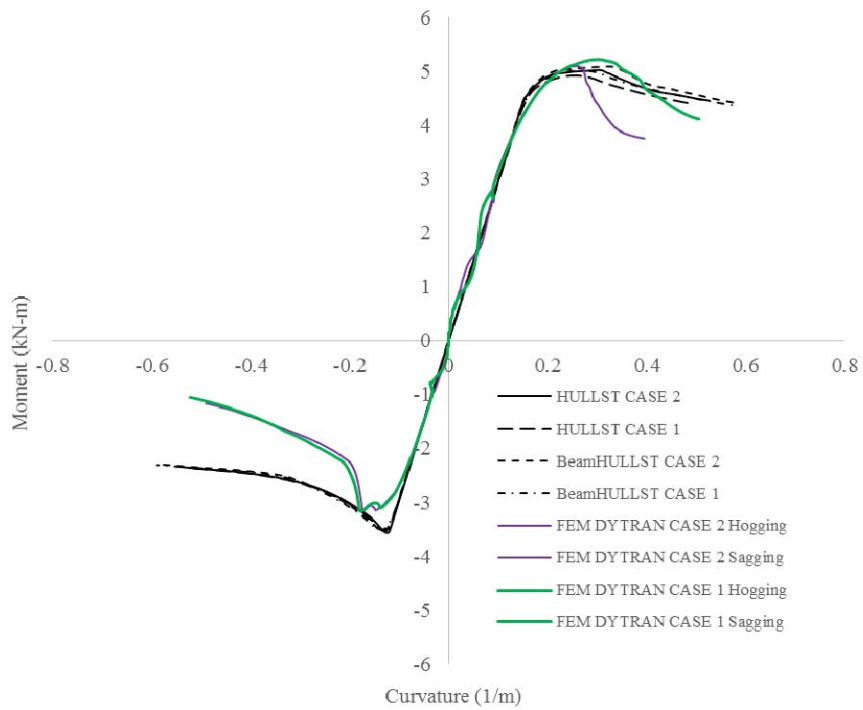


Fig.5.23 Moment-Curvature relationship of one-frame space for 20% damage

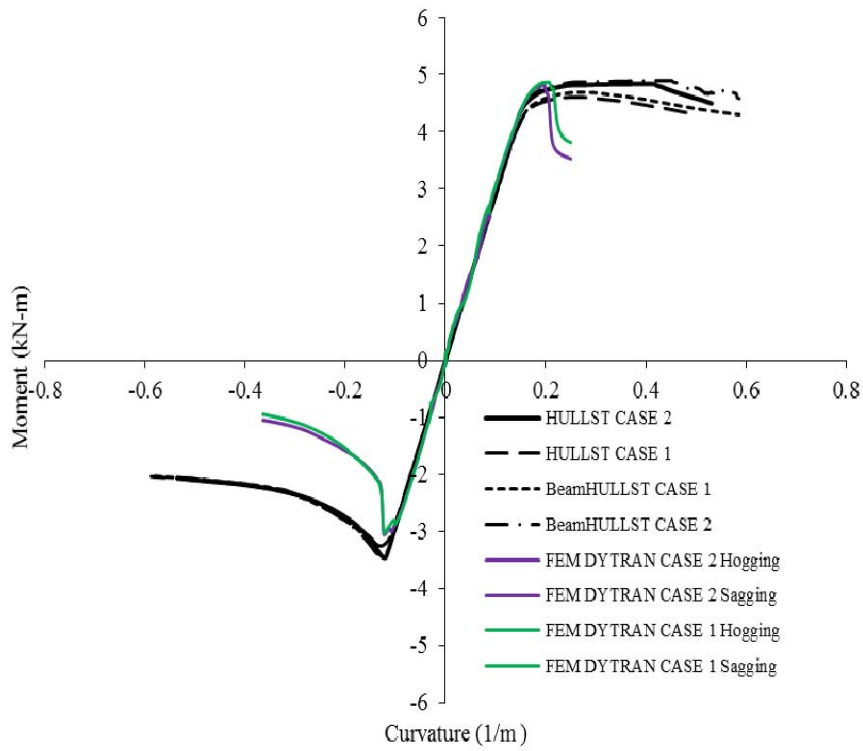


Fig.5.24 Moment-Curvature relationship of three-hold model for 70% damage

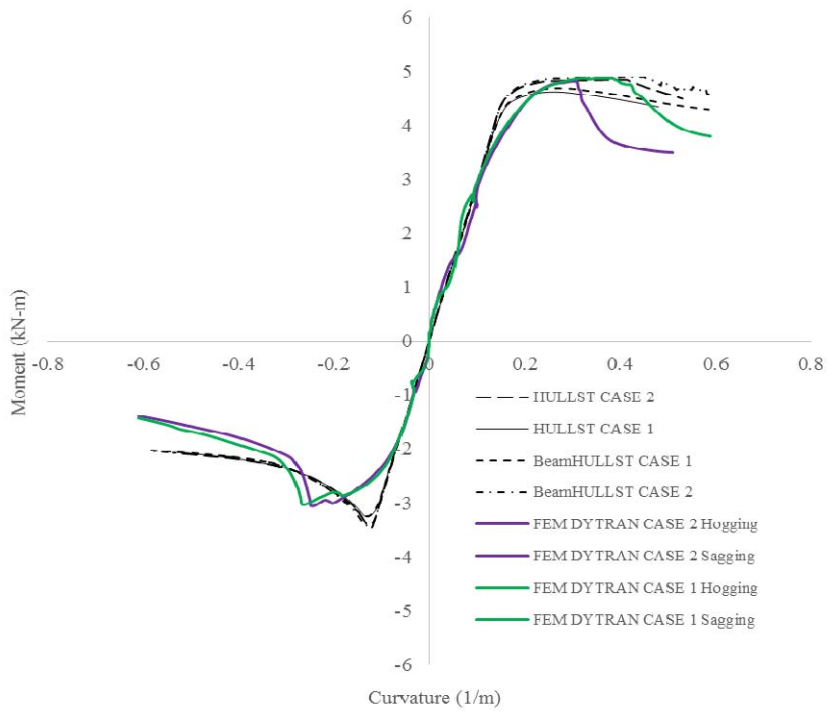


Fig.5.25 Moment-Curvature relationship of three-hold model for 70% damage

Fig.5.26 shows the bending moment-average curvature relationships calculated for the five frame-space model using the Beam-HULLST and DYTRAN for the 70% damage. It is known that the Beam HULLST that can consider the length of damage and the localization of the plastic deformation at the damage can predict the post-ultimate strength behavior as well as the residual strength with a reasonable accuracy.

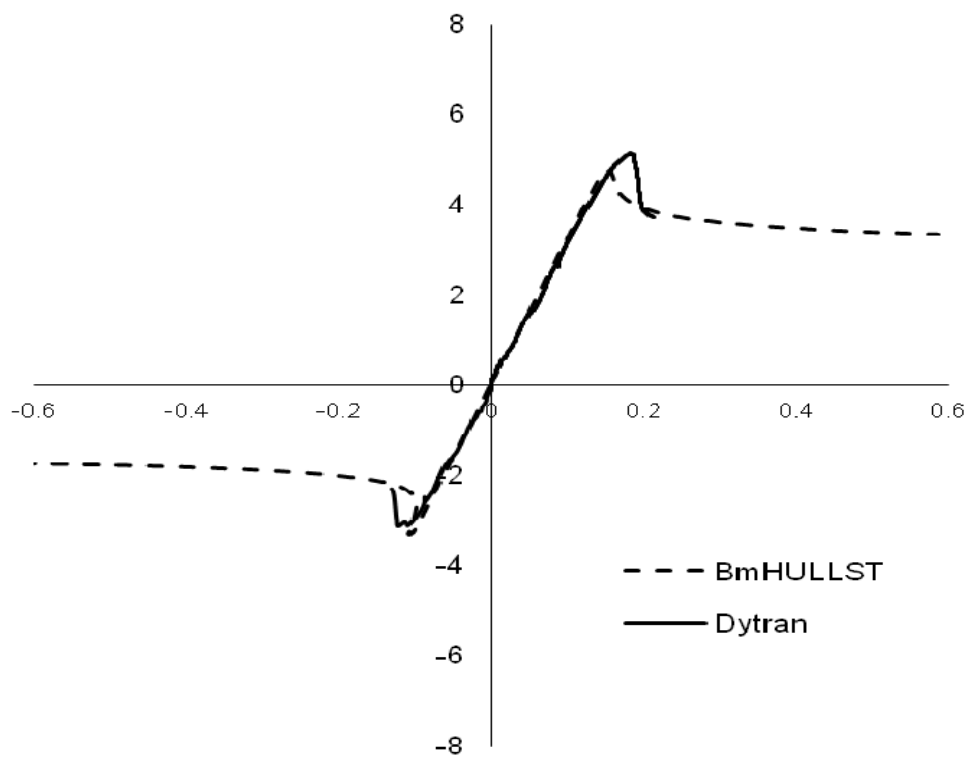


Fig. 5.26 Moment-curvature relationship of three-hold model (70% damage)

## 5.7 Conclusion

The ultimate strength analysis of ship's hull girder has been performed using Finite Element Method. The single hull bulk carrier is taken as the object ship for the assessment of the progressive collapse behavior under longitudinal bending. An asymmetric damage is assumed at the top side part based on the IACS draft CSR-H. The progressive collapse analyses using the HULLST and the Beam-HULLST are also performed and the applicability of these simplified methods is examined through a comparison with the FEM analysis. The following conclusions can be drawn:

1. The rotation of the neutral axis has a significant influence on the residual hull girder strength of the asymmetrically damaged ship. When it is neglected, the residual strength is overestimated. However, compared to the beam model analyses using HULLST or Beam-HULLST, the effect obtained by the shell FE analysis is smaller. The reduction rate of the residual strength due to the rotation of the neutral axis is about 2.3% for 20 % damage and 2.7% for 70 % for the hogging condition. This is primarily because of the possible deformation and load-redistribution as a 3D shell structure at the damaged part. The 10% reduction proposed in IACS draft CSR is on the very conservative side in this respect.
2. HULLST and Beam HULLST give the intact strength with a very good accuracy. However, in the damaged condition, particularly when the damaged part is on the compression side of hull girder bending, they tend to over-predict the ultimate strength than the FEM. The improvement of the estimate of the ultimate strength and post-ultimate strength behavior of the stiffened panel members at the

damaged part is essentially needed for the rational assessment of both the residual strength and the neutral axis effect.

3. The Beam-HULLST which can consider the damage extent in the longitudinal direction and the localization of the plastic deformation can predict the post-ultimate strength behavior as well as the ultimate residual capacity with a reasonable accuracy. It is expected to be effectively utilized for the quick assessment of the risk of the hull girder in the damaged I condition.

## **Chapter 6**

### **Concluding Remarks**

#### **6.1 Conclusion**

The investigation of the progressive collapse behavior of an asymmetrically damaged ship's hull girder subjected to longitudinal bending has been carried out. The incremental formulation of the progressive bending collapse behavior of damaged ship's hull girder is presented based on the Smith's method. The beam finite element with the bending moment-curvature relationship predicted by the Smith's method is developed and applied to the damaged hull girder. A simple formula to estimate the residual hull girder strength under the sagging condition is proposed. Finally the nonlinear Finite Element analysis is performed to validate the proposed methods. The conclusions of the thesis may be summarized as follows.

1. The reduction ratio of the residual hull girder strength due to the rotation of the neutral axis is about 8% at maximum for the case of bulk carriers and almost negligible for the case of oil tankers having outer shell damage. The reduction rate considered in the draft common structural rules is on the conservative side.
2. The influence of the damage on the residual hull girder strength under biaxial moment depends on the applied moment ratio. Larger influence is induced when biaxial moments produce the axial stress in the same direction in the damaged part. The residual strength interaction relationship obtained under the proportional moment loading almost coincides with that obtained by the proportional curvature loading.
3. The influence of the rotation of the neutral axis at the damaged part is reduced by the presence of the adjacent intact part with no neutral axis rotation. The Beam-HULLST

program developed in the present work can simulate this effect within the framework of the Smith's method. The post-ultimate behavior of the damaged hull girder predicted by the Beam-HULLST has shown a good agreement with the shell FEM analysis including the effect of the localization of the plastic deformation on the whole hull girder behavior.

4. The developed closed-form formulae of the residual hull girder strength under the sagging condition give the predictions of the residual hull girder strength and the neutral axis effect which are in good agreement with the results of the progressive collapse analysis by HULLST and Beam-HULLST.
5. Progressive collapse analysis of a damaged hull girder is performed using the explicit shell FEM code. It is found from a comparison with the FE analysis that HULLST and Beam-HULLST give a reasonable prediction of the progressive collapse behavior. However, the residual strength predicted by HULLST or Beam-HULLST under the assumption of beam theory tends to be larger than the shell FEM, particularly when the damage is located on the compression side of hull girder bending. Further improvement of the estimate of the capacity at the damaged part is necessary.
6. The effect of the rotation of the neutral axis obtained by the shell FE analysis is smaller than that predicted by HULLST or Beam-HULLST because of larger possibility of deformation and load-redistribution. This again shown that the 10% reduction rate of the residual hull girder strength of considered in the draft common structural rules is over-pessimistic and more reasonable assessment should be made.

## **6.2 Future Works**

As described above, the developed HULLST and Beam-HULLST programs gives a reasonable prediction of the neutral axis effect on the residual strength of the asymmetrically damaged ship. However, since they are based on the beam theory that assumes a rigid cross-sectional geometry and a plane cross section, the stress concentration at the damaged part and the change in the boundary condition for the damaged stiffened and plate panels are not been accounted. The improvement of the average stress-average strain relationship used for the Smith's method is needed by properly using FE analysis.

In the present study, only the bending collapse is considered. However, hull girder shear strength may be reduced more significantly than the bending strength depending on the damage location and load condition. The extension of the Beam-HULLST to the combined bending and shear load condition is expected and needs future researches.

## References

Abu Bakar, A. and Dow, RS. (2013). "Simulation of Ship Grounding Damage Using the Finite Element Method," *J Solid and Structure*, Vol 50, 623-636.

Choung, J, Nam, JM. and Ha, TB. (2011). "A New Convergence Criterion of Progressive Collapse Method for the Assessment of Residual Ultimate Strength of Asymmetrically Damaged Hulls," *Proc 25th Asian-Pacific Technical Exchange and Advisory Meeting on Marine Structure*, TEAM, Incheon, Korea, 143-150.

Choung, J, Nam, JM. and Ha, TB. (2012). "Assessment of Residual Ultimate Strength of an Asymmetrically Damaged Tanker Considering Rotational and Translational Shifts of Neutral Axis Plane," *J Marine Structures*, Vol 25, 71-84.

Downes, J, Collette, M. and Incecik, A. (2006). "Analysis of Hull Girder Strength in the Damage Condition," *3rd International ASRANet Colloquium*, ASRANet, Glasgow, UK.

Fang, C. and Das, PK. (2004). "Hull Girder Ultimate Strength of Damaged Ship," *Proc 9th Int Sym on Practical Design of Ships and Other Floating Structures*, PRADS, Luebeck-Travemuende, Germany, Vol 1, 309-316.

Hussein, AW. and Guedes Soares, C. (2009). "Reliability and Residual Strength of Double Hull Tankers Designed According to the New IACS Common Structural Rules," *J Ocean Engineering*, Vol 36, 1446-1459.

IACS (2012). Common Structural Rules for Bulk Carriers and Double Hull Oil Tankers.

International Maritime Organization (2009). "Goal-Based New Ship Construction Standards," MSC 86/5.

International Ship and Offshore Structure Congress (2006). "Collision and Grounding," Vol 2, Southampton, UK.

International Ship and Offshore Structure Congress (2009). "Damage Assessment after Accidental Events," Vol 2, Seoul, Korea.

K. Ishibashi, T. Shigemi and M. Harada (2008), "Effect of Local Pressure on Ultimate Hull Girder Strength, *Proc of Annual Meeting of Japan Society of Naval Architects and Ocean Engineers*, No 8, 391-394.

Kang, SH, Lee, SH. and Lee, JS. (2011). "Residual Ultimate Strength of Hull Girder Structures," *Proc 25th Asian-Pacific Technical Exchange and Advisory Meeting on Marine Structure*, TEAM, Incheon, Korea, 621-626.

Lee, TK et al. (2008). "A study of Ultimate Collapse Strength in Sagging of Ship Structures with Collision Damage," *Proc 18th International Offshore and Polar Engineering Conference*, ISOPE, Vancouver, Canada.

Luis, RM, Teixeira AP, Soares CG. (2009). "Longitudinal Strength Reliability of a Tanker Hull Accidentally Grounded," *J Structural Safety*, Vol 31, 224-233.

Muis Alie, MZ et al. (2011). "Ultimate Longitudinal Bending Strength of Ship Hull Girder Damages," *Proc 25th Asian-Pacific Technical Exchange and Advisory Meeting on Marine Structure*, TEAM, Incheon, Korea, 636-640.

Naar, H. (2006). "Ultimate Strength of Hull Girder for Passenger Ship," *Doctor Dissertation*, Helsinki University of Technology, Finland.

Nam, JM. and Choung,J. (2011). "Residual Longitudinal Strength of Hull Girder Considering Probabilistic Damage Extents," *Proc 25th Asian-Pacific Technical Exchange and Advisory Meeting on Marine Structure*, TEAM, Incheon, Korea, 657-667.

Notaro, G. et al. (2010). "Residual Hull Girder Strength of Ships with Collision or Grounding Damages," *Proc 11th International Symposium on Practical Design of Ships and Other Floating Structures*, PRADS, Rio de Janeiro, Brazil, 941-951.

Ohtsubo, H, Kawamoto, Y. and Kuroiwa, T. (1994). "Experimental and Numerical Research on Ship Collision and Grounding of Oil Tankers," *J Nuclear Engineering and Design*, Vol 150, 385-396.

Ozguç, O. and Barltrop, NDP. (2008). "Analysis on the Hull Girder Ultimate Strength of a Bulk Carrier Using Simplified Method Based on an Incremental- Iterative Approach," *J Offshore Mechanics and Arctic Engineering*, Vol 130, 021013-1.

Ozguç, O, Das, PK. and Barltrop, N. (2005). "A Comparative Study on the Structural Integrity of Single and Double Side Skin Bulk Carriers under collision Damage," *J Marine Structures*, Vol 18, 511-547.

Paik, JK, Thayamballi, AK. and Yang, SH. (1998). "Residual Strength Assessment of Ships after Collision and Grounding," *Marine Technology*, Vol 35, 38-54.

Pedersen, PT. (1994). "Ship Grounding and Hull Girder Strength," *J Marine Structures*, Vol 7,1-29.

Pedersen, PT. (2000). "Effect of Ship Structure and Size on Grounding and Collision Damage Distribution," *J Marine Structures*, Vol 27,1161-1179.

Servis, D. and Samuelides, M. (1999). "Ship Collision Analysis Using Finite Element," EURORO Spring Meeting, Nantes.

Smith, CS. (1977). "Influence of Local Compression Failure on Ultimate Longitudinal Strength of a Ship's Hull," *Proc Int Sym on Practical Design of Shipbuilding*, PRADS, Tokyo, Japan, 73-79.

Smith, MJ. and Pegg, NG. (2003). "Automated Assessment of Ultimate Hull Girder Strength," *J Offshore Mechanics and Arctic Engineering*, Vol 125, 211-218.

Soares, CG. et al. (2008). "Benchmark Study on the Use of Simplified Structural Codes to Predict the Ultimate Strength of a Damaged Ship Hull," *J International Shipbuilding Progress*, Vol 55, 87-107.

Toh, K, Maeda, M., and Yoshikawa, T. (2012). "The Effect of Initial Imperfection on the Hull Girder Ultimate Strength of Intact and Damaged Ships," *Proceeding of the 22nd International Offshore and Polar Engineers*, ISOPE, Rhodes, Greece, 823-830.

Wang, G. et al. (2002). "Longitudinal Strength of Ships with Accidental Damages," *J Marine Structures*, Vol 15, 119-138.

Yao, T. and Nikolov, P.I. (1992). "Progressive Collapse Analysis of a Ship's Hull Girder under Longitudinal Bending (2nd Report)," *J Soc. Naval Arch. of Japan*, Vol 172, 437-446.